Non-Equilibrium Physics II — NS-TP466M
Hydrodynamics with Applications in Soft and Active Matter

Joost de Graaf[1, *]

[1] *Institute for Theoretical Physics, Center for Extreme Matter and Emergent Phenomena, Utrecht University, Princetonplein 5, 3584 CC Utrecht, The Netherlands*

(Dated: April 7, 2025)

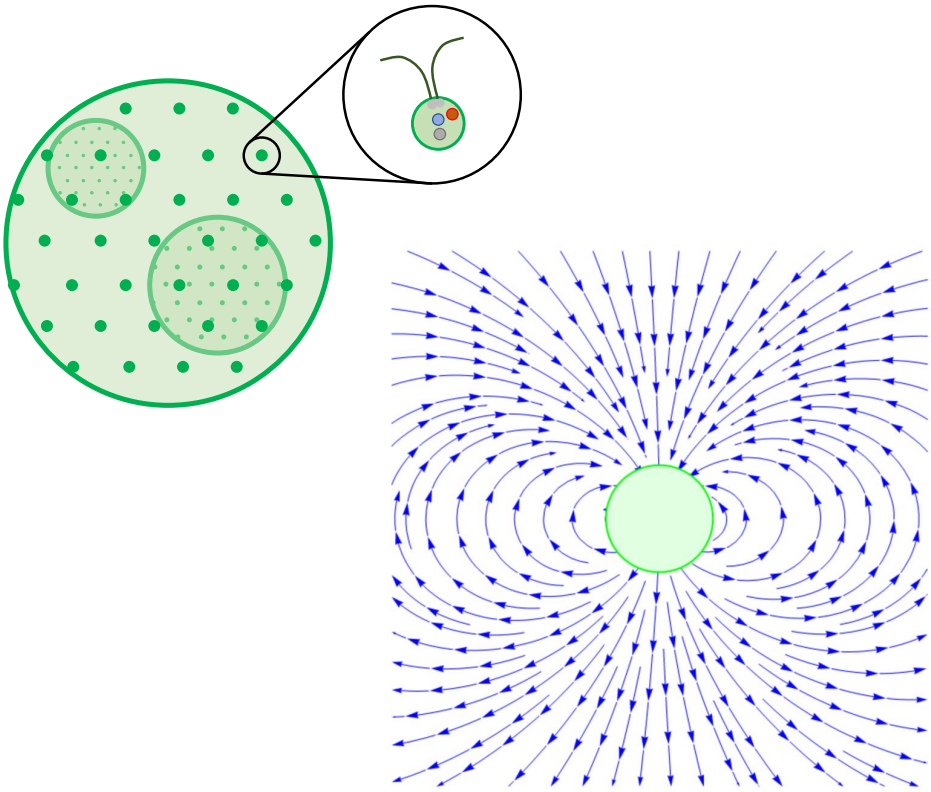

FIG. 1. **Sketch of a Volvox algae and a simple physical model for it.** (top left) A Volvox green algae is covered in tiny hairs called cilia, see inset, which beat in steady pattern to cause fluid motion. (bottom right) The flow field around this microorganism can be approximated using a neutral squirmer model [1]. Here, a cut-through along the central squirming axis is shown.

* j.degraaf@uu.nl

I. INTRODUCTION

This lecture series will concern itself with the principles of flow from a classical perspective. We will both introduce and go beyond the classical hydrodynamic equations that describe the flow of common fluids and gases, such as water, alcohol, and air, at the continuum level. These equations are commonly referred to as the Navier-Stokes (NS) equations, in honor of Claude-Louis Navier's and Sir George Gabriel Stokes' contribution to solving the problem of mathematically describing the flow of viscous fluids. The form with which you are most likely familiar and throughout this course will become familiar

$$\nabla_{\boldsymbol{r}} \cdot \boldsymbol{u} = 0; \tag{1}$$

$$\rho\left(\frac{\partial}{\partial t} + \boldsymbol{u}\cdot\nabla_{\boldsymbol{r}}\right)\boldsymbol{u} = -\nabla_{\boldsymbol{r}} p + \mu\underline{\boldsymbol{\Delta}}_{\boldsymbol{r}}\boldsymbol{u} + \boldsymbol{f}, \tag{2}$$

describes[1] the velocity $\boldsymbol{u}$ of *incompressible*, *viscous* fluids. Incompressibility is given by Eq. (1), while momentum transport is given by Eq. (2). Fluids described by the latter are called *simple* or *Newtonian*, because the stress — the forces due to deformation of the fluid — is linear in the rate of strain, *i.e.*, the rate of deformation. In Eq. (2), this is expressed by the term $\mu\underline{\boldsymbol{\Delta}}_{\boldsymbol{r}}\boldsymbol{u}$, which represents the viscous dissipation in the fluid. However, we should note that this way of writing the relation somewhat obscures the linear dependence of stress on the strain rate, as we will see.

In these notes, we will derive a general set of equations that govern flow from a perturbation perspective. This paradigm will allow us to extend our continuum description to *complex* or *non-Newtonian* fluids. In such fluids, the stress response will be nonlinear in the applied strain rate, which will have unexpected consequences. The example you will know from home is that of dough or thick cake batter, which climbs the stirrers when you mix it with an electric whisk[2]. This is very different from the behavior observed for water, where the stirrers cause (deep) dimples to form in the fluid during mixing. Before we get to the mathematically consistent framework that describes these systems, we will introduce a few general flow behaviors and means by which to characterize these. This will help motivate the theory development that is needed to describe these fluids' *rheology* — this term also refers to the branch of physics that studies flow behavior.

These notes further cover the inertia and viscosity dominated regimes, although we will only briefly touch upon the former. The linear flow regime may appear 'simple' especially for Newtonian fluids, but we will show that it is anything but. In particular, the introduction of a small amount of polymer to an otherwise Newtonian fluid, can drastically alter its behavior, even leading to the emergence of turbulence at essentially zero *Reynolds number* [3]. This number is the dimensionless group that gives the ratio between inertia and viscous dissipation, with zero implying there is no nonlinearity in Eq. (2), *i.e.*, the left-hand term drops out. This flow regime is the one commonly encountered by microorganisms, while we generally experience flows as inertia dominated on our length scale. The key to generating turbulence for dissipation-dominated systems is that the polymers endow the fluid with an (entropic) elastic response, which reintroduces nonlinear behavior, albeit on the right-hand side of an appropriately modified version of Eq. (2).

Another way to make simple, low-Reynolds-number fluids complex, is by adding many hard particles to it. This leads to a dynamical particle system with long-ranged, many-body interactions mediated by the presence of the suspending Newtonian fluid. Since this fluid's response is linear,

[1] Here, ρ is a constant mass density, t represents time, '$\cdot$' is the inner product, $\nabla_{\boldsymbol{r}}$ is the gradient with respect to the position $\boldsymbol{r}$, p is the pressure, μ is the (constant) dynamic viscosity, $\underline{\boldsymbol{\Delta}}_{\boldsymbol{r}}$ indicates the vector Laplacian, and $\boldsymbol{f}$ is an externally applied force per volume. Note that the explicit position and time dependence of $\boldsymbol{u}$, p, and (potentially) $\boldsymbol{f}$ have been dropped to ease notation. Also, technically, this set of equations needs to be supplemented for one that describes energy transport / temperature throughout the system and a set of boundary conditions.

[2] There are many interesting flow phenomena that can be found in our kitchen and we highly recommend the interested reader to have a look at the recent review paper "Culinary fluid mechanics and other currents in food science" by Mathijssen *et al.* [2], which gives a comprehensive overview.

the dynamics of the particles can be cast into the language of matrix-vector operations. We will introduce the first steps in setting up the theoretical framework required to do make this translation. We will also have a look at the numerical methods by which we can study such particle suspensions. Finally, we examine how active systems can be described in the language of fluid dynamics and how active particles — bacteria, man-made chemical swimmers, fish, and so on — interact with each other through the suspending fluid medium.

The nature of this course is somewhat eclectic, as flow and hydrodynamic interactions are truly ubiquitous in the description of the world around us. We will go into depth on some of the elements that underlie theory development, in particular frame transformations, while also doing justice to the broad scope of the field and its relation to applications.

A. Course Goals and Prerequisites

Throughout this course, you will be confronted with advanced vector calculus and linear algebra, and how these can be used in a modern scientific setting. We will also rely on Fourier transformations and give a (curt) nod to complex analysis. However, we will not be using the framework of field theory, as this course does *not* require knowledge of either Statistical or Quantum Field Theory. This should help make it accessible to a wider audience within the Physics Department. The focus is on analytic approaches, as well as understanding scaling and parameter relevance through dimensional analysis. However, there will also be numerical elements to the course, which help illustrate features of a few flowing systems, *e.g.*, microswimmers and other active matter. Since we generally stay away from the statistical aspects of fluid dynamics, we will also not dive deeply into the turbulent regime and how this brings together classical mechanics and statistical physics.

By the end of this lecture series, you will be able to derive basic hydrodynamic equations and perform the necessary frame transformations. You will understand how these transformations come about and what properties of a fluid give rise to certain flow behaviors. You will have familiarity with rheological analysis and understand how to characterize complex fluids. In addition, you will have become proficient in analytically solving fluid dynamical equations for (certain) complex fluids in simple geometries in the linear regime. You will also be able to solve analytically using Green's functions the behavior of (an)isotropic particles in a Newtonian fluid. Lastly, you will have a basic understanding of how microorganisms self-propel and how this influences their interaction with each other and their environment.

B. Hand-in Exercise and Exam

This course has one hand-in exercise that tests both theory and numerical aspects, with a stronger emphasis on the latter. It will count toward 30% of your final mark. The final exam will count toward the remaining 70% and will test, whether you

- have basic knowledge on rheology and the behavior of non-Newtonian fluids.
- are able to formulate (elasto)hydrodynamic equations and perform dimensional analysis on these to understand the regimes wherein non-linearities play a role.
- understand how to solve Stokes flows using Green's functions and the potential-flow formalism and understand the dynamics of suspended particles therein.
- know basic properties of wet and dry active-matter systems and how active matter and hydrodynamic theory interact.

- have been exposed to some algorithm development for solving Stokes flow problems with and without suspended particles.

Again, the final point will be tested predominantly in the hand-in exercise. A retake for the course will be offered to students who scored higher than a 5.0 on the hand-in exercise, in addition to meeting the overall requirement of a mark greater than 4.0 (and below 5.5) for the course.

C. A Brief History of Fluid Dynamics

Before we delve into the theory behind flow, it is worthwhile to give a perspective on the development of fluid dynamics. The Navier-Stokes equations, *e.g.*, see Eqs. (1) and (2), are the cumulation of centuries of experimental and theoretical effort aimed at solving the problem of describing flow. One of the oldest works on this topic stems from the first century AD, in which Sextus Julius Frontinus comments on the flow of water in aqueducts and fountains [4]. Many of the finest minds in science have worked on solving the hydrodynamic problem since the time of Frontinus, including: Torricelli, Pascal, Newton, Bernoulli, Venturi, d'Alembert, Cauchy, Poisson, Euler, Navier, and Stokes. We will not do justice to all these researchers here, but it suffices to say that flow has been and continues to be of significant interest.

Euler was the first to advance the calculus of coordinate transformations sufficiently to obtain a set of differential equations that describes flow, which was around the middle of the 18th century [5]. He showed that the equations of motion arise naturally by transforming from a co-moving to a laboratory frame. In modern mathematical language, flow may be represented by a continuous transformation of Euclidean space onto itself, parameterized by a scalar (time). This then leads to the appearance of the total derivative as a means to connect the two perspectives, though we will see that there are subtleties that were only picked up much more recently.

Euler's equations presented a major step forward for the field of fluid dynamics, however, they have one major drawback: they describe ideal fluids, *i.e.*, Eulerian fluids do not possess internal friction (viscosity). At the time, there were no experimental examples of fluids that behaved in this way and the predictions obtained from these equations were not descriptive of reality. The issue was pointed out by d'Alembert [6], who showed analytically that a falling ball does not experience friction in Euler's formalism, which became known as d'Alembert's Paradox.

From a physicist's perspective this is clearly a case of a theory that lacked predictive power and should therefore be disregarded in describing nature. However, in due time, the set of equations proposed by Euler has found its applications: the behavior of rarefied gasses subjected to adiabatic flow can be well approximated by solutions to Euler's equations [7]. More recently, the ideal-fluid description has seen a resurgence with the realization of superfluids [8], which display many of the counter-intuitive behaviors that were a cause for concern to Euler's contemporaries.

It took until 1821, before Euler's equations could be extended to describe viscous fluid flow; a challenge that was completed by Navier [9]. Navier's work was subsequently improved upon throughout the middle of the 19th century by Stokes. The resulting Navier-Stokes equations revolutionized the way physicists could describe flow phenomena, despite them being notoriously difficult to tackle analytically. They have been successfully applied in a wide range of settings, from understanding the fluid flow through tiny tubes in our body driven by ion gradients [10], to analyzing the motion of microorganisms [1, 11, 12] (see Fig. 1), optimizing the design of boats and airplanes [7], predicting the weather [13, 14], studying oceanic currents [15, 16], computing the motion of the earth's mantle and core [17], and understanding the evolution of galaxies [18].

Lastly, many generalized versions of the Navier-Stokes equations have been formulated by incorporating additional conservation laws. For example, magnetohydrodynamics combines these

equations with Maxwell's laws [19], which is relevant to the description of plasma physics, magnetism induced by the rotation of the Earth's core, and stellar dynamics. The presence of polymers can be accounted for through a second set of differential equations [20, 21].

D. Acknowledgements

These notes gather material from various sources and it is positive to acknowledge these. The continuum route toward hydrodynamic equations is based primarily on the books/notes "Complex Fluids in Biological Systems" edited by Saverio Spangolie [20]; "Microhydrodynamics: Principles and Selected Applications" by Sangtae Kim and Seppo Karrila [22]; "Fluid Mechanics" by Lev Landau and Evgeny Lífshítz [23]; "Navier-Stokes Equations: An Introduction with Applications" by Grzegorz Łukaszewicz and Piotr Kalita [24]; "Ocean Dynamics" by Dirk Olbers, Jürgen Willebrand, and Carsten Eden [25]; "Mathematical Principles of Classical Fluid Mechanics" by James Serrin [26]; "Objectivity and Objective Time Derivatives in Continuum Physics" by Franco Bampi and Antoni Morro [27], "Covariance and objectivity in mechanics and turbulence" by Michael Frewer [28]; "Polymeric Fluids" by Helen Wilson [29], and "A note about convected time derivatives for flows of complex fluids" by Howard Stone, Michael Shelley, and Evgeniy Boyko [30]. We also reproduced material and parts of the text from the papers "Hydrodynamics and phases of flocks" by John Toner, Yuhai Tu, and Sriram Ramaswamy [31], "Three-dimensional active turbulence in microswimmer suspensions: simulations and modelling" by Antonio Gascó, Ignacio Pagonabarraga, and Andrea Scagliarini [32], and "Active Turbulence" by Richard Alert, Jaume Casademunt, and Jean-François Joanny [33].

Sections of these lecture notes have been taught in the context of an *Advanced Topics in Theoretical Physics* course and as a standalone lecture for the *Dutch Research School of Theoretical Physics*. The student feedback provided during these courses has been taken into account in updating the lecture series. Lastly, some of the elements taught here rely on discussions with and the work of William Torre (Stokesian dynamics and previous TA of the course), Georg Rempfer (Fourier transformations), Alexander Morozov (slender body and resistive-force theory), Deb Panja (general discussions on the Green's function route). If you find any issues or mistakes in these notes, please let us know and we will endeavor to fix these as soon as possible.

CONTENTS

II. AN INTRODUCTION TO SIMPLE AND COMPLEX FLUIDS

In this chapter, we will consider the behavior of complex fluids, which possess a non-Newtonian response[3]. This is (roughly) equivalent to the statement that the (deviatoric) part of the stress tensor $\underline{\boldsymbol{\tau}} \neq \mu\underline{\dot{\boldsymbol{\gamma}}}$, where μ is the dynamic viscosity and $\underline{\dot{\boldsymbol{\gamma}}}$ represents the strain rate[4]. There is, however, a lot of subtlety that is obscured by this simple expression. We will start by building a bit of intuition for rheology and introducing some of the basic models, before criticizing these and pointing out the need for introducing upper-convected derivatives, as discussed in Chapter III. When we have these tools at our disposal, we will return to the topic of complex fluids in Chapter VIII.

A. Deforming Materials: The Basis for Rheology

Arguably the simplest way in which a material can be characterized is by subjecting it to shear. You have had plenty of experience with this yourself in testing the properties of various food stuffs and household products [2, 34] by rubbing them between your fingers. Let us first 'regain' this intuition and then formalize this. Imagine a solid block of foam glued between two wooden plates, see Fig. 2. You have also drawn a Cartesian coordinate frame on the block at rest and we will assume it responds linearly to small applied external forces for the sake of convenience.

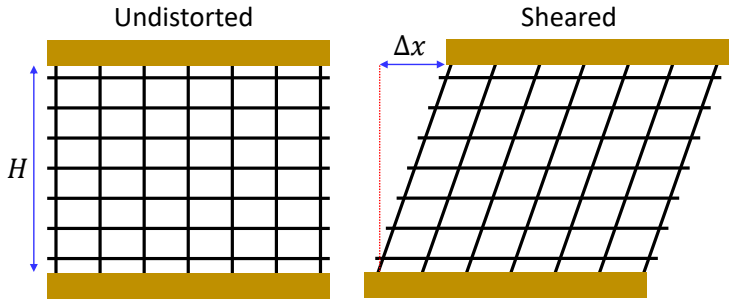

FIG. 2. **A uniform deformation applied to a linear material undergoing simple shear.** (left) A solid material between two plates (ochre) separated by a distance H is marked using a rectangular grid (black). (right) The top plate is shifted to the right by Δx, which deforms each rectangle into a parallelogram.

Applying *simple shear* to this block is equivalent to imposing a uniform deformation. For example, you could pull on both plates 'in plane' and you would find that your Carthesian squares distort uniformly to parallelograms, see Fig. 2. The level of distortion in this situation is simply given by the shift Δx divided by the height H between the plates, also known as the *shear strain* $\gamma = \Delta x/H$. The *shear stress* τ is then the force F applied to impose this shear divided by the area of the plates — it has units of pressure and is applied parallel to the plates in this situation. For convenience, we will assume that H does not change during this operation, which need not hold in practice. Applying a normal force to the block instead, will either stretch or compact it, corresponding to *tensional* or *compressional stress*, respectively. The deformation is referred to as *normal strain*. These deformations are called *elastic* when the solid returns to its original state, when the stresses are removed, and *plastic* when they are not. Solid materials often have an elastic regime of deformation followed by a plastic one and eventually fracture or rupture.

[3] The content of this chapter hybridizes elements from Refs. [20, 29].

[4] We will introduce these quantities in a more precise manner shortly. At that time, we will deal with the wide range of conventions that 'plague' the fields of fluid dynamics and rheology in greater depth. For now, bold-faced quantities are vectors and underlined bold quanties are tensors, typically 3×3 matrices in this context.

If we have a fluid, then it cannot support shear deformation like a solid. This is because the molecules would simply rearrange to accommodate the new boundary condition. It is also our experience that after applying a distortion to a cup of coffee, the spoon we used to stir does not rotate back to its original position. This is because viscous dissipation carries away the momentum we have injected into the system. To study stress in fluids, we could instead apply a constant rate of shear deformation, or *shear rate*, denoted by $\dot{\gamma}$. Referencing our solid example, simple shear can be applied by keeping the bottom plate stationary and having the top one move with a constant velocity v, such that $\dot{\gamma} = v/H$. Extensional strain may also be applied, but again for fluid we are interested in a rate of strain, rather than strain itself. In both situations, a constant stress must be applied to effect the displacement or motion, respectively.

Many modern-day rheometers operate on this principle. The measurement is either of the force required to maintain a shear rate (*controlled strain*), or of the mechanical response[5] ($\dot{\gamma}$) when a constant stress (τ) (*controlled stress*) is applied. In analyzing a material, it is commonly *initially* assumed that the relation between $\dot{\gamma}$ and τ is not dependent on the history of the system. For a Newtonian fluid we expect to find $\tau = \mu\dot{\gamma}$, where μ is the viscosity[6], *i.e.*, a straight line through the origin in a τ-$\dot{\gamma}$ plot, see Fig. 3. This is the linear stress-strain relation we alluded to in Chapter I.

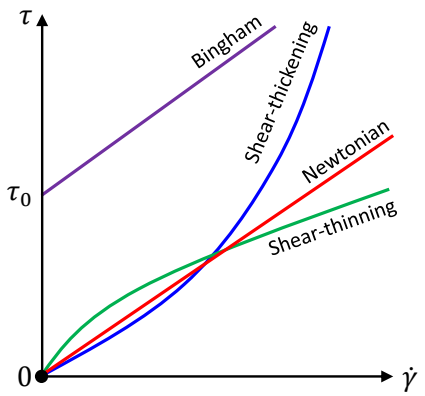

FIG. 3. **The stress / rate of shear curve for various materials.** The stress τ is graphed as a function of the shear rate $\dot{\gamma}$, showing a Newtonian (red), a shear-thinning (green), and a shear-thickening (blue) fluid-like response. The purple line shows the behavior of the Bingham model, which has a yield-stress τ_0. Figure inspired by a similar representation in Ref. [29].

When the stress increases more slowly than linearly with applied $\dot{\gamma}$ the fluid is called *shear-thinning*, while the opposite regime is called *shear-thickening*. One way of dealing with this non-linear response is to absorb the dependence on $\dot{\gamma}$ into the viscosity, thereby implying that the only effect of shear on a suspension is to change the instantaneous viscosity. In this *generalized Newtonian model*, we write $\underline{\boldsymbol{\tau}} = \mu(\dot{\gamma})\underline{\dot{\boldsymbol{\gamma}}}$. It will turn out that this approach leaves much to be desired for, as we will see in Section II C. For now, we will state that in this context $\dot{\gamma}$, which means that we work with Galilei invariant measure of the tensorial shear rate in modifying μ.

There are several historical models that take the generalized-Newtonian-model route to capture non-linearities observed in experiment. A *power-law fluid* is characterized by $\mu(\dot{\gamma}) = \mu|\dot{\gamma}|^{n-1}$, where $n = 1$ corresponds to a Newtonian response, $n > 1$ is shear thickening, and $0 < n < 1$ is

[5] Technically, this is a geometric response, as γ measures distortion.

[6] Note that in many pieces of literature the viscosity is denoted by η instead, but we will stick with our choice here. Additionally, many textbooks will use the label σ for the shear stress. Be careful in checking consistency with your own notation and interpretation, when consulting the literature! We will make things more clear in Chapter IV.

shear-thinning. A *Carreau-Yasuda fluid* is described by $\mu(\dot{\gamma}) = \mu_\infty + (\mu_0 - \mu_\infty)[1 + (\lambda\dot{\gamma})^a]^{(n-1)/a}$, where λ is a relaxation time and a sets the crossover region's size. Again for $n = 1$ the fluid is Newtonian, but here we require $0 < n \leq 1$. As the shear rate goes to zero, the viscosity reduces to μ_0 and for very high shear rates the viscosity tends to μ_∞. You can think of a suspension for which you probe the fluid + particle-induced behavior at low shear rate and predominantly the response of the suspending fluid at very high rates. The Carreau-Yasuda model has been used to describe the behavior of blood, which is shear thinning. Lastly, we consider the *Bingham model*, which is given by $\tau = \mu\dot{\gamma} + \tau_0$, whenever $\tau > \tau_0$. This model behaves like a solid below the *yield stress* τ_0, *i.e.*, it does not support a shear rate, and flows like a fluid above this yield stress. Many materials have such features, think of shaving cream, toothpaste, hummus, butter, *etc.* [34].

Exercise 1: In order to illustrate the typical features of flows of shear-thinning materials, we now consider the flow of a power-law fluid in a cylindrical pipe. We choose the cylindrical coordinate system with the z-direction along the axis of the pipe, which has radius R. The flow is assumed to be laminar[7], unidirectional, and axisymmetric, $\boldsymbol{u} = (0, 0, U(r))$.

(a) Argue that $\dot{\gamma} = |U'(r)|$ using only a *few* words, where the where the prime denotes the r-derivative. Hint: use the simple definition of a rate of distortion and symmetry.

(b) For a pressure-driven, incompressible flow of a power-law fluid in a microfluidic device, we can write

$$\nabla_{\boldsymbol{r}} \cdot \boldsymbol{u} = 0; \tag{3}$$

$$\nabla_{\boldsymbol{r}} \cdot \left(\mu|\dot{\gamma}|^{n-1}\underline{\boldsymbol{\tau}}\right) = \nabla_{\boldsymbol{r}} p, \tag{4}$$

where $\underline{\boldsymbol{\tau}}$ is the deviatoric stress in the fluid and p denotes the pressure. Show that in the pipe geometry these Stokes equations reduce

$$-\frac{\partial p}{\partial z} + \frac{1}{r}\frac{\partial}{\partial r}(r\tau_{rz}) = 0, \tag{5}$$

where the subscript indicates the relevant elements of the tensor in the cylindrical coordinates and we have

$$\tau_{rz}(r) = \mu U'(r)|U'(r)|^{n-1}. \tag{6}$$

Assume that the flow is driven by the applied constant pressure gradient $-(\partial p/\partial z) = \Delta P/L$, with L the pipe length and ΔP the pressure difference between the ends.

(c) Integrate Eq. (5) and insist that τ_{rz} remains finite on the center line, to obtain that $\tau_{rz} = -\tau_w r/R$ with τ_w the shear stress on the wall and R the radius of the pipe. Why can we call τ_w a shear stress? Explain using a *few* words only.

(d) Assume no-slip boundary conditions on the wall[8], argue that the velocity satisfies

$$\mu|U'(r)|^n = \tau_w r/R, \tag{7}$$

paying careful attention to the signs in your argument.

[7] Not turbulent, see Chapter V for additional details.
[8] The velocity of the fluid is the same as that of the wall, here zero.

(e) Integrate the equation to obtain a general expression for the pipe flow. Check your expression by verifying that you obtain a parabolic flow profile for $n = 1$. Normalize your expression by the mean pipe velocity $\bar{U}$, which is the velocity averaged over the area to obtain

$$\frac{U(r)}{\bar{U}} = \frac{3n+1}{n+1}\left[1 + \left(\frac{r}{R}\right)^{\frac{n+1}{n}}\right]. \tag{8}$$

(f) Graph this for several values of n. What do you conclude about the limit $n \downarrow 0$? Explain whether this situation is physical using a *few* words only.

B. Memory and Rheology

Thus far, we have assumed that the fluid's response to an applied stress is an instantaneous change of the shear rate, or *vice versa*. This is generally not the case, in most experimental systems there will be a memory in the response to stress. Turning back to our block of foam from Section II A, we know that even when a foam cushion returns to its original shape eventually, pressing it typically leaves an impression that stays around for a while.

For a fluid, this time dependence can be captured using the convolution of the applied shear rate with a Green's function G that accounts for relaxation

$$\tau(t) = \int_{-\infty}^{t} \mathrm{d}t'\, G(t-t')\dot{\gamma}(t'), \tag{9}$$

where the integral runs over the entire history of the fluid, which is formally denoted to start at $t = -\infty$. Note that $G(t < 0) = 0$, because the fluid cannot have knowledge of the future (*causality*). Physically, we would additionally expect $G(t)$ to decrease with increasing t, as perturbations of the material in a more distant past should contribute less. When we use $G(t) = \mu\delta(t)$, we recover the behavior of a simple fluid, and when $G(t) = G_0 =$ constant, we have an elastic solid. That is, for the latter, the stress in the material only depends on the total deformation. Other common choices involve a single-relaxation approximation $G(t) = G_0 \exp(-t/t_0)$ or a multi-relaxation approximation, which is simply a sum of exponents with different decay times and amplitudes.

Exercise 2: Let us consider a step-strain experiment to gain some insight into Eq. (9). For shear flow this means that you would set up your material between two plates and leave it to settle, so it loses the memory of the flow that put it there. Once it has had time to relax, you shear it through one shear unit (*i.e.*, until the top plate has moved a distance equal to the separation between the plates). Then you stop the shear dead. Suppose the time that you apply this shear is given by T, then the expression for the shear rate should be

$$\dot{\gamma} = \begin{cases} 0 & t < -T \\ 1/T & -T < t < 0 \\ 0 & t > 0 \end{cases}. \tag{10}$$

Compute the associated $\tau(t)$ using Eq. (9) and take the limit $T \downarrow 0$ to conclude that $\tau(t) \approx G(t)$. What do you now conclude about the physical interpretation of $G(t)$ in terms of the system's response to applied shear? Explain your answer using a *few* words.

A step-shear experiment as examined in Exercise 2 is not trivial to accomplish in any real-world device, since this would require $\dot{\gamma}(t) = \delta(t)$. Thus, to gain information about the features of $G(t)$

another form of rheology needs to be considered. In practice, oscillatory shear is applied, where the applied shear is given by $\gamma = \alpha \sin(\omega t)$ with α the amplitude[9] and ω the angular frequency. We now find that the shear rate is given by $\dot{\gamma} = \alpha\omega \cos(\omega t)$ and that the stress built up by continued oscillatory shear up to time t reads

$$\tau(t) = \alpha\omega \int_{-\infty}^{t} \mathrm{d}t'\, G(t-t') \cos(\omega t') = \alpha\omega \int_{0}^{\infty} \mathrm{d}s\, G(s) \cos(\omega(t-s)), \tag{11}$$

where the second identity follows by introducing $s = t - t'$. Writing $\cos(\omega(t-s)) = \mathsf{Re}\left[\exp(i\omega(t-s))\right]$ and realizing that $G(t)$ is real-valued, we obtain

$$\tau(t) = \alpha\omega \mathsf{Re}\left[e^{i\omega t} \int_{0}^{\infty} \mathrm{d}s\, G(s) \exp(-i\omega s)\right]. \tag{12}$$

Here, we recognize a single-sided Fourier transform, which can be readily extended to the entire integration domain (recall $G(t<0) = 0$). The convention for the *complex* shear modulus is thus

$$G^* \equiv i\omega \int_{-\infty}^{\infty} \mathrm{d}s\, G(s) \exp(-i\omega s) \equiv G' + iG'', \tag{13}$$

where we have introduced the storage modulus G' (real part) and the loss modulus G'' (complex part) of G^*. Substituting this back in the definition of $\tau(t)$, we arrive at

$$\tau(t) = G'\gamma(t) + \frac{G''}{\omega}\dot{\gamma}(t). \tag{14}$$

Exercise 3: Let us now further develop our intuition for the storage and loss modulus and use it to understand when a material is solid-like and when it is fluid-like instead.

(a) Perform the algebraic manipulations to arrive at Eq. (14) and provide expressions for G^* for a purely viscous fluid, a purely elastic solid, and a fluid with a single relaxation time t_0.

(b) Analyze the limits $\omega t_0 \ll 1$ and $\omega t_0 \gg 1$ for such a single-relaxation fluid under oscillatory shear. That is, determine how the fluid responds.

(c) Graph G' and G'' and determine the crossover point. Does your result make sense?

(d) When you are confronted with a set of G' and G'' curves for a general complex fluid, what is the criterion for identifying it as a fluid or as a solid? Explain using a *few* words.

Viscoelastic fluids are materials that exhibit both viscous and elastic responses to forces, as can be characterized in the linear-response regime via G'' and G', respectively. The shear stress created in an elastic solid obeys (for example) Hooke's law with proportionality constant G_0, while for a Newtonian fluid there is a linear relationship between shear stress and velocity gradient with proportionality constant μ. This motivates the representation of viscoelastic materials using a mechanical diagram with springs and dashpots, see Fig. 4. The simplest viscoelastic fluid is a dashpot and spring in series (Maxwell fluid), while these two elements in parallel represent a simple viscoelastic solid (Kelvin-Voight solid). Most real materials have a more complicated rheology that

[9] It is implicitly assumed that α is sufficiently small to be in the linear-response regime of the material being studied.

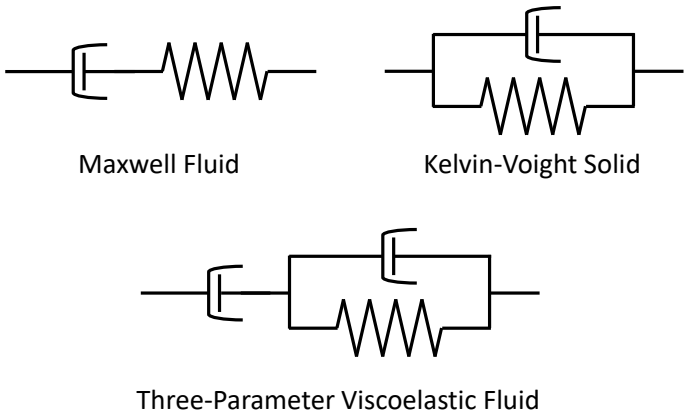

FIG. 4. **Spring-dashpot representations of viscoelastic materials.** The Maxwell fluid consists of a dashpot (left) and a spring (right) in series, while a Kelvin-Voight solid consists of these elements connected in parallel. The dashpot and spring elements can be used to create more complex mechanical diagrams, as shown for the three-parameter viscoelastic fluid, which possesses two damping rates and a single elastic relaxation time. This figure is inspired by a similar representation in Ref. [20].

requires a more involved mechanical circuit representation, with a simple example given in Fig. 4. Returning to the Maxwell fluid, this satisfies the differential equation

$$\tau + \frac{\mu}{G_0}\dot{\tau} = \mu\dot{\gamma}, \tag{15}$$

where $\lambda = \mu/G_0$ represents the time scale of relaxation. From Eq. (15) the frequency-dependent viscosity and elastic modulus are readily established, see Exercise 4. A more in-depth analysis of the rheological characterization of fluids and solids may be found in Refs. [35, 36].

Exercise 4: Let us consider the Maxwell model of Eq. (15) and determine its rheological properties.

(a) Use separation of variables to arrive at the expression $G(t-t') = (\mu/\lambda)\exp(-(t-t')/\lambda)$ in the notation of Eq. (9).

(b) Consider a shear of the form $\gamma(t) = \gamma_0 \sin\omega t$ and obtain expressions for the frequency-dependent viscosity $\mu(\omega)$ and shear modulus $G(\omega)$ by writing $\tau(\omega) = \mu(\omega)\dot{\gamma} + G(\omega)\gamma$.

(c) Examine the short- and long-time behavior of these expressions using an expansion and argue how the Maxwell model has both solid- and fluid-like properties, respectively.

(d) Look up the expression for the Kelvin-Voight model and repeat the above calculations. Does your result make sense in terms of the obtained limiting behavior?

C. Generalizing the Maxwell Model

It is tempting to generalize the Maxwell fluid to tensorial form to describe situations with flow profiles that are not captured by a scalar shear rate $\dot{\gamma}$ alone. Naively, we would assume this reads

$$\underline{\boldsymbol{\tau}} + \lambda\frac{\partial}{\partial t}\underline{\boldsymbol{\tau}} = \mu\underline{\dot{\boldsymbol{\gamma}}}, \tag{16}$$

where we have simply introduced the deviatoric stress tensor and the shear-rate tensor. There is, however, a significant problem with this naive way of working with tensors. Let us consider this here as a motivation to the introduction of frame-invariant derivatives in Chapter III.

Assume that we are performing two identical experiments on the same general Maxwell fluid, *i.e.*, one that can be described using the tensorial form of Eq. (16). One of these experiments is conducted in the stationary lab frame, and the other on a platform moving at constant velocity $\boldsymbol{u}_0$ with respect to the lab frame. The researchers in the lab frame express the stress in the moving-frame experiment as

$$\frac{\partial}{\partial t}\underline{\boldsymbol{\sigma}}(\boldsymbol{r}+\boldsymbol{u}_0 t, t) = \frac{\partial}{\partial t}\underline{\boldsymbol{\sigma}} + \boldsymbol{u}_0 \cdot \nabla_{\boldsymbol{r}}\underline{\boldsymbol{\sigma}}. \tag{17}$$

This leads to an issue. Both experiments should be described by the same equations, since a constant velocity added to each point in the fluid does not result in any velocity gradients. That is, no additional stress should be created in the fluid. However, the time derivatives differ by a term proportional to $\boldsymbol{u}_0$. Clearly, Eq. (16) is not frame-invariant and it should not be used.

Exercise 5: There are other issues with generalized models, in particular ones that have strong shear-thinning behavior. Consider a plane Couette flow (linear shear flow) of a shear-thinning fluid. The fluid is confined between two parallel plates located at $y = 0$ and $y = h$ in a two-dimensional (2D) Cartesian coordinate system $\boldsymbol{x} = (x, y)$. The base flow is given by $\boldsymbol{u}(\boldsymbol{x}) = (\dot{\gamma} y_0, 0) = (u(y), 0)$, and the equations of motion and the constitutive equation are given by

$$\rho\left(\frac{\partial}{\partial t} + \boldsymbol{u}\cdot\nabla_{\boldsymbol{x}}\right)\boldsymbol{u} = \nabla_{\boldsymbol{x}}\cdot\underline{\boldsymbol{\sigma}}; \tag{18}$$

$$\underline{\boldsymbol{\sigma}} = -p\mathbb{I}_3 + \mu(\dot{\gamma})\,\underline{\dot{\boldsymbol{\gamma}}}, \tag{19}$$

where ρ is the density, $\partial/(\partial t)$ denotes the partial derivative with respect to time t, $\nabla_{\boldsymbol{x}}$ represents the gradient operator, '$\cdot$' is the inner product, $\underline{\boldsymbol{\sigma}}$ is the stress in the fluid, p the pressure, $\mathbb{I}_3$ is the three-dimensional (3D) identity tensor, $\mu(\dot{\gamma})$ represents a generalized viscosity, and $\underline{\dot{\boldsymbol{\gamma}}}$ is the shear-rate tensor. Note that the upper wall moves with the velocity $\dot{\gamma}_0 h$ in its plane, while the lower wall is kept stationary. We will now consider an infinitesimal perturbation to the base flow profile of the form

$$\boldsymbol{u}(\boldsymbol{x}, t) = (\dot{\gamma}_0 y, 0) + (\delta u(y, t), 0), \tag{20}$$

where δu is the function that represents the small perturbation.

(a) Show that the equation of motion for the perturbation reduces to

$$\rho\frac{\partial}{\partial t}\delta u(y,t) = \frac{\partial}{\partial y}\left[\mu\left(\dot{\gamma}_0 + \frac{\partial}{\partial y}\delta u(y,t)\right)\left(\dot{\gamma}_0 + \frac{\partial}{\partial y}\delta u(y,t)\right)\right], \tag{21}$$

where the first term $\mu(\cdots)$ is read "μ as a function of the argument."

(b) Assume that the perturbation is small relative to the background shear flow and linearize Eq. (21), such that you obtain

$$\rho\frac{\partial}{\partial t}\delta u(y,t) = \left[\mu(\dot{\gamma}_0) + \dot{\gamma}_0\left.\frac{\partial\mu(x)}{\partial x}\right|_{x=\dot{\gamma}_0}\right]\frac{\partial^2}{\partial y^2}\delta u(y,t). \tag{22}$$

The no-slip boundary conditions are already satisfied by the base profile, so that the perturbation must have $\delta u(0,t) = \delta u(h,t) = 0$. Therefore, without loss of generality, the perturbation can be written as

$$\delta u(y,t) = \sum_{m=1}^{\infty} \delta u_m \exp(\alpha_m t) \sin\left(\frac{m\pi y}{h}\right), \tag{23}$$

where δu_m are expansion coefficients.

(c) Justify the expansion presented in Eq. (23) using a *few* words, referencing features of the differential equation (22) and standard analytic solving techniques.

(d) Perform the explicit substitution of Eq. (23) into Eq. (22) and obtain an expression form α_m that reads

$$\alpha_m = -\left(\frac{m\pi}{h}\right)^2 \left[\mu\left(\dot{\gamma}_0\right) + \dot{\gamma}_0 \left.\frac{\partial \mu(x)}{\partial x}\right|_{x=\dot{\gamma}_0}\right]. \tag{24}$$

(e) Now assume that the generalized viscosity adheres to the form given for a power-law fluid, *i.e.*, $\mu(\dot{\gamma}) = K\dot{\gamma}^{n-1}$. Use this power-law-fluid expression to reduce Eq. (24) further. What do you conclude about the range of stability for the power-law fluid in terms of n? Explain your answer using a *few* words.

More generally, Eq. (24) implies that any shear flow is unstable if its shear stress σ_{xy} decreases with $\dot{\gamma}$. It turns out that in dilute polymer solutions this condition is never satisfied and steady shear flows are possible for these fluids. However, linear shear flows of semi-dilute wormlike micellar solutions have been demonstrated to split into piecewise linear shear flow with regions of different shear rates [37]. This phenomenon of shear-banding is well studied and is usually attributed to the region of the flow where $\partial\sigma_{xy}/(\partial\dot{\gamma}) < 0$.

Where to next? In this chapter, we have briefly touched upon aspects of the rheology of fluids. We noted how these can have nonlinearities and time-dependence, and their response can be generally probed using G' and G'' in oscillatory shear. The way fluids respond in general is of great importance, not only to manufacturing but also in terms of identifying healthy and diseased tissues [38]. Along these lines, using non-invasive probes to measure the behavior of fluids is attracting strong attention [39]. Examples of this include the use of light to probe opaque, dense samples (optical coherence tomography), ultrasound with and without contrast agents, and even magnetic resonance imaging (μMRI). There are good opportunities for physicists to work in areas where these techniques are applied or developed, and conduct interesting research that has a positive impact on people's lives. There also remain many unanswered fundamental questions as to how microstructure and rheology are linked [34].

III. COORDINATE FRAMES AND GALILEI INVARIANCE

In this chapter, we follow the standard approach to obtaining the classic hydrodynamic transport equations in three-dimensional (3D) space, following the approach outlined in Refs. [20, 23, 27, 30]. Classical flow is described by a continuous transformation from 3D space onto itself. This implies that there are two coordinate frames, the untransformed one and the one resulting from the transformation. In physical terms, these can be identified as the co-moving and laboratory frames. Using these two frames interchangeably will facilitate the formulation of balance equations in their integral and differential form, as we will see in Chapter IV.

A. Transforming between Lagrangian and Eulerian Coordinates

There are two ways to examine a flow, one is from the perspective of an outside observer. This observer reports on flow quantities as a function of space $\boldsymbol{r}$ and time t, and their frame of reference is mapped out in *Eulerian* coordinates. Think of a person standing on the side of a riverbank looking at the water flowing past. The second is from the perspective of an observer who drifts along with the flow, but who effectively does not perturb it. This 'probe' observer reports on quantities in terms of *co-moving* or *Lagrangian* coordinates, also referred to as *material* or *referential* coordinates.

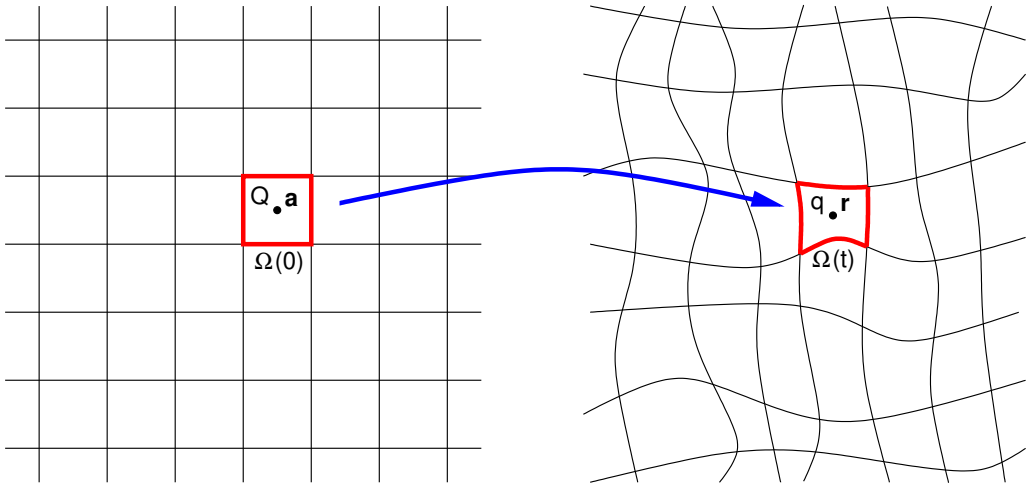

FIG. 5. **Sketch of a coordinate transform that represents flow.** A point a in the Lagrangian reference frame at time $t = 0$ is transformed under the mapping $\boldsymbol{r}(a, t)$ into the Eulerian reference frame. The coordinate transform associated with the mapping represents a flow that takes a Lagrangian volume element $\Omega(0)$ associated with the point $\boldsymbol{a}$ to its Eulerian counterpart $\Omega(t)$, as indicated by the red outlined area. The volume element does not deform for the Lagrangian observer, who reports on quantities Q, while it does for the Eulerian one, who reports on equivalent quantities labeled q. Figure inspired by Ref. [20].

We can connect the observations in both frames to each other via coordinate transformations. To do this properly, we must assume that at some point $t = 0$ we have their coordinate description coincide. This is the situation sketched in the left-hand side of Fig. 5. At some later time t, the material will have flowed. We would then expect that for the Eulerian observer, the original gridlines that were on the fluid appear distorted. Or in other words, they will see some Lagrangian observers now closer together and others further apart. Note that both the Eulerian and Lagrangian observers still measure along their own rectangular Cartesian grid. That is, the right-hand side of Fig. 5 only shows the deformation of the $t = 0$ grid due to the flow.

Now let us consider an infinitesimal[10] volume of fluid, labeled by the coordinate of its center $\boldsymbol{a}$ at time $t = 0$ in both frames, see Fig. 5. The path followed by the Lagrangian observer (fluid parcel) in the Eulerian coordinate frame is given by $\boldsymbol{r}(\boldsymbol{a}, t)$, with the property $\boldsymbol{r}(\boldsymbol{a}, 0) = \boldsymbol{a}$. We assume here that this path is continuous and sufficiently smooth, *i.e.*, the flow is physical, such that there exists the inverse $\boldsymbol{a}(\boldsymbol{r}, t)$. Note that $\boldsymbol{r}(\boldsymbol{a}, t)$ is associated with a continuous transformation of 3D space onto itself, parameterized by a scalar t (identified here as time, but this could be generalized).

The Lagrangian observer measures a scalar quantity Q on the parcel — Q could be density, energy, *etc.* — which is related to the parcel's dynamical history. The Eulerian observer can report on the same quantity, which we will denote by q to distinguish the two observers. The rate of change of the quantities Q and q on the fluid parcel are now related through the coordinate transformation

$$\frac{d}{dt}Q(\boldsymbol{a}, t) = \frac{d}{dt}q(\boldsymbol{r}(\boldsymbol{a}, t), t) = \frac{\partial}{\partial t}q(\boldsymbol{r}(\boldsymbol{a}, t), t) + \sum_{i=1}^{3}\left(\frac{\partial}{\partial p_i}q(\boldsymbol{p}, t)\bigg|_{\boldsymbol{p}=\boldsymbol{r}(\boldsymbol{a},t)}\right)\left(\frac{\partial}{\partial t}r_i(\boldsymbol{a}, t)\right). \tag{25}$$

In the first identity, we impose that the two quantities as measured by the different observers should be equal. This is fairly obvious for scalar quantities like the temperature and density, but there will be subtleties that creep in when working with vectors and tensors, see Section III B. The chain rule leads to the partial derivatives with respect to time in the second identity. On the right-hand side of Eq. (25) we recognize

$$\frac{\partial}{\partial t}r_i(\boldsymbol{a}, t) = \frac{d}{dt}r_i(\boldsymbol{a}, t) \equiv u_i(\boldsymbol{r}, t) \tag{26}$$

as the i-th component of the velocity $\boldsymbol{u}$ of the material in the Eulerian coordinate frame, which is naturally taken at the point $\boldsymbol{r}$ at time t. Note that we can transition from a partial derivative to a total derivative with respect to time in Eq. (26), because $\boldsymbol{a}$ does not depend on time. Combining Eqs. (25) and (26) we arrive at

$$\frac{d}{dt}Q(\boldsymbol{a}, t) = \left(\frac{\partial}{\partial t} + \boldsymbol{u}(\boldsymbol{r}, t)\cdot\nabla_{\boldsymbol{r}}\right)q(\boldsymbol{r}, t) \equiv \frac{D}{Dt}q(\boldsymbol{r}, t), \tag{27}$$

where '$\cdot$' denotes the inner product and $\nabla_{\boldsymbol{r}}$ the gradient with respect to position in the Eulerian frame[11]. Here, we have introduced the *material derivative* D/Dt, which is a time derivative that follows the material as it deforms (Lagrangian frame). It should be stressed that D/Dt measures the Lagrangian rate of change, which is expressed in Eulerian quantities in the center of Eq. (27). Lastly, we dropped the notation $(\boldsymbol{a}, t)$ for the position $\boldsymbol{r}$, since the relation between the two is implicit through the mapping.

Coordinate transformations impact integration domains and we require the Jacobian of these transformations to transform a Lagrangian into an Eulerian domain. We only consider the Jacobian of the forward transformation here, which is specified by

$$\underline{\boldsymbol{J}}(\boldsymbol{a}, t) = \frac{d}{d\boldsymbol{s}}\boldsymbol{r}(\boldsymbol{s}, t)\bigg|_{\boldsymbol{s}=\boldsymbol{a}}. \tag{28}$$

In Eq. (28) have taken a total derivative of a vector-valued function[12]. Introducing the determinant of the Jacobian

$$J(\boldsymbol{a}, t) = \det\left(\underline{\boldsymbol{J}}(\boldsymbol{a}, t)\right), \tag{29}$$

[10] This avoids complications in terms of finite extension of the material in Eulerian coordinates. In principle all the arguments can be made in terms of a limiting form, but here it is understood that this can always be done.

[11] Honestly, this is a lot of words and index work to arrive at a relatively sensible mathematical identity. However, it is important to recognize the connection between the two frames and what this implies for the observer in each.

[12] We avoid confusion with the material derivative here by using the mathematical notation of a total derivative: $(d\boldsymbol{x}/d\boldsymbol{r})_{ij} = \partial x_i/\partial r_j$ in index notation with $\boldsymbol{x}$ some vector-valued function depending on $\boldsymbol{r}$. Note that the material derivative is simply a total derivative with respect to time.

we have that $J(\boldsymbol{a},0) = \det(\mathbb{I}_3) = 1$ with $\mathbb{I}_3$ the 3D identity matrix. One readily finds

$$\frac{d}{dt}J(\boldsymbol{a},t) = \big(\nabla_{\boldsymbol{r}}\cdot\boldsymbol{u}(\boldsymbol{r},t)\big)\,J(\boldsymbol{a},t), \tag{30}$$

which makes sense, since the divergence of the velocity is related to the rate of change in volume. Physically, a material is volume preserving when $J(\boldsymbol{a},t) = 1$, for all $\boldsymbol{r}$ and t, such that $\nabla_{\boldsymbol{r}}\cdot\boldsymbol{u}(\boldsymbol{r},t) = 0$. When this holds, the fluid is referred to as *incompressible*.

Exercise 6: Show that Eq. (30) follows from the definition of the determinant in Eq. (29). It may help to rewrite the expressions using the Einstein summation and the Levi-Civita symbol. Alternatively, the 3D determinant can be expressed in terms of a cross and dot product of the columns comprising the total derivative.

B. Objectivity and Derivatives

Thinking in terms of a material (Lagrangian) and a laboratory (Eulerian) coordinate frame can be extremely convenient in order to derive transport equations, as we will do in Chapter IV, where we consider a simple liquid like water. However, when generalizing fluid dynamics to encompass complex fluids (*e.g.*, polymer suspensions, Oobleck, and dough), as we will consider again in Chapter VIII, we can resort to the concept of *objectivity*. That is, a constitutive equation — *e.g.*, the relation between stress and rate of strain, see Chapter II — needs to be frame independent, see Section II C for a non-objective example that highlights the need for a new type of time derivative. Let us start by building the physical intuition before solving the issue in terms of frame-invariant differential operators that act on tensors.

In classical physics, the time evolution of a scalar field is the same regardless of which observer is measuring it. In simple language, we would tend to agree that the local mass density of a small piece of the river Thames should not change, irrespective of whether someone is observing it standing on the embankment (observer #1) or cycling along the embankment at a constant speed (observer #2). It should also not change when considering this quantity from a small rubber boat that is being pulled down along with the observed piece of river into an eddy that has spontaneously formed (observer #3). Other than being needlessly dramatic, the point is that the last frame is not an inertial frame of reference, and the observer is a Lagrangian one. Section III A revealed that when taking a time derivative, the motion of the fluid needs to be taken into account, when comparing the quantity in the frames of observer #1 and #3, respectively.

There are further subtleties that crop up in this seemingly straightforward concept, when considering time derivatives of vectorial and tensorial quantities. That is, they cannot be dealt with by simply applying a material derivative to each of the components of a vector or tensor. The velocity that #3 measures, the time derivative of the displacement, will need to be corrected for the fact that this observer is rotating with respect to observer #1, when they compare notes. That is, when observer #1 sees a constant velocity vector, such as observer #2 speeding along on the embankment, observer #3 will report a velocity with a time dependence in their own coordinate frame[13]. As observer #3 is pulled further down into the eddy the coordinate frame that all observers agreed upon at time $t = 0$, is getting distorted further and further. Nonetheless, the fluid remains the same and should adhere to the same constitutive relation[14].

[13] Note that both observers do report on a vector quantity, which is the concept of *form invariance* rather than *frame indifference* and makes so much sense that it typically goes uncommented.

[14] Importantly, we cannot bypass the issue by imposing constraints on the types of observers that we work with as in classical mechanics. There, we would write down Newton's equations of motion and only deal with transformations between initial frames, which only differ from each other by a constant velocity. That is, we consider only observers #1 and #2 and ignore observer #3, for which we would otherwise have to introduce 'fictitious forces'.

The issue of taking time derivatives of tensorial quantities for describing flow was first addressed by James Oldroyd [40]. We start working toward this by first introducing the concept of *objectivity*[15]. Let $\underline{\boldsymbol{R}}(t)$ represent a rotation and $\boldsymbol{h}(t)$ a translation connecting two observers. That is, one observer reports on spatial distances and time intervals using the notation $(\boldsymbol{r}, t)$ and the other using the starred notation $(\boldsymbol{r}^*, t^*)$. We will insist that time is measured in the same (classical) way and thus $t^* = t$ from now on. If distances between points and time between events must remain the same for both observers then the most general possible transformation is $\boldsymbol{r}^* = \boldsymbol{h}(t) + \underline{\boldsymbol{R}}(t)\boldsymbol{r}$. It follows that objective vectors $\boldsymbol{q}$ transform as $\boldsymbol{q}^* = \underline{\boldsymbol{R}}(t)\boldsymbol{q}$, that is, vectors that are rotated between observers maintain their length.

Exercise 7: We will now develop our understanding of objectivity. Here, we will do so by measuring a changing distance in two frames and obtaining the velocity and acceleration.

(a) Consider two vectors $\boldsymbol{r}$ and $\boldsymbol{r}_0$. Subject these to the general transformation and show that the difference vector is objective $\boldsymbol{r}^* - \boldsymbol{r}_0^* = \underline{\boldsymbol{R}}(t)\,(\boldsymbol{r} - \boldsymbol{r}_0)$.

(b) Next, demonstrate that velocity and acceleration do not transform in an objective manner, *i.e.*, they do not transform *via* $\underline{\boldsymbol{R}}(t)$ alone.

(c) Provide the condition on the frame transformation in terms of $\boldsymbol{h}(t)$ and $\underline{\boldsymbol{R}}(t)$ under which the velocity transforms objectively. Does this requirement make physical sense?

(d) What do the additional terms you obtain for the acceleration represent physically? Explain your answer using a *few* words only, referencing your knowledge of classical mechanics.

Hint: if you cannot solve (b) and want to move on with (c) and (d) you can intuit that the extra terms should contain single time derivatives of $\underline{\boldsymbol{R}}(t)$ and $h(t)$ for the velocity and double time derivatives and mixed terms for the acceleration.

In Exercise 7, we have seen that for general distance-preserving transformations the velocity and acceleration do not transform exclusively by $\underline{\boldsymbol{R}}(t)$, *i.e.*, the time derivative of a vector does not inherit the objectivity of the original. The same holds for rank-two tensors (matrices). Let $\underline{\boldsymbol{Q}}(\boldsymbol{r}, t)$ be some time- and position-dependent matrix, then length-preservation imposes that objective tensors transform according to $\underline{\boldsymbol{Q}}^*(\boldsymbol{r}^*, t) = \underline{\boldsymbol{R}}(t)\underline{\boldsymbol{Q}}(\boldsymbol{r}, t)\underline{\boldsymbol{R}}^T(t)$. This is simply the time-dependent analogue to what you are already familiar with from linear algebra.

Exercise 8: Suppose that we have a rank-two tensor that is constructed by means of a dyadic, *i.e.*, $\underline{\boldsymbol{S}}(\boldsymbol{r}, t) = \boldsymbol{v}(\boldsymbol{r}, t) \otimes \boldsymbol{w}(\boldsymbol{r}, t)$ with $\boldsymbol{v}$ and $\boldsymbol{w}$ two vectors. For two vectors $\boldsymbol{a}$ and $\boldsymbol{b}$, the dyadic product is defined here[16] as $(\boldsymbol{a} \otimes \boldsymbol{b})_{ij} \equiv a_i b_j$. Show that the dyadic transformation has the correct form for an objective tensor, whenever both vectors transform objectively.

The above discussion of objectivity for tensors can be used to show that time-derivatives of scalar quantities are objective. Simply consider $\underline{\boldsymbol{Q}}$ as the identity matrix multiplied by a number $s(\boldsymbol{r}, t)$ and work out the definitions. This gives us $s^*(\boldsymbol{r}^*, t) = s(\boldsymbol{r}, t)$, which means that we do not pick up any time derivatives of the transformation, when taking a time derivative of s^*, which is what we intuitively understand to be the case. However, tensors, similar to vectors, typically do

[15] This is related to transformations of the Euclidean group — distance preserving transformations, such as translation, rotation, and mirroring. We shall restrict ourselves to rotations and translations here; mirroring is not allowed, which has favorable implications for the properties of the Jacobian of transformations). In mathematical language, we will work with the special Euclidean group.

[16] In the following sections, we will use vector and tensor notation, but the exercises may be simpler to solve by writing them out in index notation.

not preserve their objectivity upon time differentiation, unless we redefine these time derivatives to explicitly account for frame transformations. Consider

$$\frac{d\underline{\boldsymbol{Q}}^*}{dt} = \frac{d\underline{\boldsymbol{R}}\underline{\boldsymbol{Q}}\underline{\boldsymbol{R}}^T}{dt} = \frac{d\underline{\boldsymbol{R}}}{dt}\underline{\boldsymbol{Q}}\underline{\boldsymbol{R}}^T + \underline{\boldsymbol{R}}\frac{d\underline{\boldsymbol{Q}}}{dt}\underline{\boldsymbol{R}}^T + \underline{\boldsymbol{R}}\underline{\boldsymbol{Q}}\frac{d\underline{\boldsymbol{R}}^T}{dt}, \tag{31}$$

and realize that there is *a priori* no reason to believe that derivatives of $\underline{\boldsymbol{R}}$ with respect to time are zero for a general distance-preserving transformation (*e.g.*, a rotation).

To make the discussion more pertinent to fluid dynamics, we will consider the transformation from the Eulerian to Lagrangian coordinate frame

$$\underline{\boldsymbol{J}}(\boldsymbol{a},t) = \nabla_{\boldsymbol{p}}\boldsymbol{r}(\boldsymbol{p},t)|_{\boldsymbol{p}=\boldsymbol{a}} = \frac{d\boldsymbol{r}}{d\boldsymbol{a}}, \tag{32}$$

where we introduced the final form for notational convenience. Similarly, we can write $\underline{\boldsymbol{J}}^* = (d\boldsymbol{r}^*)/(d\boldsymbol{a})$. Referencing our definition $\boldsymbol{r}^* = \underline{\boldsymbol{R}}\boldsymbol{r} + \boldsymbol{h}$, we realize that only $\boldsymbol{r}$ can be derived with respect to $\boldsymbol{a}$; $\boldsymbol{h}$ is independent of this quantity. We conclude that $\underline{\boldsymbol{J}}^* = \underline{\boldsymbol{R}}\,\underline{\boldsymbol{J}}$, which means that the tensor $\underline{\boldsymbol{J}}$ transforms as a vector and therefore cannot have objectivity. The physical reason for this is that while Eulerian vectors may transform with $\underline{\boldsymbol{R}}$, Lagrangian ones do not. This is why we are one transformation ($\underline{\boldsymbol{R}}^T$) short of having $\underline{\boldsymbol{J}}$ transform like a tensorial quantity. We will now fix this issue by defining

$$\underline{\boldsymbol{U}}(\boldsymbol{a},t) = \frac{d\underline{\boldsymbol{J}}(\boldsymbol{a},t)}{dt}\underline{\boldsymbol{J}}^{-1}(\boldsymbol{a},t). \tag{33}$$

Exercise 9: Show that $\underline{\boldsymbol{U}}(\boldsymbol{a},t)$ corresponds to $(\nabla_{\boldsymbol{r}}\boldsymbol{u})^T$, with $\boldsymbol{u}$ the fluid velocity and $\nabla_{\boldsymbol{r}}\boldsymbol{u}$ a 3×3-tensor that represents the total derivative of the velocity. Show that in general $\underline{\boldsymbol{U}}$ is also not objective. You should arrive at

$$\underline{\boldsymbol{U}}^* = \left(\frac{d}{dt}\underline{\boldsymbol{R}}\right)\underline{\boldsymbol{R}}^T + \underline{\boldsymbol{R}}\,\underline{\boldsymbol{U}}\,\underline{\boldsymbol{R}}^T. \tag{34}$$

Introduce the notation

$$\underline{\boldsymbol{\Omega}}(t) = \frac{d\underline{\boldsymbol{R}}(t)}{dt}\underline{\boldsymbol{R}}^T(t), \tag{35}$$

for the correction factor. What does $\underline{\boldsymbol{\Omega}}(t)$ represent physically? Explain using a *few* words only.

The quantity $\underline{\boldsymbol{U}}(\boldsymbol{a},t)$ may be decomposed in a symmetric $\underline{\boldsymbol{U}}_S(\boldsymbol{a},t) = \underline{\boldsymbol{U}}(\boldsymbol{a},t) + \underline{\boldsymbol{U}}^T(\boldsymbol{a},t)$ and antisymmetric $\underline{\boldsymbol{U}}_A(\boldsymbol{a},t) = \underline{\boldsymbol{U}}(\boldsymbol{a},t) - \underline{\boldsymbol{U}}^T(\boldsymbol{a},t)$ part. We will come back to the meaning of this in Chapter IV, but for now it will suffice to know that this decomposition can be associated with deformations and rotations, respectively, of the volume elements comprising the flow. This allows us to write[17] for the decomposition $2\underline{\boldsymbol{U}}^* = \underline{\boldsymbol{U}}_S^* + \underline{\boldsymbol{U}}_A^* = \underline{\boldsymbol{R}}\left(\underline{\boldsymbol{U}}_S + \underline{\boldsymbol{U}}_A\right)\underline{\boldsymbol{R}}^{-1} + \underline{\boldsymbol{\Omega}}$. The contribution $\underline{\boldsymbol{\Omega}}$ is generally anti-symmetric, which can be seen realizing that interchanging $\underline{\boldsymbol{R}}$ and $\underline{\boldsymbol{R}}^T$ leads to a backward rotation in our example (or backward transformation in general). As there is a time derivative for only one of the $\underline{\boldsymbol{R}}$, this should lead to a change in sign between $\underline{\boldsymbol{\Omega}}(t)$ and $\underline{\boldsymbol{\Omega}}^{-1}(t)$. We also realize that the symmetry of a tensor cannot be altered by sandwiching it between $\underline{\boldsymbol{R}}$ and $\underline{\boldsymbol{R}}^T$, hence the symmetric part will behave in a frame-independent manner — it is already objective —

[17] The factor two may be absorbed into the definition of the symmetric and antisymmetric part, but we will not do so here for reasons that will become clear soon and again in Chapter IV.

and the antisymmetric part will not.

Exercise 10: Isolate the antisymmetric part of the gradient of the velocity and let $\underline{\boldsymbol{R}}$ act on this from the right. Show that you obtain

$$\frac{d\underline{\boldsymbol{R}}(t)}{dt} = \underline{\boldsymbol{U}}_A^*(\boldsymbol{a},t)\underline{\boldsymbol{R}}(t) - \underline{\boldsymbol{R}}(t)\underline{\boldsymbol{U}}_A(\boldsymbol{a},t), \tag{36}$$

and argue that therefore the antisymmetric part does not transform objectively.

Now consider an Eulerian vector field $\boldsymbol{B}(\boldsymbol{r},t)$ which is related to a Lagrangian vector field $\boldsymbol{b}(\boldsymbol{a},t)$ *via* the relation $\boldsymbol{B}(\boldsymbol{r},t) = \underline{\boldsymbol{J}}(\boldsymbol{a},t)\boldsymbol{b}(\boldsymbol{a},t)$. Taking the material derivative of $\boldsymbol{B}(\boldsymbol{r},t)$ using the above definitions, we find

$$\frac{D}{Dt}\boldsymbol{B} = \frac{D}{Dt}(\underline{\boldsymbol{J}}\boldsymbol{b}) = \left(\frac{d}{dt}\underline{\boldsymbol{J}}\right)\boldsymbol{b} + \underline{\boldsymbol{J}}\frac{d}{dt}\boldsymbol{b}. \tag{37}$$

The right-most term transforms like a vector. This is because the Lagrangian vector does not transform and the tensor $\underline{\boldsymbol{J}}$ transforms as a *vector* quantity, as we saw earlier. Turning to the first term on the right-hand side, we note that the time derivative of $\underline{\boldsymbol{J}}$ does not transform correctly. Removing the offending part, allows us to introduce the (objective) *upper-convected derivative*[18]:

$$\overset{\triangledown}{\boldsymbol{B}}(\boldsymbol{r},t) = \frac{D\boldsymbol{B}(\boldsymbol{r},t)}{Dt} - \underline{\boldsymbol{U}}(\boldsymbol{a},t)\boldsymbol{B}(\boldsymbol{r},t). \tag{38}$$

Exercise 11: Use the definitions to write Eq. (38) in a form that shows the dependence on the fluid velocity explicitly. It is important to do this, because the form in Eq. (38) can lead to confusion, due to the way $\underline{\boldsymbol{U}}$ has been defined.

It is relatively straightforward to show that the upper-convected derivative is frame independent:

$$\begin{aligned}
\left(\overset{\triangledown^*}{\boldsymbol{B}^*}\right) &= \frac{D\underline{\boldsymbol{R}}\boldsymbol{B}}{Dt} - \underline{\boldsymbol{U}}^*\underline{\boldsymbol{R}}\boldsymbol{B} = \frac{D\underline{\boldsymbol{R}}\boldsymbol{B}}{Dt} - \left(\underline{\boldsymbol{R}}\underline{\boldsymbol{U}}\underline{\boldsymbol{R}}^T + \underline{\boldsymbol{\Omega}}\right)\underline{\boldsymbol{R}}\boldsymbol{B} \\
&= \underline{\boldsymbol{R}}\frac{D\boldsymbol{B}}{Dt} + \frac{D\underline{\boldsymbol{R}}}{Dt}\boldsymbol{B} - \underline{\boldsymbol{R}}\underline{\boldsymbol{U}}\underline{\boldsymbol{R}}^T\underline{\boldsymbol{R}}\boldsymbol{B} - \underline{\boldsymbol{\Omega}}\underline{\boldsymbol{R}}\boldsymbol{B} \\
&= \underline{\boldsymbol{R}}\frac{D\boldsymbol{B}}{Dt} + \frac{D\underline{\boldsymbol{R}}}{Dt}\boldsymbol{B} - \underline{\boldsymbol{R}}\underline{\boldsymbol{U}}\boldsymbol{B} - \frac{D\underline{\boldsymbol{R}}}{Dt}\boldsymbol{B} \\
&= \underline{\boldsymbol{R}}\left(\frac{D\boldsymbol{B}}{Dt} - \underline{\boldsymbol{U}}\boldsymbol{B}\right) = \underline{\boldsymbol{R}}\,\overset{\triangledown}{\boldsymbol{B}}\,.
\end{aligned} \tag{39}$$

Considering that there is an upper-convected derivative, it would be natural to assume that there should also be a "lower-convected" derivative, which acts on the covariant vector. We will not go into this here, as lower convected derivatives are not as commonly used to describe physical transport phenomena. We recommend the interested reader to take a course on manifold theory (for physicists[19]) for more information.

---

[18] Wait! Why does the definition of the upper-convected derivative look different from the ones of other literature sources? Just have a look at Exercise 9 and you will see where the perceived difference comes from. Here, we mean by $\underline{\boldsymbol{U}}\boldsymbol{B} = \sum_k U_{ik}B_k$, which together with our result from the aforementioned exercise brings our result in line with other definitions in the literature. There is a decided lack of elegance here, but since vector notation is encountered throughout the literature, we will use it and focus instead on making you aware of its shortcomings.

[19] There is a naming convention conflict between the mathematics and physics communities regarding covariant and contravariant forms.

Before we turn to tensors, it is useful to interpret Eq. (38) physically. When we think of an infinitesimal line segment $\boldsymbol{d}$, then the expression

$$\overset{\triangledown}{\boldsymbol{d}} = \boldsymbol{0} \Rightarrow \frac{D}{Dt}\boldsymbol{d} = \underline{\boldsymbol{U}}\boldsymbol{d}, \tag{40}$$

implies that as the segment moves with the flow (D/Dt), it is rotated and stretched *via* $\underline{\boldsymbol{U}}$. However, there are no other processes by which it is changed. When we imagine such line segments to be springs that have a natural rest length, we can start to see how the deformation imposed by the fluid will lead to natural counteracting forces from objects suspended in the fluid[20]. This simple picture lies at the heart of what will govern a large class of complex fluids, *e.g.*, see Refs. [20, 29, 30, 35, 41], and we will extend it to cover tensors next.

Exercise 12: Use the definition $\underline{\boldsymbol{Q}}^*(\boldsymbol{r}^*, t) = \underline{\boldsymbol{R}}(t)\underline{\boldsymbol{Q}}(\boldsymbol{r}, t)\underline{\boldsymbol{R}}^T(t)$ to derive

$$\overset{\triangledown}{\underline{\boldsymbol{Q}}} = \frac{D\underline{\boldsymbol{Q}}}{Dt} - \underline{\boldsymbol{U}}\underline{\boldsymbol{Q}} - \underline{\boldsymbol{Q}}\underline{\boldsymbol{U}}^T. \tag{41}$$

Also show that it is a frame-invariant time derivative[21]. What is the upper-convected derivative of $\mathbb{I}_3$ and what does that tell you about this derivative?

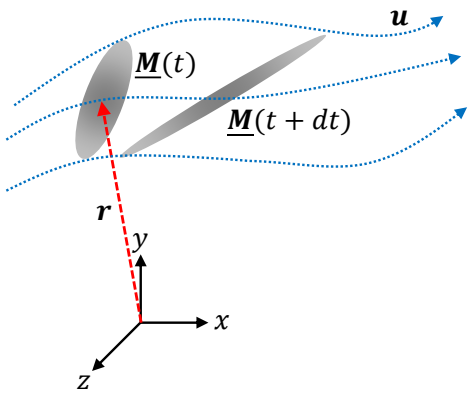

FIG. 6. **Understanding the upper-convected derivative.** Distortion of a material element (gray ellipse) due to flow (blue dotted lines), which leads to a natural definition of the upper-convected derivative for a tensor. Figure inspired by Ref. [30].

To interpret the above relation, we consider deformation of some local microstructure — think of how a suspended polymer responds to the local flow — that is measured using the reduced tensor $\underline{\boldsymbol{M}} = \langle \boldsymbol{d} \otimes \boldsymbol{d} \rangle / d_{\text{eq}}^2$. Here, the brackets denote an ensemble average and the dyadic product characterizes the state of deformation with respect to some equilibrium extent d_{eq}. If the shape of this tensor looks unfamiliar, you can think back on what you have learned for the moment-of-inertia tensor for rigid bodies. To compute this tensor, you would integrate mass-density weighted second-order terms in the coordinates, *e.g.*, $x^2 + z^2$ for the yy component of the tensor. The full set of coordinate components is given by $(x^2 + y^2 + z^2)\mathbb{I}_3 - (x, y, z) \otimes (x, y, z)$. Here, the first term measures isotropic and the second term asymmetric contributions. Thus, our microstructure the

[20] Do not be alarmed if this is still a bit nebulous at this time, we will return to the topic in Chapter VIII.
[21] Again, do not be fooled by the notation in terms of $\underline{\boldsymbol{U}}$!

tensor $\underline{\boldsymbol{M}}$ measures non-isotropic distortions of the material. Figure 6 sketches the idea of how the tensor charts distortion. Taking the material derivative of $\underline{\boldsymbol{M}}$ and using Eq. (40), we arrive at

$$\begin{aligned}\frac{D}{Dt}\underline{\boldsymbol{M}} &= \frac{D}{Dt}\frac{\langle \boldsymbol{d}\otimes\boldsymbol{d}\rangle}{d_{\mathrm{eq}}^2} = \frac{1}{d_{\mathrm{eq}}^2}\left(\left\langle\frac{D\boldsymbol{d}}{Dt}\otimes\boldsymbol{d}\right\rangle + \left\langle\boldsymbol{d}\otimes\frac{D\boldsymbol{d}}{Dt}\right\rangle\right);\\ &= \frac{1}{d_{\mathrm{eq}}^2}\left(\langle(\underline{\boldsymbol{U}}\boldsymbol{d})\otimes\boldsymbol{d}\rangle + \langle\boldsymbol{d}\otimes(\underline{\boldsymbol{U}}\boldsymbol{d})\rangle\right) = \underline{\boldsymbol{U}}\,\underline{\boldsymbol{M}} + \underline{\boldsymbol{M}}\,\underline{\boldsymbol{U}}^T,\end{aligned} \tag{42}$$

using Eq. (40). This then leads to a natural definition for the upper convected derivative, that matches that of Eq. (41). That is, one that leaves the time derivative of $\underline{\boldsymbol{M}}$ the same irrespective of the observer reporting on the constitutive relation. We will leave the topic of upper-convected derivatives for now and return to this in Chapter VIII.

Where to next? In this chapter, we have covered the Lagrangian and Eulerian perspective and introduced the notion of objectivity referencing physical examples. The latter was applied to the transformation between the Eulerian and Lagrangian frames leading to the introduction of upper-convected derivatives. The work by Bampi and Morrow [27] gives a more mathematical introduction to the concept. Frames, mappings, and transformations eventually leads into the theory of manifolds, Lie groups, Lie derivatives, *etc.* We refer any student interested in the more formal aspects of frame invariance and its consequences on the permissible forms of derivatives to a course on manifolds — preferably one with examples deriving from physics.

IV. CLASSICAL ROUTE TO HYDRODYNAMIC EQUATIONS

In this section, we follow the standard approach to obtaining the classic hydrodynamic transport equations in three-dimensional (3D) space, closely following the approach outlined in Refs. [20]. In essence, we will see that conservation of a quantity leads to a natural transport equation, an aspect that you should be familiar with for particle systems from your classical mechanics lectures. The only difference here is that we are considering continua rather than individual particles.

A. Balance Equations for Mass, Momentum, and Energy

Using the definitions in Section III A, we can now write down the basic balance equations in the Eulerian frame, which give rise to transport equations of local quantities in a natural way.

1. *Mass Conservation*

The mass $M(t)$ of a volume $\Omega(t)$ is determined by integrating the mass density $\rho(\boldsymbol{r},t)$ over this volume. When no mass is created or destroyed — a sensible condition in classical systems — we may write

$$0 = \frac{d}{dt}M(t) = \frac{d}{dt}\int_{\Omega(t)} \mathrm{d}\boldsymbol{r}\, \rho(\boldsymbol{r},t) = \frac{d}{dt}\int_{\Omega(0)} \mathrm{d}\boldsymbol{a}\, \rho(\boldsymbol{r}(\boldsymbol{a},t),t)J(\boldsymbol{a},t). \tag{43}$$

In the last equality, we transformed to the Lagrangian description to eliminate the time dependence of the control volume[22]. Now pulling the time derivative into the integral, we find

$$\begin{aligned}\frac{d}{dt}M(t) &= \int_{\Omega(0)} \mathrm{d}\boldsymbol{a} \left(\frac{D}{Dt}\rho(\boldsymbol{r}(\boldsymbol{a},t),t) + \rho(\boldsymbol{r}(\boldsymbol{a},t),t)\nabla_{\boldsymbol{r}}\cdot\boldsymbol{u}(\boldsymbol{r}(\boldsymbol{a},t),t)\right)J(\boldsymbol{a},t);\\ &= \int_{\Omega(t)} \mathrm{d}\boldsymbol{r} \left(\frac{D}{Dt}\rho(\boldsymbol{r},t) + \rho(\boldsymbol{r},t)\nabla_{\boldsymbol{r}}\cdot\boldsymbol{u}(\boldsymbol{r},t)\right) = 0.\end{aligned} \tag{44}$$

Since this holds for all volumes $\Omega(t)$, we obtain

$$\frac{D}{Dt}\rho(\boldsymbol{r},t) + \rho(\boldsymbol{r},t)\nabla_{\boldsymbol{r}}\cdot\boldsymbol{u}(\boldsymbol{r},t) = 0, \tag{45}$$

for the conservation of mass. This can be rewritten in the (more common) form

$$\frac{\partial}{\partial t}\rho(\boldsymbol{r},t) = -\nabla_{\boldsymbol{r}}\cdot\big(\rho(\boldsymbol{r},t)\boldsymbol{u}(\boldsymbol{r},t)\big). \tag{46}$$

Equation (46) implies that the density on a fluid parcel can only change through convective[23] transport from adjacent parcels, which takes the form of a mass-density flux. In the above derivation, we have seen the consequences of conservation in action: a conservation law leads to an associated transport equation when things move around.

---

[22] Note that we have sneakily omitted the absolute bars that are necessary to perform integration by substitution. This is permissible, since *physical* deformations of a fluid parcel cannot invert the sign of the volume, which is what the determinant of the Jacobian indicates and why the absolute value is taken in general. Thinking back to our discussion in Chapter III, this is why we did not permit mirroring.

[23] Convection pertains to the movement of the fluid itself, while advection describes the co-movement of a material dissolved or suspended in the fluid with the whole.

Exercise 13: Verify that $\rho(\boldsymbol{a},t)J(\boldsymbol{a},t) = \rho(\boldsymbol{a},0)$ follows from the above calculations. What does this identity imply physically? Explain using a *few* words only. Also show that when $\nabla_{\boldsymbol{r}}\left(\nabla_{\boldsymbol{r}}\cdot\boldsymbol{u}(\boldsymbol{r},t)\right) = \boldsymbol{0}$, the density as a function of time is given by

$$\rho(\boldsymbol{r},t) = \rho(\boldsymbol{a})\exp\left(-\int_0^t \mathrm{d}t'\,\nabla_{\boldsymbol{r}}\cdot\boldsymbol{u}(\boldsymbol{r},t')\right). \tag{47}$$

Here, $\rho(\boldsymbol{a})$ the density distribution of the fluid at time $t = 0$ and we have assumed a weaker condition than incompressibility. Why does this assumption need to be made? What is the implication of Eq. (47) and how does it relate to the assumptions made for our fluid parcel in Section III A?

2. *Linear and Angular Momentum Transport*

We may obtain the Cauchy equation of motion for the fluid velocity by considering the conservation of momentum and using a similar approach of exchanging integration and differentiation. However, it will turn out that this situation is more complicated than that for mass conservation. The momentum contained in the volume $\Omega(t)$ is given by

$$\boldsymbol{p}(t) = \int_{\Omega(t)}\mathrm{d}\boldsymbol{r}\,\rho(\boldsymbol{r},t)\boldsymbol{u}(\boldsymbol{r},t), \tag{48}$$

which leads to

$$\frac{d}{dt}\boldsymbol{p}(t) = \int_{\Omega(t)}\mathrm{d}\boldsymbol{r}\left(\boldsymbol{u}(\boldsymbol{r},t)\frac{D}{Dt}\rho(\boldsymbol{r},t) + \rho(\boldsymbol{r},t)\frac{D}{Dt}\boldsymbol{u}(\boldsymbol{r},t) + \rho(\boldsymbol{r},t)\boldsymbol{u}(\boldsymbol{r},t)\left(\nabla_{\boldsymbol{r}}\cdot\boldsymbol{u}(\boldsymbol{r},t)\right)\right). \tag{49}$$

This expression can be rewritten to read

$$\frac{d}{dt}\boldsymbol{p}(t) = \int_{\Omega(t)}\mathrm{d}\boldsymbol{r}\,\rho(\boldsymbol{r},t)\frac{D}{Dt}\boldsymbol{u}(\boldsymbol{r},t), \tag{50}$$

where we have canceled two of the terms using Eq. (45). In the situation where there is no internal friction and no external forces applied to the system (no sources or sinks of momentum), we may set $d\boldsymbol{p}(t)/dt = 0$ to obtain that

$$\rho(\boldsymbol{r},t)\frac{D}{Dt}\boldsymbol{u}(\boldsymbol{r},t) = \boldsymbol{0} \Rightarrow \frac{\partial}{\partial t}\boldsymbol{u}(\boldsymbol{r},t) = -\left(\boldsymbol{u}(\boldsymbol{r},t)\cdot\nabla_{\boldsymbol{r}}\right)\boldsymbol{u}(\boldsymbol{r},t), \tag{51}$$

which is nothing more than an expression of how coordinate transforms work.

The above is a rather uninteresting situation from a classical physics perspective, describing a fully frictionless fluid that is not subjected to external forces. We will need to extend the equations, because we are interested in systems that are externally perturbed, *i.e.*, $d\boldsymbol{p}(t)/dt \neq \boldsymbol{0}$. That is, we need to put in physics that drives the way the mapping evolves over time. The momentum in the control volume may change through the application of external forces $\boldsymbol{f}(\boldsymbol{r},t)$ acting on the fluid[24] and surface forces which act on the boundary of the fluid element $\partial\Omega(t)$, *i.e.*, traction forces $\boldsymbol{t}(\boldsymbol{r},t)$. Traction forces will turn out to be an expression of internal friction within the fluid.

Let $\hat{\boldsymbol{n}}(\boldsymbol{r},t)$ be the outward-pointing normal vector to the surface $\partial\Omega(t)$ of $\Omega(t)$. Then Cauchy's theorem[25] guarantees that there exists a rank-two tensor field, called the Cauchy stress tensor, that

[24] We assume $\boldsymbol{f}$ is a force density (a force per volume), rather than a external body-force density field, which is what most textbooks assume. The latter choice requires an additional multiplication with ρ to obtain the right units and is appropriate for describing gravity.

[25] We refer to Ref. [42] for a formal proof of the theorem and to Ref. [43] for an extensive discussion of its limitations in a modern materials-science context.

relates the traction to the surface normal, and this tensor is independent of the normal itself[26]: $\boldsymbol{t}(\boldsymbol{r},t) = \hat{\boldsymbol{n}}(\boldsymbol{r},t)\cdot\underline{\boldsymbol{\sigma}}(\boldsymbol{r},t)$. The stress tensor is symmetric, whenever there are no body torques acting on the fluid[27], *i.e.*, angular momentum is conserved. This assumption is sensible for the fluids that we will consider from here on out.

We add the terms, applying Newton's second law by balancing the various force contributions, thereby obtaining

$$\frac{d}{dt}\boldsymbol{p}(t) = \int_{\Omega(t)} \mathrm{d}\boldsymbol{r}\, \rho(\boldsymbol{r},t)\frac{D}{Dt}\boldsymbol{u}(\boldsymbol{r},t) = \int_{\Omega(t)} \mathrm{d}\boldsymbol{r}\, \boldsymbol{f}(\boldsymbol{r},t) + \int_{\partial\Omega(t)} \mathrm{d}\boldsymbol{s}\, \hat{\boldsymbol{n}}(\boldsymbol{s},t)\cdot\underline{\boldsymbol{\sigma}}(\boldsymbol{s},t). \tag{52}$$

The last integral is a surface integral, as indicated by the use of the integration variable $\boldsymbol{s}$. Using the divergence theorem, we may write

$$\int_{\Omega(t)} \mathrm{d}\boldsymbol{r}\, \rho(\boldsymbol{r},t)\frac{D}{Dt}\boldsymbol{u}(\boldsymbol{r},t) = \int_{\Omega(t)} \mathrm{d}\boldsymbol{r}\, \left(\boldsymbol{f}(\boldsymbol{r},t) + \nabla_{\boldsymbol{r}}\cdot\underline{\boldsymbol{\sigma}}(\boldsymbol{r},t)\right), \tag{53}$$

with $\nabla_{\boldsymbol{r}}\cdot\underline{\boldsymbol{\sigma}}(\boldsymbol{r},t)$ the three vector that has components $\sum_{j=1}^{3}\partial\sigma_{ji}/\partial r_j$, such that the momentum transport equation becomes

$$\rho(\boldsymbol{r},t)\left(\frac{\partial}{\partial t} + \boldsymbol{u}(\boldsymbol{r},t)\cdot\nabla_{\boldsymbol{r}}\right)\boldsymbol{u}(\boldsymbol{r},t) = \nabla_{\boldsymbol{r}}\cdot\underline{\boldsymbol{\sigma}}(\boldsymbol{r},t) + \boldsymbol{f}(\boldsymbol{r},t), \tag{54}$$

which is the general form of the Cauchy equation of motion for the velocity of a fluid (in differential form). Note that it is nonlinear in the fluid velocity, *i.e.*, the second term on the left-hand side, which we will come back to in Section V A.

Exercise 14: In this exercise, we will gain a better feeling for the stress tensor and its symmetries.

(a) Demonstrate that the Cauchy equation of motion can be rewritten in the following form

$$\frac{\partial}{\partial t}\left(\rho(\boldsymbol{r},t)\boldsymbol{u}(\boldsymbol{r},t)\right) = \nabla_{\boldsymbol{r}}\cdot\left(\underline{\boldsymbol{\sigma}}(\boldsymbol{r},t) - \rho(\boldsymbol{r},t)\boldsymbol{u}(\boldsymbol{r},t)\otimes\boldsymbol{u}(\boldsymbol{r},t)\right) + \boldsymbol{f}(\boldsymbol{r},t) \tag{55}$$

and explain how this form may readily be interpreted as a conservation equation.

(b) Let $\boldsymbol{H}$ be the net angular momentum in a fluid element, verify that arguments similar to the ones given above for the linear momentum lead to the differential form

$$\frac{d}{dt}\boldsymbol{H}(t) = \frac{d}{dt}\int_{\Omega(t)} \mathrm{d}\boldsymbol{r}\, \rho(\boldsymbol{r},t)\left(\boldsymbol{r}\times\boldsymbol{u}(\boldsymbol{r},t)\right) = \int_{\Omega(t)} \mathrm{d}\boldsymbol{r}\, \left(\boldsymbol{r}\times\boldsymbol{f}(\boldsymbol{r},t)\right) + \int_{\partial\Omega(t)} \mathrm{d}\boldsymbol{s}\, \left(\boldsymbol{r}\times\boldsymbol{t}(\boldsymbol{s},t)\right), \tag{56}$$

where we have introduced the cross product '×'. It should be noted that above conservation law only holds when all torques arise from macroscopic forces.

(c) Show that Eq. (56) with $d\boldsymbol{H}/dt = \boldsymbol{0}$ is equivalent to the condition that the stress tensor is symmetric. Hint: Use Green's theorem to rewrite the surface integral and move the time derivative into the integral. This will allow you to isolate a cross-product term, $\boldsymbol{r}\times$, acting on a term that includes all terms of Eq. (54), from an integral over differences in off-diagonal elements of $\underline{\boldsymbol{\sigma}}(\boldsymbol{r},t)$. The former is zero by definition, hence the stress tensor must be symmetric.

---

[26] We use the dot-product notation to relate to the standard vector-based way of writing the equations used in the literature. Admittedly, this notation is a bit awkward when index notation gives a clearer representation: $\boldsymbol{b}\cdot\underline{\boldsymbol{A}}$ may be written as $\sum_j b_j A_{ji}$ for some vector $\boldsymbol{b}$ and some rank-two tensor $\underline{\boldsymbol{A}}$. Here, it is important to realize that there is a flexibility in writing a vector acting on a stress tensor *via* the dot product, or simply having the stress tensor act on the vector $\sum_j A_{ij}b_j$, whenever this tensor is symmetric $A_{ij} = A_{ji}$. Hence, you will also see the notation $\underline{\boldsymbol{\sigma}}\hat{\boldsymbol{n}}$, which does not help with in general with the legibility of the literature.

[27] Body torques can, for example, occur when magnetic fields are applied to ferrofluids [44].

3. The Closure Relation for a Newtonian Fluid

A host of fluids can be modeled using Eq. (54) by specifying $\underline{\boldsymbol{\sigma}}(\boldsymbol{r},t)$: water, polymer suspensions, blood, corn starch, *etc.* That is, the behavior of a fluid is set by specifying a *constitutive relation*, generally in the form of an evolution equation for $\underline{\boldsymbol{\sigma}}(\boldsymbol{r},t)$, see Chapter II. This is a phenomenological approach, since general conservation principles do not have molecular details baked into them. In this section, we will only provide the closure relation for a *simple* or *Newtonian* fluid. A Newtonian fluid captures well the behavior of monoatomic media with short-ranged interactions, such as inert gases, but also water, ethanol, and many others.

We start by rewriting $\underline{\boldsymbol{\sigma}}(\boldsymbol{r},t) = -p(\boldsymbol{r},t)\mathbb{I}_3 + \underline{\boldsymbol{\tau}}(\boldsymbol{r},t)$, with $p(\boldsymbol{r},t)$ the pressure and $\underline{\boldsymbol{\tau}}(\boldsymbol{r},t)$ the deviatoric stress tensor, which contains viscous and other stresses. This rewrite does nothing more than to isolate the normal stresses from the shear stresses. The normal stresses on the diagonal are equal in the case of fluids[28] and are therefore grouped in a term that can *a posteriori* be identified as the negative of the pressure. In fact, it will turn out that for most intents and purposes the equation of state of the fluid will not be of huge importance to the discussion in these lecture notes.

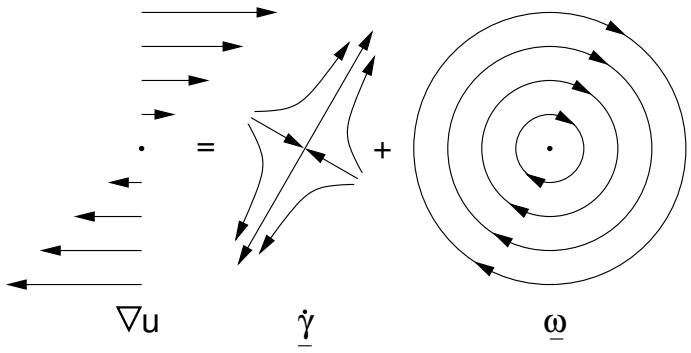

FIG. 7. **Decomposition of linear shear as extensional and rotational flow.** The variation of the flow velocity in linear shear flow, as given by $\nabla_{\boldsymbol{r}}\boldsymbol{u}(\boldsymbol{r},t)$, may be decomposed into a purely extensional component and a rotational one. The former is given by the symmetric strain-rate tensor $\underline{\dot{\boldsymbol{\gamma}}}(\boldsymbol{r},t)$ and the latter by the vorticity tensor $\underline{\boldsymbol{\omega}}(\boldsymbol{r},t)$, which represents rotations around an axis, pointing out of the plane in this case. This figure is inspired by an analogous one in Ref. [20].

The strain rate is defined as follows. If we consider a fluid velocity field $\boldsymbol{u}(\boldsymbol{r},t)$, the Taylor series of the velocity around the point $\boldsymbol{r}$ is given by

$$\boldsymbol{u}(\boldsymbol{r}+\mathrm{d}\boldsymbol{r}) = \boldsymbol{u}(\boldsymbol{r},t) + \big(\nabla_{\boldsymbol{r}}\boldsymbol{u}(\boldsymbol{r},t)\big)\,\mathrm{d}\boldsymbol{r} + \text{h.o.t.}, \tag{57}$$

where we have taken the total derivative of the velocity $\nabla_{\boldsymbol{r}}\boldsymbol{u}(\boldsymbol{r},t)$, which is a rank-two tensor that acts on the infinitesimal line segment $\mathrm{d}\boldsymbol{r}$. We now decompose the total derivative of the velocity into symmetric and anti-symmetric parts

$$\nabla_{\boldsymbol{r}}\boldsymbol{u}(\boldsymbol{r},t) \equiv \frac{1}{2}\Big(\underline{\dot{\boldsymbol{\gamma}}}(\boldsymbol{r},t) + \underline{\boldsymbol{\omega}}(\boldsymbol{r},t)\Big); \tag{58}$$

$$\underline{\dot{\boldsymbol{\gamma}}}(\boldsymbol{r},t) \equiv \big(\nabla_{\boldsymbol{r}}\boldsymbol{u}(\boldsymbol{r},t)\big) + \big(\nabla_{\boldsymbol{r}}\boldsymbol{u}(\boldsymbol{r},t)\big)^T; \tag{59}$$

$$\underline{\boldsymbol{\omega}}(\boldsymbol{r},t) \equiv \big(\nabla_{\boldsymbol{r}}\boldsymbol{u}(\boldsymbol{r},t)\big) - \big(\nabla_{\boldsymbol{r}}\boldsymbol{u}(\boldsymbol{r},t)\big)^T, \tag{60}$$

[28] Fluids cannot support (heterogeneous) loads in the same way solids can, as we already discussed in Chapter II.

with $\underline{\dot{\gamma}}(\boldsymbol{r},t)$ the strain-rate tensor[29], $\underline{\boldsymbol{\omega}}(\boldsymbol{r},t)$ the vorticity tensor, and T denoting transposition. This way of expanding the fluid field locally gives insight into the action of the two quantities that we have introduced. The strain-rate tensor indicates how a control volume is deformed, see Fig. 7. For instance, the application of a nonzero $\underline{\dot{\gamma}}(\boldsymbol{r},t)$ will transform a spherical control volume into an ellipsoid. The dot in the notation for the strain-rate tensor indicates that the variation of deformation over time is being considered[30]. The vorticity tensor gives rise to rigid-body rotations of a control volume about the axis $\boldsymbol{\omega}(\boldsymbol{r},t) = \nabla_{\boldsymbol{r}} \times \boldsymbol{u}(\boldsymbol{r},t)$, see Fig. 7. This quantity is called the *vorticity* of the fluid, and the rotation rate is equal to $\omega(\boldsymbol{r},t) = |\boldsymbol{\omega}(\boldsymbol{r},t)|$.

Exercise 15: Argue using linear algebra to show that the strain-rate tensor indeed gives rise to such deformations and that the vorticity tensor leads to rotations about the axis defined by the vorticity at a rate equal to the norm of this vector. Be mindful of pesky factors of two and have a look the footnote if you get confused by their appearance.

Returning to the closure relation, we have that $\underline{\boldsymbol{\tau}}(\boldsymbol{r},t)$ is symmetric, because we assumed conservation of angular momentum, and we know that $\underline{\dot{\gamma}}(\boldsymbol{r},t)$ is symmetric, therefore, one can directly relate these using some prefactor. Clearly, the vorticity is not going to enter the closure for a Newtonian fluid, because this would imply that angular-momentum conservation is broken. Note that this also makes sense in the context of objectivity, see Chapter III, as $\underline{\dot{\gamma}}(\boldsymbol{r},t)$ corresponds to the symmetric (and therefore objective) part of $\underline{\boldsymbol{U}}$[31]. Here, we also make the reduction that there is no relaxation involved in the evolution of the stress field, which would require us to write down a differential form for the strain-rate tensor involving convected derivatives.

It will turn out to be physically relevant to break the strain rate up into a traceless part and one that has a nonzero trace, which may have different prefactors in the closure relation. We thus introduce $(\nabla_{\boldsymbol{r}} \cdot \boldsymbol{u}(\boldsymbol{r},t))\mathbb{I}_3$ and write the *linear* stress-strain relation for an isotropic fluid as:

$$\underline{\boldsymbol{\tau}}(\boldsymbol{r},t) = \mu\left(\underline{\dot{\gamma}}(\boldsymbol{r},t) - \frac{2}{3}\left(\nabla_{\boldsymbol{r}} \cdot \boldsymbol{u}(\boldsymbol{r},t)\right)\mathbb{I}_3\right) + \mu'\left(\nabla_{\boldsymbol{r}} \cdot \boldsymbol{u}(\boldsymbol{r},t)\right)\mathbb{I}_3. \tag{61}$$

Here, the prefactor μ in front of the traceless part of $\underline{\boldsymbol{\tau}}(\boldsymbol{r},t)$ is called the *dynamic fluid viscosity*, and is a measure for internal friction or equivalently momentum diffusion, because the combination μ/ρ has the dimensionality of a diffusion constant. There will be an exercise about this in Chapter VI, where we consider the laminar flow regime. Lastly, take note of the factor of 2 in Eq. 61, this is due to our choice in defining the strain-rate tensor, also see the footnote accompanying Eq. (59).

The prefactor μ' is called the *dilatational viscosity* and is related to the level of compressibility that the medium exhibits. This can be readily understood by its pairing with the factor $\left(\nabla_{\boldsymbol{r}} \cdot \boldsymbol{u}(\boldsymbol{r},t)\right)$, which is zero in case of an incompressible medium. Lastly, note that Eq. (61) can be proven to be the most general form of a linear relation between the fluid deformation and the deviatoric stress. So not only is the expression physically relevant but covers all linear relations.

Exercise 16: We will now use the form provided in Eq. (61) to rewrite the Navier-Stokes equations. Assume that the fluid is incompressible and use this to rewrite Eq. (54) into the more familiar form given by Eq. (2).

---

[29] Unfortunately, we have reached a point of contention within the field. Why do we not add a factor of 1/2 to the definition the symmetric and antisymmetric part, rather than to Eq. (58)? In the literature, one often sees $\underline{\dot{\boldsymbol{e}}} = (1/2)\left(\nabla_{\boldsymbol{r}}\boldsymbol{u}\right) + \left(\nabla_{\boldsymbol{r}}\boldsymbol{u}\right)^T$ for the definition of the strain-rate tensor. Our reasoning is simple, if you examine the definition of the upper-convected derivative in Eq. (41) and the final part to Exercise 12, you will see that $\underline{\dot{\gamma}}$ is the object that naturally emerges by taking the upper-convected derivative of the identity tensor $\mathbb{I}_3$. This does mean that in examining the literature you should be aware that you must be careful with factors of two.

[30] Ignoring more complicated scenarios where there is a yield stress, it is clear that a fluid would relax under a rigid deformation (strain) and does not build up stress as a consequence thereof.

[31] We know $\underline{\boldsymbol{U}}$ to be equal to $\left(\nabla_{\boldsymbol{r}}\boldsymbol{u}\right)^T$ as per Exercise 9. Be mindful of the transposition!

The most interesting thing about Eq. (61) is that the prefactors[32] μ (and μ') do not depend on the density of a gas and therefore do not vary in time and space[33]. Maxwell was the first to derive this property of μ using kinetic theory and was himself highly surprised by the result, writing [45]: "*Such a consequence of the mathematical theory is very startling and the only experiment I have met with on the subject does not seem to confirm it.*" He therefore took matters into his own hands, building a device capable of measuring the viscosity and performing the experiment that confirmed his own prediction [46][34]. Historically, this provided (indirect) evidence for the existence of molecules. At that time, the molecular nature of matter had met with considerable skepticism. Unfortunately, despite Maxwell's efforts, it continued to be called into question well into the early 20th century, when the work of Perrin [48], and Geiger, Marsden, and Rutherford [49] managed to silence the last remaining protagonists of the microscopic continuum picture of matter.

4. Energy, Entropy, and Heat Transport

Let us now return to the matter at hand, establishing transport equations. We only have to deal with one more quantity, the internal energy per unit mass $\tilde{U}(\boldsymbol{r},t)$ — note that this is per mass (or equivalently per particle) rather than per volume, as the density may change over space. Energy balance is expressed in terms of the first law of thermodynamics

$$\frac{d}{dt}\int_{\Omega(t)}\mathrm{d}\boldsymbol{r}\,\rho(\boldsymbol{r},t)\left(\frac{1}{2}|\boldsymbol{u}(\boldsymbol{r},t)|^2+\tilde{U}(\boldsymbol{r},t)\right)= \int_{\Omega(t)}\mathrm{d}\boldsymbol{r}\,\boldsymbol{f}(\boldsymbol{r},t)\cdot\boldsymbol{u}(\boldsymbol{r},t)+\int_{\partial\Omega(t)}\mathrm{d}\boldsymbol{s}\,\boldsymbol{t}(\boldsymbol{s},t)\cdot\boldsymbol{u}(\boldsymbol{s},t)-\int_{\partial\Omega(t)}\mathrm{d}\boldsymbol{s}\,\boldsymbol{q}(\boldsymbol{s},t)\cdot\boldsymbol{n}(\boldsymbol{s},t). \tag{62}$$

The terms on the right-hand side of Eq. (62) represent the work done by the force density, the work done by the stress, and the total heat flux $\boldsymbol{q}(\boldsymbol{r},t)$ *into* the volume; hence the minus sign.

The two surface integrals can be recast into the following expressions using the divergence theorem

$$-\int_{\partial\Omega(t)}\mathrm{d}\boldsymbol{s}\,\boldsymbol{q}(\boldsymbol{s},t)\cdot\boldsymbol{n}(\boldsymbol{s},t)=-\int_{\Omega(t)}\mathrm{d}\boldsymbol{r}\,\nabla_{\boldsymbol{r}}\cdot\boldsymbol{q}(\boldsymbol{r},t); \tag{63}$$

$$\int_{\partial\Omega(t)}\mathrm{d}\boldsymbol{s}\,\boldsymbol{t}(\boldsymbol{s},t)\cdot\boldsymbol{u}(\boldsymbol{s},t)=\int_{\partial\Omega(t)}\mathrm{d}\boldsymbol{s}\,\left(\hat{\boldsymbol{n}}(\boldsymbol{s},t)\cdot\underline{\boldsymbol{\sigma}}(\boldsymbol{s},t)\right)\cdot\boldsymbol{u}(\boldsymbol{s},t)\quad=\int_{\Omega(t)}\mathrm{d}\boldsymbol{r}\,\nabla_{\boldsymbol{r}}\cdot\left(\underline{\boldsymbol{\sigma}}(\boldsymbol{r},t)\boldsymbol{u}(\boldsymbol{r},t)\right). \tag{64}$$

Grouping all the terms on the right-hand side of Eq. (62) gives rise to the following 'input' term for the energy transport equation

$$\boldsymbol{f}(\boldsymbol{r},t)\cdot\boldsymbol{u}(\boldsymbol{r},t)+\nabla_{\boldsymbol{r}}\cdot\left(\underline{\boldsymbol{\sigma}}(\boldsymbol{r},t)\boldsymbol{u}(\boldsymbol{r},t)-\boldsymbol{q}(\boldsymbol{r},t)\right) \tag{65}$$

Turning our attention to the left-hand side of Eq. (62), we may separate it out in an internal and kinetic term

$$\frac{D}{Dt}\left(\rho(\boldsymbol{r},t)\tilde{U}(\boldsymbol{r},t)\right)+\rho(\boldsymbol{r},t)\tilde{U}(\boldsymbol{r},t)\nabla_{\boldsymbol{r}}\cdot\boldsymbol{u}(\boldsymbol{r},t)=\rho(\boldsymbol{r},t)\frac{D}{Dt}\tilde{U}(\boldsymbol{r},t); \tag{66}$$

$$\frac{1}{2}\frac{D}{Dt}\left(\rho(\boldsymbol{r},t)|\boldsymbol{u}(\boldsymbol{r},t)|^2\right)+\frac{1}{2}\rho(\boldsymbol{r},t)|\boldsymbol{u}(\boldsymbol{r},t)|^2\nabla_{\boldsymbol{r}}\cdot\boldsymbol{u}(\boldsymbol{r},t)= \rho(\boldsymbol{r},t)\boldsymbol{u}(\boldsymbol{r},t)\cdot\left(\frac{\partial}{\partial t}\boldsymbol{u}(\boldsymbol{r},t)+\frac{1}{2}\nabla_{\boldsymbol{r}}|\boldsymbol{u}(\boldsymbol{r},t)|^2\right)=\boldsymbol{u}(\boldsymbol{r},t)\cdot\left(\nabla_{\boldsymbol{r}}\cdot\underline{\boldsymbol{\sigma}}(\boldsymbol{r},t)+\boldsymbol{f}(\boldsymbol{r},t)\right), \tag{67}$$

---

[32] In the literature, you will often find the symbol η being used for viscosity. This has the advantage that there is no confusion with particle mobility, as we will encounter in Chapter VII, which is also often denoted using the symbol μ. Check the convention that is taken, when you read a book or paper. At this point you may have become very frustrated with the state of affairs in fluid dynamics, but you should remember that this has come out of the historical developments of fields that operated in their own, isolated manner. Even basic physics is full of contradictory conventions that are similar in origin and refuse to go away.

[33] This is, of course, subject to some constraints.

[34] Anecdotally, Maxwell's wife was apparently heavily involved in the experimentation, though she was not — as was common at the time — acknowledged for her efforts [47].

respectively. Equations (66) and (67) were obtained by eliminating the mass density transport terms that result from expanding the material derivative. We employed Eq. (54) and the vector calculus identity $\nabla_{\boldsymbol{r}}|\boldsymbol{u}(\boldsymbol{r},t)|^2 = 2(\boldsymbol{u}(\boldsymbol{r},t)\cdot\nabla_{\boldsymbol{r}})\boldsymbol{u}(\boldsymbol{r},t)$ to obtain the final equality in Eq. (67). Note that this equation defines the transport of kinetic energy.

Exercise 17: Perform the necessary algebra to convince yourself of the above result. It is not a particularly insightful calculation, but you will be able to train your frame-transformation and vector-calculus skills, if they still need sharpening.

Combining the above equations results in the following form for internal energy density transport

$$\rho(\boldsymbol{r},t)\frac{D}{Dt}\tilde{U}(\boldsymbol{r},t) + \boldsymbol{u}(\boldsymbol{r},t)\cdot\left(\nabla_{\boldsymbol{r}}\cdot\underline{\boldsymbol{\sigma}}(\boldsymbol{r},t)\right) = \nabla_{\boldsymbol{r}}\cdot\left(\underline{\boldsymbol{\sigma}}(\boldsymbol{r},t)\boldsymbol{u}(\boldsymbol{r},t) - \boldsymbol{q}(\boldsymbol{r},t)\right). \tag{68}$$

Grouping terms we obtain

$$\rho(\boldsymbol{r},t)\frac{D}{Dt}\tilde{U}(\boldsymbol{r},t) = \underline{\boldsymbol{\sigma}}(\boldsymbol{r},t) : \nabla_{\boldsymbol{r}}\boldsymbol{u}(\boldsymbol{r},t) - \nabla_{\boldsymbol{r}}\cdot\boldsymbol{q}(\boldsymbol{r},t), \tag{69}$$

where ':' denotes the tensor double dot product, defined as $\underline{\boldsymbol{A}} : \underline{\boldsymbol{B}} \equiv \sum_{i=1}^{3}\sum_{j=1}^{3} A_{ij}B_{ji}$ for two tensors $\underline{\boldsymbol{A}}$ and $\underline{\boldsymbol{B}}$. There are several ways in which to contract two tensors, and it is important to examine how the double dot product is defined in another article/textbook, whenever you encounter it[35].

Surprisingly, we obtained a relatively simple expression from a fairly unpleasant calculation. Let us briefly touch upon the physical interpretation of Eq. (69). On the left-hand side, we see the familiar form of a transported time derivative for the internal energy. This form makes sense, as $\tilde{U}(\boldsymbol{r},t)$ is a scalar and its time derivative should therefore have a similar shape to that of a quantity like the density. On the right-hand side, we see that the internal energy can be modified by injecting heat into the system via $\boldsymbol{q}(\boldsymbol{r},t)$. In addition, we have the term $\underline{\boldsymbol{\sigma}}(\boldsymbol{r},t) : \nabla_{\boldsymbol{r}}\boldsymbol{u}(\boldsymbol{r},t)$, which captures internal energy dissipation. It can also be read as the trace over the matrix product between the stress and the local deformation of the fluid. Thus, the stress caused by fluid deformation multiplied by the rate of deformation itself gives rise to a local change of internal energy.

Equation (69) may be rewritten further. Note that $\nabla_{\boldsymbol{r}}\boldsymbol{u}(\boldsymbol{r},t)$ is the definition of the total derivative. We also have that $\underline{\boldsymbol{\sigma}}(\boldsymbol{r},t)$ is symmetric, hence only the symmetric part of the total derivative of the velocity will remain in taking the tensor double dot product. This is exactly the definition of the strain-rate tensor, so that

$$\rho(\boldsymbol{r},t)\frac{D}{Dt}\tilde{U}(\boldsymbol{r},t) = \underline{\boldsymbol{\sigma}}(\boldsymbol{r},t) : \underline{\dot{\boldsymbol{\gamma}}}(\boldsymbol{r},t) - \nabla_{\boldsymbol{r}}\cdot\boldsymbol{q}(\boldsymbol{r},t). \tag{70}$$

Exercise 18: Show that when the medium is incompressible and Newtonian, Eq. (70) reduces to

$$\rho(\boldsymbol{r},t)\frac{D}{Dt}\tilde{U}(\boldsymbol{r},t) = \mu\underline{\dot{\boldsymbol{\gamma}}}(\boldsymbol{r},t) : \underline{\dot{\boldsymbol{\gamma}}}(\boldsymbol{r},t) - \nabla_{\boldsymbol{r}}\cdot\boldsymbol{q}(\boldsymbol{r},t). \tag{71}$$

The interpretation of Eq. (71) is more straightforward. Here, we see that in a(n incompressible) Newtonian medium, the internal energy must increase by the dissipation in the fluid. The double dot product is also a nicely Galilei-invariant way of making $\underline{\dot{\boldsymbol{\gamma}}}(\boldsymbol{r},t)$ into a scalar.

We can now recover the heat equation by using the fundamental thermodynamic relation $\mathrm{d}U = T\mathrm{d}S - p\mathrm{d}V$ with U the internal energy, S the entropy, T the temperature, and V the volume. The

[35] For the more mathematically minded audience, you might recognize the Frobenius inner product or the Hilbert–Schmidt inner product.

local variants of the internal energy and entropy are $\tilde{U}(\boldsymbol{r},t)$ and $s(\boldsymbol{r},t)$, respectively, and these are given in terms of mass density. In this case, we may recast the combined first and second law in terms of material derivatives

$$\rho(\boldsymbol{r},t)\frac{D}{Dt}\tilde{U}(\boldsymbol{r},t) = \rho(\boldsymbol{r},t)T(\boldsymbol{r},t)\frac{D}{Dt}s(\boldsymbol{r},t) + \frac{p(\boldsymbol{r},t)}{\rho(\boldsymbol{r},t)}\frac{D}{Dt}\rho(\boldsymbol{r},t), \tag{72}$$

where we have implicitly assumed that there is no increase of internal energy *via* mass transport and introduced the local temperature $T(\boldsymbol{r},t)$. The assumption is not unreasonable as we make use of mass conservation on the control volume $\Omega(t)$ throughout our calculations. Note that this is also used to interchange the mass densities and material derivatives here.

Exercise 19: Derive Eq. (72) from the fundamental thermodynamic relation $\mathrm{d}U = T\mathrm{d}S - p\mathrm{d}V$ paying attention to assumptions made on the control volume.

Employing Eq. (45) it is possible to rewrite Eq. (72) in the following form

$$\rho(\boldsymbol{r},t)\frac{D}{Dt}\tilde{U}(\boldsymbol{r},t) = \rho(\boldsymbol{r},t)T(\boldsymbol{r},t)\frac{D}{Dt}s(\boldsymbol{r},t) - p(\boldsymbol{r},t)\nabla_{\boldsymbol{r}}\cdot\boldsymbol{u}(\boldsymbol{r},t). \tag{73}$$

Subsequently plugging this expression into Eq. (70) results in

$$\begin{aligned}\rho(\boldsymbol{r},t)T(\boldsymbol{r},t)\frac{D}{Dt}s(\boldsymbol{r},t) &= \underline{\boldsymbol{\sigma}}(\boldsymbol{r},t):\underline{\dot{\boldsymbol{\gamma}}}(\boldsymbol{r},t) + p(\boldsymbol{r},t)\nabla_{\boldsymbol{r}}\cdot\boldsymbol{u}(\boldsymbol{r},t) - \nabla_{\boldsymbol{r}}\cdot\boldsymbol{q}(\boldsymbol{r},t)\\ &= \underline{\boldsymbol{\tau}}(\boldsymbol{r},t):\underline{\dot{\boldsymbol{\gamma}}}(\boldsymbol{r},t) - \nabla_{\boldsymbol{r}}\cdot\boldsymbol{q}(\boldsymbol{r},t),\end{aligned} \tag{74}$$

through the definition of $\underline{\boldsymbol{\sigma}}(\boldsymbol{r},t)$. Next, we assume that Fourier's law of heat conduction applies: $\boldsymbol{q}(\boldsymbol{r},t) = -k(\boldsymbol{r},t)\nabla_{\boldsymbol{r}}T(\boldsymbol{r},t)$, with $k(\boldsymbol{r},t)$ the thermal conductivity. This results in the general form for entropy transport

$$\rho(\boldsymbol{r},t)T(\boldsymbol{r},t)\left(\frac{\partial}{\partial t}s(\boldsymbol{r},t) + \boldsymbol{u}(\boldsymbol{r},t)\cdot\nabla_{\boldsymbol{r}}s(\boldsymbol{r},t)\right) = \underline{\boldsymbol{\tau}}(\boldsymbol{r},t):\underline{\dot{\boldsymbol{\gamma}}}(\boldsymbol{r},t) + \nabla_{\boldsymbol{r}}\cdot\left(k(\boldsymbol{r},t)\nabla_{\boldsymbol{r}}T(\boldsymbol{r},t)\right). \tag{75}$$

In the case of an 'incompressible' medium this can be reduced further through the relations

$$T(\boldsymbol{r},t)\frac{\partial s(\boldsymbol{r},t)}{\partial t} = T(\boldsymbol{r},t)\left(\frac{\partial s(\boldsymbol{r},t)}{\partial T(\boldsymbol{r},t)}\right)_{p(\boldsymbol{r},t)}\frac{\partial T(\boldsymbol{r},t)}{\partial t} = c_p(\boldsymbol{r},t)\frac{\partial T(\boldsymbol{r},t)}{\partial t}; \tag{76}$$

$$T(\boldsymbol{r},t)\nabla_{\boldsymbol{r}}s(\boldsymbol{r},t) = T(\boldsymbol{r},t)\left(\frac{\partial s(\boldsymbol{r},t)}{\partial T(\boldsymbol{r},t)}\right)_{p(\boldsymbol{r},t)}\nabla_{\boldsymbol{r}}T(\boldsymbol{r},t) = c_p(\boldsymbol{r},t)\nabla_{\boldsymbol{r}}T(\boldsymbol{r},t), \tag{77}$$

where we have assumed that the pressure is constant and not the density to introduce the specific heat at constant pressure $c_p(\boldsymbol{r},t) = T(\boldsymbol{r},t)(\partial s(\boldsymbol{r},t)/\partial T(\boldsymbol{r},t))_{p(\boldsymbol{r},t)}$. Using these equations we finally arrive at the familiar form of the heat equation

$$\rho(\boldsymbol{r},t)c_p(\boldsymbol{r},t)\frac{D}{Dt}T(\boldsymbol{r},t) = \underline{\boldsymbol{\tau}}(\boldsymbol{r},t):\underline{\dot{\boldsymbol{\gamma}}}(\boldsymbol{r},t) + \nabla_{\boldsymbol{r}}\cdot\left(k(\boldsymbol{r},t)\nabla_{\boldsymbol{r}}T(\boldsymbol{r},t)\right). \tag{78}$$

The condition of incompressibility is used here to imply that small density variations are permitted through the temperature heterogeneity, but that pressure variations as a result of motion may be assumed small, *i.e.*, the fluid does not approach the speed of sound.

Exercise 20: Derive Eq. (78) using the above exchange of variables.

In general, one should be careful in using the term incompressible. An incompressible medium is not the same as a homogeneous incompressible medium: the mass density need not be spatially constant[36]. Incompressibility as expressed by $\nabla_{\boldsymbol{r}} \cdot \boldsymbol{u}(\boldsymbol{r},t) = 0$ is merely an observation about the volume conserving nature of the flow (the mapping). The notation in Eqs. (76) and (77) is not particularly elegant, due to the local nature of all the quantities, but as we just observed some heterogeneity must be present. In addition, we did not make assumptions about the ideality of the gas or fluid that is flowing; hence the heat capacity may be dependent on position, through the position dependence of the temperature.

B. The Hydrodynamic Transport Equations

Summarizing the above discussion, we obtain the following set of transport equations, the NS equations, for an incompressible Newtonian medium

$$\nabla_{\boldsymbol{r}} \cdot \boldsymbol{u}(\boldsymbol{r},t) = 0; \tag{79}$$

$$\frac{D}{Dt}\rho(\boldsymbol{r},t) = 0; \tag{80}$$

$$\rho(\boldsymbol{r},t)\frac{D}{Dt}\boldsymbol{u}(\boldsymbol{r},t) = -\nabla_{\boldsymbol{r}} p(\boldsymbol{r},t) + \mu \underline{\boldsymbol{\Delta}}_{\boldsymbol{r}} \boldsymbol{u}(\boldsymbol{r},t) + \boldsymbol{f}(\boldsymbol{r},t); \tag{81}$$

$$\rho(\boldsymbol{r},t)c_p(\boldsymbol{r},t)\frac{D}{Dt}T(\boldsymbol{r},t) = \mu\underline{\dot{\gamma}}(\boldsymbol{r},t) : \underline{\dot{\gamma}}(\boldsymbol{r},t) + \nabla_{\boldsymbol{r}} \cdot \left(k(\boldsymbol{r},t)\nabla_{\boldsymbol{r}} T(\boldsymbol{r},t)\right). \tag{82}$$

Here, Eq. (79) is an expression of incompressibility, Eq. (80) of mass conservation, Eq. (81) of momentum conservation, and Eq. (82) of energy conservation. Note that we have introduced the vector Laplacian[37] $\underline{\boldsymbol{\Delta}}_{\boldsymbol{r}} \equiv \mathbb{I}_3 \nabla^2_{\boldsymbol{r}}$ in Eq. (81). If the medium is also homogeneous, then $\rho(\boldsymbol{r},t)$ may be replaced by ρ_0 and we can drop Eq. (80). Lastly, one should specify the heat capacity at constant pressure and the thermal conductivity of the medium as a function of the temperature to close the system, *i.e.*, we require an equation of state.

Exercise 21: Write down the transport equations for a compressible ideal gas, taking care to rederive the associated heat equation from Eq. (75) using the appropriate assumptions for the form of the first law of thermodynamics in this case. Also comment on the implications of incompressibility for the energy, entropy, and heat transport.

Where to next? In this chapter, we have seen how conservation laws and suitably chosen terms for the input of momentum/energy give rise to the standard Navier-Stokes equations. In Chapter V, we will cover the physical regimes of flow, while in Chapter VIII, we will extend the equations to encompass non-Newtonian flow behavior. We will not cover the topic of multiphasic flows [50] in these notes, but this would be a natural (albeit challenging) extension of the above discussion. For such systems, you would need to deal with topics like (im)miscibility, phase separation, *etc.* There are approximate descriptions that work well when one of the species is dilute in the fluid medium, and these are frequently used in, for example, the field of soft matter.

---

[36] Think, for instance, about the situation wherein ocean currents with different salinities or temperatures meet. They will behave in an essentially incompressible manner, but their mass densities may differ substantially.

[37] You might wonder why these notes are so obsessed with the use of the vector Laplacian. Would a regular Laplacian not work, when applied to the individual coordinates? Indeed it would, until you forget that it looks different on each component of a vector in spherical coordinates. One day you will think back on this footnote after spending way too much time staring confused at a page, not understanding why your result does not line up with the literature. Then you will know why we do it like this here.

V. PROPERTIES OF THE HYDRODYNAMIC EQUATIONS

In this section, we cover the consequences of solving the Navier-Stokes equations for incompressible simple media, *i.e.*, fluids with a (linear) Newtonian response characterized by a single dissipation coefficient μ (the dynamic viscosity). We further impose that the mass density ρ is spatially constant, and we will drop the explicit time and position dependencies to ease notation. Then, the classical Navier-Stokes equations read

$$\nabla_{\boldsymbol{r}} \cdot \boldsymbol{u} = 0; \tag{83}$$

$$\rho\left(\frac{\partial}{\partial t} + \boldsymbol{u}\cdot\nabla_{\boldsymbol{r}}\right)\boldsymbol{u} = -\nabla_{\boldsymbol{r}} p + \mu\underline{\boldsymbol{\Delta}}_{\boldsymbol{r}}\boldsymbol{u} + \boldsymbol{f}; \tag{84}$$

$$\rho\left(\frac{\partial}{\partial t} + \boldsymbol{u}\cdot\nabla_{\boldsymbol{r}}\right)\tilde{U} = \mu\underline{\dot{\gamma}} : \underline{\dot{\gamma}} + \nabla_{\boldsymbol{r}}\cdot\left(k\nabla_{\boldsymbol{r}} T\right). \tag{85}$$

The first equation, Eq. (83), implies incompressibility of the fluid medium. Equation (84) follows from conservation of momentum. The final equation follows from a more detailed analysis of energy, entropy, and heat transport in the fluid medium, see Section IV A 4.

A. Characterizing Flow via the Reynolds Number

Singling out Eq. (84), we note that there are nonlinear terms in the fluid velocity $\boldsymbol{u}$, due to the second term on the left-hand side. One can estimate the importance of these nonlinearities by means of a dimensional analysis. We write $t = \mathsf{T}t^\star$, $\boldsymbol{r} = \mathsf{L}\boldsymbol{r}^\star$, $\boldsymbol{u} = \mathsf{U}\boldsymbol{u}^\star$, $p = \mu\mathsf{U}p^\star/\mathsf{L}$, and $\boldsymbol{f} = \mu\mathsf{U}\boldsymbol{f}^\star/\mathsf{L}^2$, where we have introduced dimensionless (starred) quantities and the following representative properties of the system: a characteristic (oscillatory) time T, length L, and speed[38] U. Expressing the momentum transport equation in terms of these parameters results in

$$\mathsf{Re}\left(\mathsf{St}\frac{\partial}{\partial t^\star} + \boldsymbol{u}^\star\cdot\nabla_{\boldsymbol{r}^\star}\right)\boldsymbol{u}^\star = -\nabla_{\boldsymbol{r}^\star} p^\star + \underline{\boldsymbol{\Delta}}_{\boldsymbol{r}^\star}\boldsymbol{u}^\star + \boldsymbol{f}^\star, \tag{86}$$

where we have introduced the Reynolds number

$$\mathsf{Re} = \frac{\rho\mathsf{U}\mathsf{L}}{\mu}, \tag{87}$$

and the Strouhal number

$$\mathsf{St} = \frac{\mathsf{L}}{\mathsf{U}\mathsf{T}}. \tag{88}$$

Exercise 22: Perform the necessary calculations to de-dimensionalize the Navier-Stokes equations and arrive at the definitions of the Reynolds and Strouhal number, respectively.

The Reynolds number is a measure for the importance of inertia in the system, compared to viscous dissipation. For a high Reynolds number, inertia dominates as represented by the time derivatives and convective transport on the left-hand side of Eq. (86), while for low Reynolds numbers, the right-hand side of the equation dominates which represents viscous effects. The

[38] It is not immediately obvious why we cannot simply introduce $U = L/T$ or equivalently write $T = L/U$. This way of introducing reducing variables is more general and will reveal an additional condition on the fluid motion.

Strouhal number is a measure for the relative importance of convective transport to temporal perturbations of the flow field with natural time scale T. For example, in systems wherein the fluid is subjected to oscillatory drive, like in a dynamic shear rheometer, the driving frequency may be such that velocity perturbations are produced on a time scale that is shorter or comparable to that of the overall dissipative transport.

When $\mathsf{Re} \ll 1$, but the combination $\mathsf{ReSt} \gtrsim 1$, the nonlinear term drops out of the Navier-Stokes equations, but the time derivative remains important. This form of the Navier-Stokes equations is sometimes referred to as the *unsteady Stokes equations*, for which the momentum transport is given by:

$$\rho \frac{\partial}{\partial t} \boldsymbol{u} = -\nabla_{\boldsymbol{r}} p + \mu \underline{\boldsymbol{\Delta}}_{\boldsymbol{r}} \boldsymbol{u} + \boldsymbol{f}. \tag{89}$$

When both $\mathsf{Re} \ll 1$ and $\mathsf{St} \lesssim 1$ viscous dissipation dominates over inertia and Eq. (86) can be approximated by the linear Stokes form

$$\mu \underline{\boldsymbol{\Delta}}_{\boldsymbol{r}} \boldsymbol{u} = \nabla_{\boldsymbol{r}} p - \boldsymbol{f}, \tag{90}$$

which describes fluid flows that are referred to as *laminar* and for which we have reinstated the dimensionful notation. Laminarity refers to a tendency of the fluid to flow in parallel layers. We will come back to this in Exercise 26. This feature can be readily observed in a setup where fluid flows through a tube and dyes are injected at various distances from the center. The streams of dye flow along with the fluid, without significant lateral mixing due to the fluid motion; they mix only through diffusion. Such experiments were carried out by Osborne Reynolds, who considered the transition from laminar to turbulent flow in a smooth pipe [51]. The turbulent regime is characterized by chaotic changes in pressure and flow velocity, resulting in significant convective mixing.

Exercise 23: Look up the characteristic quantities that describe: the motion of microscopic bacteria, human swimmers, weather patterns like a cyclone, oceanic currents, and flow in the earth's mantle, and compute their Reynolds number to determine whether the Stokes equations may be used to describe such flow or if the full Navier-Stokes equations need to be solved.

B. From Laminar to Turbulent Flow

As you have seen by completing Exercise 23, there are a few ways to obtain laminar flow. Low values of Re may be obtained by reducing the length scale and/or speed, whilst keeping the medium's properties ρ and μ constant. At very large length scales, low Re are obtained through very small speeds, incredibly high viscosities, or ultra-low densities. In our daily experience, we are typically confronted with turbulent flow, as is visualized by smoke billowing out of a chimney. The enhanced mixing that turbulence can bring about in these settings is quite desirable, as it makes the surroundings of factories relatively habitable[39].

The most striking aspect of the Reynolds number, compared to other dimensionless control parameters that you have encountered in physics thus far, is the location where the transition between turbulence and laminarity takes place. A control parameter typically assumes the value 1 roughly in the middle of the transition region between the two limiting behaviors. Through significant experimental effort in a wide range of hydrodynamic settings, it has become clear that

[39] Interestingly, this observation — turbulence facilitates mixing — has significant consequences for the way microscopic structures in our body and microorganisms have to deal with their waste management. Laminarity imposes that mixing is diffusion dominated on these length scales, but there are some clever ways to move around this condition: either by outrunning diffusion oneself, or by generating recirculating flow patterns that draw in fresh "food" and flush away waste. We will come back to this in Section VI B and Exercise 33.

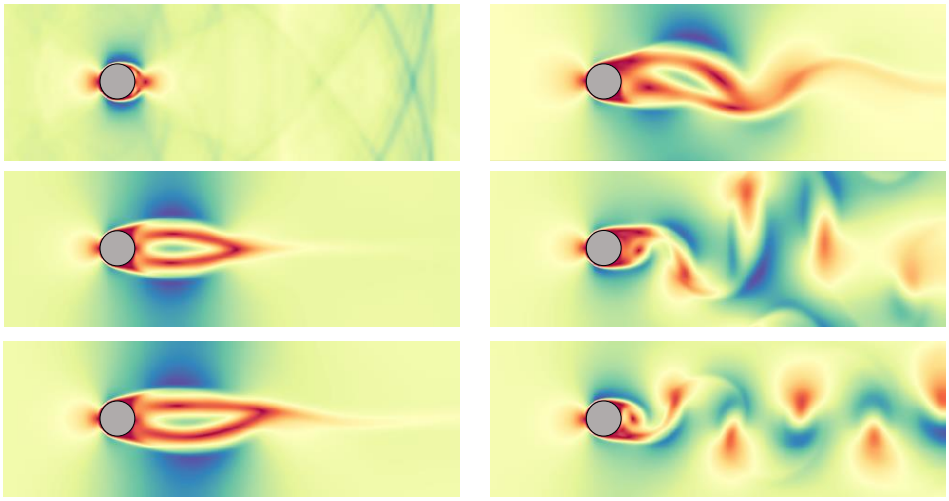

FIG. 8. **Numerical study of the development of the Kármán vortex street.** This figure shows the time evolution of a flow field around a cylindrical obstacle at $\mathsf{Re} \approx 220$. These solutions were obtained using a lattice-Boltzmann Python solver that is based on a `FlowKit` example [52]. Blue indicates regions of low and red of high fluid speed. Time increases from top to bottom and left to right. Initially, sound waves scatter off the obstacle as a result of the initial conditions of homogeneous fluid flow. Next, a symmetric set of high-velocity fluid layers form around the obstacle, of which the symmetry destabilizes and leads to the generation of a stead street of vortices being shed behind the pillar.

$\mathsf{Re} < 1$ (typically $\ll 1$) is a sufficient condition for obtaining laminar flow, but $\mathsf{Re} > 1$ is an insufficient condition to observe turbulence.

The issues with the Reynolds number are best illustrated by considering the onset of turbulence from a situation that is laminar by, *e.g.*, increasing the flow speed. For example, the Kármán vortex street, see Fig. 8, occurs when fluid flows past a cylindrical object in 3D. Deep into the laminar regime, $\mathsf{Re} \ll 1$, the profile can be computed by solving Stokes' equations using a stream-function approach, which we will return to in Chapter VII. For sufficiently high $\mathsf{Re} \leq 49$ two symmetrically placed vortices develop behind the cylinder, which comprise the wake of the flow. When the flow speed is increased further, $49 < \mathsf{Re} \lesssim 140$ to 190 [53], the recirculation region develops instabilities leading to vortices being shed behind the obstacle in a regular pattern[40]. This is what Theodore von Kármán observed experimentally [54], after whom the effect is named; although it should be noted that the effect had been observed earlier, see Refs. [55, 56]. The vortices are attributed to the thin boundary layer of fast fluid flow around the object being shed off the wake due to the instabilities. Increasing the Reynolds number further leads to an irregular pattern of vortices and eventually the onset of turbulence.

It turns out that for flow in a (very!) smooth tube with circular cross section, laminarity may be preserved up to $\mathsf{Re} \approx 2300$ [57, 58], with L chosen as the diameter of the tube and U the flow speed in the center. Turbulence sets in above $\mathsf{Re} \approx 2600$ [57, 58]. In boundary-layer flows (along a smooth plate), this number can be even higher, with turbulence setting in above $\mathsf{Re} \approx 5 \times 10^5$ [59]. This oddly high crossover in terms of the Reynolds number is found everywhere, with the critical Reynolds number having different values for every geometry considered. Numerical solutions display similar transition trends[41]. This makes it difficult to predict whether a flow is laminar or turbulent based on dimensional analysis alone and the onset of turbulence continues to be a topic

[40] This turns out to cause very specific noise in telegraph lines and can destabilize chimneys, when the eigenfrequency of structure is reached.

[41] In certain cases the laminar flow profile may be numerically maintained if no perturbations are imposed, *i.e.*, this flow can be metastable state.

of intense fundamental study today.

Exercise 24: Examine the lattice-Boltzmann Python solver in the `FlowKit` example [52]. Reproduce the image in Fig. 8 and examine lower Reynolds numbers as well. Do you obtain the expected result for near-zero Reynolds number? Explain in a few words, why you do not observe Stokes' paradox. Reproduce the other regimes reported by Williamson at lower `Re` [53].

The solution to the above issue with the Reynolds number should be sought in the emergence of a new length scale (representing the thin boundary layer), which is substantially smaller than that of the geometry. The idea is that this length scale is the one that should enter into the expression for the Reynolds number, which is then closer to 1 at the transition to turbulence. However, this is a gross oversimplification of what happens in systems on the threshold of the turbulent regime.

Where to next? In this chapter, we have seen that the separation between the linear and nonlinear regime of Newtonian flow is involved. Solving the full Navier-Stokes equations can in general be done numerically, but even that is challenging. Spectral methods[42] are one class by which (bulk) systems can be studied. For time-dependent, turbulent flows with complicated boundary conditions, it proves efficient to turn to a mesoscale description based on the Boltzmann transport equation, rather than directly solving the Navier-Stokes equations themselves by finite-element or finite-volume methods [61]. Lattice Boltzmann [62] and associated approaches such as multiparticle collision dynamics [63] also see frequent use in solving for low-Reynolds number flows. More can be done analytically in the laminar flow regime, but often numerical methods must be used, especially when the fluids become complex. We will consider analytic (and some numerical) approaches for low-Reynolds-numbers systems next.

[42] The paper introducing the computational framework Dedalus [60] offers an entry into this way of modeling.

VI. MICROHYDRODYNAMICS AND SELF-PROPELLED ORGANISMS

We now turn to the Stokes equations for a homogeneous fluid medium, for which the time-dependence of processes is such that the Strouhal number is negligible. In this chapter, we are interested in the motion of microorganisms and what the consequences are of the low-Re flow regime in which they find themselves. We repeat the two relevant equations here

$$\mu \underline{\underline{\Delta}}_{\boldsymbol{r}} \boldsymbol{u} = \nabla_{\boldsymbol{r}} p - \boldsymbol{f}; \tag{91}$$

$$\nabla_{\boldsymbol{r}} \cdot \boldsymbol{u} = 0. \tag{92}$$

Provided we do not impose significant external temperature gradients, it is permitted to ignore the energy transport equation, which is why we say "two relevant equations." This reduction is justifiable for laminar flows, since low-Re viscous dissipation does not result in significant local heating of the fluid, see Exercise 25. The system may therefore be assumed to be isothermal.

Exercise 25: Perform the dimensional analysis on Eq. (85) that is required to show that viscous dissipation results in local temperature increases that scale as $\mu \mathsf{U}^2/\mathsf{K}$, with U the typical velocity as before, and K the characteristic thermal conductivity, *i.e.*, $k = \mathsf{K}k^\star$. Find the relevant numbers for microscale motion in water and argue that low-Re systems are effectively isothermal provided there is no external heating.

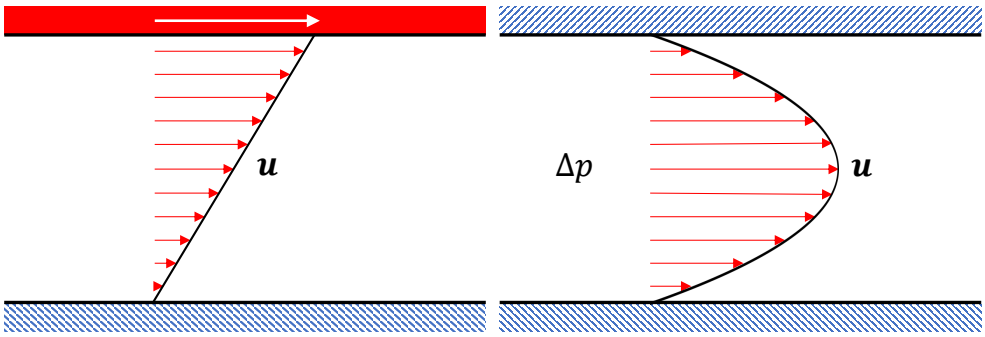

FIG. 9. **Sketches of basic geometries in which the Stokes equations may be solved analytically.** On the left Couette flow is driven by a moving plate, which leads to a linear fluid velocity profile between it and a stationary plate. The right shows the parabolic flow profile associated with pressure-driven Hagen-Poiseuille flow between two stationary plates.

Under the above conditions, we see that there are no derivatives with respect to time left in the system of equations that governs laminar flow. Time-dependent flow can be introduced into the system either via the body force $\boldsymbol{f}$ or via the boundary conditions. Despite the linearity of Eqs. (91) and (92), it is difficult to obtain analytic solutions in all but a few simple geometries. The most well-known example of an analytically solvable system is that of pressure driven flow between two parallel plates, which is called Hagen-Poiseuille flow, see the right-hand panel of Fig. 9. Here, the fluid velocity is zero on the walls and forms a parabola in the direction normal to the walls. The zero-velocity boundary condition is commonly imposed to model the interaction of a fluid with a hard wall and it manages to capture many experimental observations.

Exercise 26: Compute the velocity profile in a Hagen-Poiseuille geometry and show that the peak fluid velocity is given by $V = H^2 \Delta P/(8\mu L)$, where H is the plate separation and Δp the pressure drop over a channel of length L. Use symmetry arguments to suitably reduce Eqs. (91) and (92).

A. Achieving Motion by Irreversible Shape Changes

Elimination of the explicit time dependence from the Navier-Stokes equations in the laminar flow regime has very interesting consequences for the way self-propelled microorganisms can effect motion. Typically, $\mathsf{Re} \ll 10^{-4}$ for microswimmers and they are therefore deep in the laminar regime of fluid flow. A microswimmer and its surrounding comprise a force-free system, provided we ignore the effects of gravity[43]. The microswimmer also does not apply a body force on the fluid ($\boldsymbol{f} = \mathbf{0}$). Therefore, such an organism can only propel by changing its body shape, in much the same way that we do when we go swimming.

There is a major difference, however: we swim in the inertia dominated regime, while microorganisms cannot coast on their own momentum. Any momentum that is generated in the laminar-flow regime is instantaneously dissipated away to infinity and thus a time-wise delta-like application of force leads to negligible motion. On human length scales an analogy with swimming in honey is often made, but if you run the numbers — assuming one somehow manages to maintain the same swim speed — you would find that viscosities more in the range of pitch (a tar-like substance). Particles *can* move with a constant speed in the laminar regime, but this requires the constant application of a force, *e.g.*, gravitational sedimentation.

The dominance of viscous dissipation implies that if one reverses the arrow of time, the path followed by a microswimmer is retraced. Crucially, the speed with which you do this time reversal does not impact the retracing[44]. It is like playing back a movie at half or quarter speed, the retraced path is not affected by doing so. A further consequence is that there is no net motion when a change in boundary conditions is reciprocal in time. That is, a cyclic configurational motion that does not enclose an area in configuration space leads to zero net displacement.

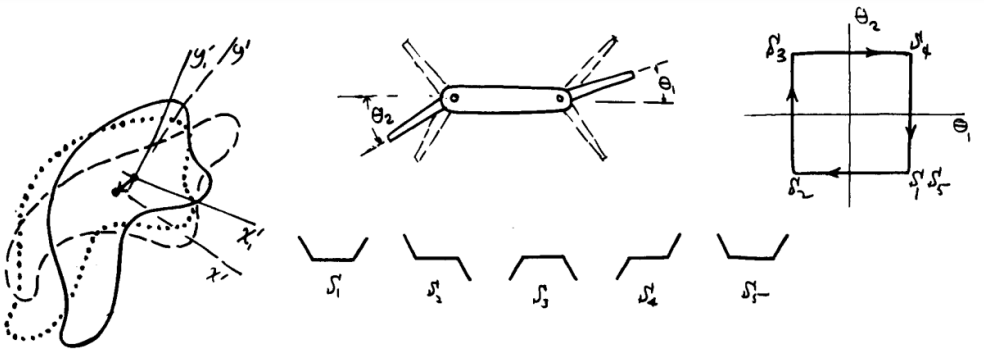

FIG. 10. **Sketches form "Life at Low Reynolds Number" by Edward Purcell.** On the left the motion of a paramecium is shown. In the middle, a double-hinged model microswimmer, which undergoes non-reciprocal actuation (bottom row). The right sketch demonstrates that this type of motion encloses an area in configurational space. Figure adapted from Ref. [12].

This was formalized by Edward Purcell[45], who considered the motion of an organism with a single hinge: a scallop. Purcell realized that the only kind of motion a scallop can achieve is reciprocal in time: it can open and close its hinge, but the speed at which it does so is irrelevant in the linear flow regime. In other words, a scallop can move just fine using inertia on our length scales, but a microscallop cannot swim. He published this observation in the lecture "Life at Low Reynolds Number" [12], see Fig. 10, and the observation has since gone under the name *Scallop Theorem*. Purcell went further to suggest a model microswimmer that had two hinges and

[43] This is often justified due to a limited density mismatch or dominance of self-propulsion over all other forces.
[44] The system must maintain a low Reynolds number to make use of the linearity of the underlying equations.
[45] Famous for sharing the 1952 Nobel Prize for Physics on the nuclear magnetic resonance in liquids and in solids.

is therefore capable of non-reciprocal motion, which formed the basis for more recent modelling efforts on microswimmers[46].

It should come as no surprise then that actual microorganisms *by necessity* employ non-reciprocal shape changes to achieve propulsion. These break the time-reversal symmetry intrinsic to the fluid and allow for directed motion. *Escherichia coli* bacteria, for instance, can have long, thin tail-like appendages, called flagella, which they spin around at a high rate [65]. These bundle together to form a cork-screw-like flagellar bundle. Because a cork screw has a chirality that breaks time-reversal symmetry, the *E. coli* can use rotation of this helical bundle to move forward. Sperm employ a similar strategy to *E. coli*, albeit typically using only a single flagellum, while *Chlamydomonas reinhardtii* algae have two "antennae" at their front, which they move in a breast-stroke like manner to self-propel [66].

B. Long-Ranged Interactions through the Fluid

As a final consequence of being immersed in a fluid medium, we will discuss hydrodynamic interactions. These are the long-ranged interactions mediated by the fluid medium. To get a feeling for this, let us consider a stream. A leaf that falls in the stream, is carried along by the flow. An object moving around in a fluid, either under the action of an external force or via self-propulsion, creates a fluid flow field around itself. Other objects in the medium are affected by this flow field, similar to the leaf in the stream. In addition, the flow field generated by a moving object can influence the motion of the object itself, when there are "obstacles" present in the system. The flow field that would be produced by the swimmer in bulk, is modified to account for the obstacles, which couples back to the motion of the swimmer itself.

We will now consider a simple model for the hydrodynamic interactions due to a swimming microorganism, in order to show how these differ from those of driven particles by virtue of the force-free condition on their motion. We will use fundamental solutions to the Stokes equations (Green's functions) in the following, which we will derive from Eqs. (91) and (92) first. Then, we will construct a simple flow field description for a swimming microorganism from the Stokeslet solutions that describe a situation where a point-force is applied to the fluid.

Without loss of generality, we assume that the body force is given by a point force $\tilde{\boldsymbol{f}}$ located at the origin $\boldsymbol{f}(\boldsymbol{r}) = \tilde{\boldsymbol{f}}\delta(\boldsymbol{r})$, with $\delta(\boldsymbol{r})$ the Dirac delta distribution. In that case, $\boldsymbol{r}$ is the point in the fluid where we want to determine the velocity. We take the divergence of Eq. (91) and use incompressibility to obtain

$$\nabla \cdot \left(-\nabla p(\boldsymbol{r}) + \mu \underline{\boldsymbol{\Delta}} \boldsymbol{u}(\boldsymbol{r})\right) = -\nabla \cdot \tilde{\boldsymbol{f}}\delta(\boldsymbol{r}) \Rightarrow \nabla^2 p(\boldsymbol{r}) = \tilde{\boldsymbol{f}} \cdot \nabla\delta(\boldsymbol{r}). \tag{93}$$

Next, we define the Fourier transform of a function ϕ and its inverse as

$$\check{\phi}(\boldsymbol{k}) \equiv \int_{\mathbb{R}^3} \mathrm{d}\boldsymbol{r}\, e^{-i\boldsymbol{k}\cdot\boldsymbol{r}}\phi(\boldsymbol{r}), \qquad \phi(\boldsymbol{r}) \equiv \frac{1}{(2\pi)^3}\int_{\mathbb{R}^3} \mathrm{d}\boldsymbol{k}\, e^{i\boldsymbol{k}\cdot\boldsymbol{r}}\check{\phi}(\boldsymbol{k}), \tag{94}$$

respectively, with i the imaginary unit. Here, we use the "check" symbol for the Fourier transform to avoid confusion with the standard "hat" notation for normalized vectors. Applying the Fourier transform (94), we obtain

$$-k^2\check{p}(\boldsymbol{k}) = i\boldsymbol{k}\cdot\tilde{\boldsymbol{f}} \Rightarrow \check{p}(\boldsymbol{k}) = -i\frac{\hat{\boldsymbol{k}}}{k}\cdot\tilde{\boldsymbol{f}}. \tag{95}$$

[46] The most well-known variant is the three-bead swimmer by Ali Najafi and Ramin Golestanian, which uses non-reciprocal actuation to achieve forward motion at low Reynolds numbers [64].

Note that $\check{p}$ is parallel to the $\hat{\boldsymbol{k}}$ vector[47]. The next step is to Fourier transform the Stokes equation (91) to obtain

$$-i\boldsymbol{k}\check{p}(\boldsymbol{k}) - \mu k^2 \check{\boldsymbol{u}}(\boldsymbol{k}) = -\tilde{\boldsymbol{f}} \Rightarrow \check{\boldsymbol{u}}(\boldsymbol{k}) = \frac{1}{\mu k^2}\left(\mathbb{I}_3 - \hat{\boldsymbol{k}}\otimes\hat{\boldsymbol{k}}\right)\tilde{\boldsymbol{f}}. \tag{96}$$

Exercise 27: Derive Eq. (96) and provide a physical interpretation for the final form. Why is it important to have incompressibility in taking the Fourier-based route?

The above results in the following expression for the velocity field and pressure using the inverse Fourier transform

$$\boldsymbol{u}(\boldsymbol{r}) = \frac{1}{(2\pi)^3}\int_{\mathbb{R}^3} \mathrm{d}\boldsymbol{k}\, e^{i\boldsymbol{k}\cdot\boldsymbol{r}} \frac{1}{\mu k^2}\left(\mathbb{I}_3 - \hat{\boldsymbol{k}}\otimes\hat{\boldsymbol{k}}\right)\tilde{\boldsymbol{f}}; \tag{97}$$

$$p(\boldsymbol{r}) = -i\frac{1}{(2\pi)^3}\int_{\mathbb{R}^3} \mathrm{d}\boldsymbol{k}\, e^{i\boldsymbol{k}\cdot\boldsymbol{r}} \frac{\hat{\boldsymbol{k}}\cdot\tilde{\boldsymbol{f}}}{k}. \tag{98}$$

Using the properties of the harmonic and biharmonic fundamental solutions, see, *e.g.*, Ref. [67, 68] for additional details, one recovers

$$\boldsymbol{u}(\boldsymbol{r}) = \frac{1}{8\pi\mu r}\left(\mathbb{I}_3 + \hat{\boldsymbol{r}}\otimes\hat{\boldsymbol{r}}\right)\tilde{\boldsymbol{f}} \equiv \frac{1}{8\pi\mu}\underline{\boldsymbol{S}}(\boldsymbol{r})\tilde{\boldsymbol{f}}, \tag{99}$$

with

$$\underline{\boldsymbol{S}}(\boldsymbol{r}) = \frac{1}{r}\left(\mathbb{I}_3 + \hat{\boldsymbol{r}}\otimes\hat{\boldsymbol{r}}\right), \tag{100}$$

where Eqs. (99) and (100) introduce the fundamental solution known as the Stokeslet $\underline{\boldsymbol{S}}(\boldsymbol{r})$. The important aspect to take away from the above is the long-ranged nature of fundamental solution, which has a $1/r$ decay. This implies that any interactions between particles that are caused by their movement in a fluid will need to be treated with care. For example, in a periodic simulation volume, Ewald summation needs to be employed [69].

Exercise 28: This exercise aims to ensure you understand the above procedure for obtaining the fundamental solution.

(a) Perform the computational steps to obtain the fundamental solution for a point force acting on an incompressible Newtonian medium at zero Reynolds number.

(b) Argue physically why flow induced by a point-force is characterized by a pinching of the fluid around the point where the force acts and graph the streamlines to the Stokeslet.

(c) Show that the expression for the pressure is

$$p(\boldsymbol{r}) = \frac{\hat{\boldsymbol{r}}}{4\pi r^2}\cdot\tilde{\boldsymbol{f}}, \tag{101}$$

and identify the relevant Green's function. It should look familiar, explain using a *few* words.

[47] This is an expression of the fact that the pressure acts as a Lagrange multiplier to impose incompressibility on the (Navier-)Stokes equations. That is, it accounts for there being four equations with only three parameters in terms of the velocity vector components. Or, in other words, in Fourier space $\check{p}$ is generated by that part of the force that lies along $\hat{\boldsymbol{k}}$.

We will return to the shape of the pressure equation in Chapter VII.

Exercise 29: In this exercise, we will consider microhydrodynamic Green's functions and the method of images to capture the presence of a no-slip wall. You will have encountered this approach in a basic electrostatics course, but the vectorial nature of fluid dynamics leads to several complications. Consider a flat no-slip (zero velocity) boundary coinciding with the xy-plane and a point force $\boldsymbol{F}$ applied to an incompressible Newtonian fluid at a height h above the origin. Assume throughout that this fluid is well-described by the Stokes equations.

(a) Use the Stokeslet to show that an oppositely directed force in a point reflected in the wall (at $z = -h$) does not give rise to the desired hydrodynamic boundary condition. Provide the physical intuition for this using only a *few* words.

(b) The following image convention corresponds to a valid hydrodynamic boundary condition, though not quite the desired no-slip one. Let the reflection point be located at $z = -h$, but only the z-component of the force applied in the reflection point $\boldsymbol{F}^*$ is flipped with respect to $\boldsymbol{F}$: $\boldsymbol{F}^* = (F_x, F_y, -F_z)$, where the subscripts indicate the Cartesian components of the original $\boldsymbol{F}$. Show that the z-component of the flow is indeed zero for this boundary condition. What is the effect of the wall on the velocity in the xy-plane? Compute the strain-rate tensor. What is the implication for traction (and thus friction) experienced at this boundary?

Deriving the form of the hydrodynamic tensor for the image is not trivial, so we provide it here. This tensor is most commonly attributed to Blake, who gave the form for two specific orientations [70]: a force directed parallel and perpendicular to the wall[48]. We introduce the following notation

$$\boldsymbol{r} = \begin{pmatrix} x \\ y \\ z \end{pmatrix}; \quad \boldsymbol{r}_{\mathrm{F}} = \begin{pmatrix} 0 \\ 0 \\ h \end{pmatrix}; \quad \boldsymbol{r}_{\mathrm{I}} = \begin{pmatrix} 0 \\ 0 \\ -h \end{pmatrix}; \quad \boldsymbol{R} = \boldsymbol{r} - \boldsymbol{r}_{\mathrm{I}}; \quad R = |\boldsymbol{R}|; \quad \underline{\boldsymbol{M}} = \begin{pmatrix} 1 & 0 & 0 \\ 0 & 1 & 0 \\ 0 & 0 & -1 \end{pmatrix};$$

which from left to right specifies: the point in the fluid $\boldsymbol{r}$, the point where the force is applied $\boldsymbol{r}_{\mathrm{F}}$, the image point $\boldsymbol{r}_{\mathrm{I}}$, the separation between fluid and image point, the corresponding length, and a reflection matrix. The Blake tensor for a force $\boldsymbol{F}$ acting on the fluid at a point $\boldsymbol{r}$ is now reads [72]:

$$\boldsymbol{u}_{\mathrm{I}}(\boldsymbol{R}) = \underline{\boldsymbol{S}}_{\mathrm{I}}(\boldsymbol{R})\boldsymbol{F}; \tag{102}$$

$$\underline{\boldsymbol{S}}_{\mathrm{I}}(\boldsymbol{R}) = -\underline{\boldsymbol{S}}_{\mathrm{O}}(\boldsymbol{R}) + \underline{\boldsymbol{S}}_{\mathrm{D}}(\boldsymbol{R}) - \underline{\boldsymbol{S}}_{\mathrm{SD}}(\boldsymbol{R}); \tag{103}$$

$$\underline{\boldsymbol{S}}_{\mathrm{O}}(\boldsymbol{R}) = \frac{1}{8\pi\mu R}\left(\mathbb{I}_3 + \hat{\boldsymbol{R}} \otimes \hat{\boldsymbol{R}}\right); \tag{104}$$

$$\underline{\boldsymbol{S}}_{\mathrm{D}}(\boldsymbol{R}) = \frac{2h^2}{8\pi\mu R^3}\left(\mathbb{I}_3 - 3\hat{\boldsymbol{R}} \otimes \hat{\boldsymbol{R}}\right)\underline{\boldsymbol{M}}; \tag{105}$$

$$\underline{\boldsymbol{S}}_{\mathrm{SD}}(\boldsymbol{R}) = \frac{2h}{8\pi\mu R^3}\left(\hat{\boldsymbol{R}} \otimes \hat{\boldsymbol{z}} - \hat{\boldsymbol{z}} \otimes \hat{\boldsymbol{R}}\right)\underline{\boldsymbol{M}} + \left(\frac{z+h}{h}\right)\underline{\boldsymbol{S}}_{\mathrm{D}}(\boldsymbol{R}). \tag{106}$$

Equations (102) and (103) introduce the fluid velocity generated by the image and the Blake tensor, respectively. The Blake tensor is comprised of three contributions, where $\hat{\boldsymbol{z}}$ is the unit vector pointing along the z-axis. N.B. The $(z+h)$ term in Eq. (106) already accounts for the fact that $\underline{\boldsymbol{S}}_{\mathrm{SD}}$ is evaluated in $\boldsymbol{R}$.

[48] Lorentz first analyzed this situation, but did not make the connection to an image formalism [71].

(c) Verify that this form gives the correct boundary condition; it would be advisable to use `Mathematica` to do so. Take $\boldsymbol{F}$ to be parallel to $\hat{\boldsymbol{x}}$ and visualize the flow field above the boundary. What do the three components to the Blake tensor for the image represent? Hint: you can find this answer in the literature.

C. Solving Stokes Equations on a Grid

We can gain intuition into the way Green's functions work by examining the incompressible Stokes equations on a grid. This will allow us to obtain numerical solutions for the dynamics in the fluid. Let us start by discretizing space on a cubic lattice with $L \times M \times N$ grid points in the x, y, and z directions respectively. The grid spacing is given by h, so that the domain lengths are $(L_x, L_y, L_z) = (L, M, N)h$. Henceforth, we will express the coordinates in a reduced form $(x, y, z) = (l, m, n)h$. At each grid point, we write scalar field as $\phi(hl, hm, hn)$, where $l \in \{0, \ldots, L-1\}$, $m \in \{0, \ldots, M-1\}$, and $n \in \{0, \ldots, N-1\}$ are indices. We also assume periodic boundary conditions in all directions, i.e., $\phi(h(l+L), h(m+M), h(n+N)) = \phi(hl, hm, hn)$. The discrete Fourier and inverse Fourier transformations are defined as

$$\check{\phi}(q,r,s) = \sum_{l=0}^{L-1}\sum_{m=0}^{M-1}\sum_{n=0}^{N-1} \exp\left[-2\pi i\left(\frac{lq}{L}+\frac{mr}{M}+\frac{ns}{N}\right)\right]\phi(hl,hm,hn); \tag{107}$$

$$\phi(hl,hm,ns) = \frac{1}{LMN}\sum_{q=0}^{L-1}\sum_{r=0}^{M-1}\sum_{s=0}^{N-1} \exp\left[2\pi i\left(\frac{lq}{L}+\frac{mr}{M}+\frac{ns}{N}\right)\right]\check{\phi}(q,r,s), \tag{108}$$

respectively. Note the presence of the volume term in the denominator of Eq. (108).

It is important to use appropriately discretized differential operators on the lattice, rather than their continuum variants, as well as have each of these be of the same order. This leads to a consistent equation set of discrete incompressible Stokes equations. In our calculations, a partial derivative with respect to the x coordinate is taken to have the form

$$\partial_x \phi(x,y,x) \to \frac{\phi(x+h,y,z)+\phi(x-h,y,z)}{2h}, \tag{109}$$

while for the Laplacian we choose a 7-point central difference scheme. In other words, we work exclusively with central differences. That is, the expression for the Laplacian of a function $\phi(x, y, z)$ is given by

$$\begin{aligned}\Delta\phi(x,y,z) \to \frac{1}{h^2}\big[&\phi(x+h,y,z)+\phi(x-h,y,z)+\phi(x,y+h,z)+\\ &\phi(x,y-h,z)+\phi(x,y,z+h)+\phi(x,y,z-h)-6\phi(x,y,z)\big].\end{aligned} \tag{110}$$

The divergence of a vector-valued function $\boldsymbol{\phi}$ can be similarly written as

$$\begin{aligned}\nabla_{\boldsymbol{r}}\cdot\boldsymbol{\phi}(x,y,z) \to \frac{1}{2h}\big[&\phi_x(x+h,y,z)-\phi_x(x-h,y,z)+\phi_y(x,y+h,z)-\phi_y(x,y-h,z)\\ &+\phi_z(x,y,z+h)-\phi_z(x,y,z-h)\big].\end{aligned} \tag{111}$$

We next work out the Fourier- or reciprocal-space expressions for the pressure and velocity. Following Section VI B the former is required to set up the appropriate projection formalism. Here, we will consider the dimensionless forms of the expressions

$$\boldsymbol{\Delta}_{\tilde{\boldsymbol{r}}}\tilde{\boldsymbol{u}} = \nabla_{\tilde{\boldsymbol{r}}}\tilde{p} - \tilde{\boldsymbol{f}}, \tag{112}$$

as working with reduced quantities is sensible from a computational perspective. We introduce $\check{p}$ for the Fourier transform of $\tilde{p}$ and similarly $\check{\boldsymbol{f}}$ for $\tilde{\boldsymbol{f}}$, respectively, where we have dropped the subscripts. We have also dropped the dependence on (hl, hm, hn) for all real-space quantities and on (q, r, s) for the checked quantities, in order to improve the legibility. Note that an important distinction with the discussion in the previous section is that $\tilde{\boldsymbol{f}}$ is not necessarily a point force, the field can act on the entire lattice.

Indexing the components of vectors and tensors using the subscripts 'a' and 'b', which take values from the set $\{x, y, z\}$, and performing the necessary algebraic manipulations, we arrive at the following form for the reduced reciprocal-space pressure

$$\check{p} = \frac{ih \sum_a \sin(k_a h) \check{f}_a}{2 \sum_b \cos(k_b h) - 6}. \tag{113}$$

Note that we have introduced the shorthand notation k_a for the components of the wave vector associated with reciprocal indices $k_x = 2\pi q/L_x$, $k_y = 2\pi r/L_y$, and $k_z = 2\pi s/L_z$, respectively.

Exercise 30: In this exercise, we verify our solution for the pressure and use it to construct the velocity field.

(a) Take the limit $h \downarrow 0$ and expanding $\sin(k_a h) \approx k_a h$ and $\cos(k_a h) \approx 1 - k_a^2 h^2/2$. Show that you arrive at the form

$$\check{p}(\boldsymbol{k}) = -\frac{i}{k} \hat{\boldsymbol{k}}^{\mathrm{T}} \check{\boldsymbol{f}}(\boldsymbol{k}). \tag{114}$$

The term on the right-hand side should look familiar.

(b) Having obtained $\check{p}$, use it to obtain the reciprocal-space velocity $\check{\boldsymbol{u}}$. You should arrive at the following component-wise expressions

$$\check{u}_a = \frac{h^2}{6 - 2\sum_c \cos(k_c h)} \sum_b \left[\delta_{ab} - \frac{\sin(k_a h) \sin(k_b h)}{6 - 2\sum_c \cos(k_c h)} \right] \check{f}_b, \tag{115}$$

where $c \in \{x, y, z\}$ also indices the coordinates.

The salient features of Eq. (96) can be recovered by taking $h \downarrow 0$, which leads to

$$\check{\boldsymbol{u}}(\boldsymbol{k}) = \frac{1}{k^2} \left(\underline{\mathbb{I}}_3 - \hat{\boldsymbol{k}} \otimes \hat{\boldsymbol{k}} \right) \check{\boldsymbol{f}}(\boldsymbol{k}), \tag{116}$$

and reveals the projection-like nature of Eq. (115).

Exercise 31: Examine the incomplete script "newtonian_force_roller_exercise.py". This gives a `Python` implementation of the above discrete-projection solver.

(a) Install `Python` and `Google`'s `JAX` library for `Python` on your own machine.

(b) Read through the provided scripts and try to understand how the projection formalism has been implemented.

(c) Now modify the script, such that you impose a force of the following form to the fluid

$$\boldsymbol{f} = A \left(\sin(2\pi x) \sin(2\pi y + \pi/2), \cos(2\pi x) \cos(2\pi y + \pi/2) \right), \tag{117}$$

with A a prefactor and x and y taking values on the unit square. You will have to introduce appropriate scaling to get it to work on an N_x by $N_y = N_x$ grid, independent of the value of N_x. You will find that there are two choices that can be made, one makes the velocity scale invariant, the other the stress. The solver is intrinsically in 3D, so additionally a sensible choice of N_z will need to be made.

(d) Visualize the flow field and explain why this setup is referred to as a four-roller mill.

(e) Compute the viscous part of the stress tensor belonging to this flow and show the xx-component.

(f) How should you choose the prefactor A, such that the xx-component to the stress in the center of the rollers is unity?

We will return to this exercise again in Chapter VIII, where we examine how the behavior changes with the introduction of viscoelasticity.

D. Theory for Microswimmers

Now that we have a solution for the application of a point force onto the fluid, we can consider the leading order decay of the flow field around a microswimmer. Recall that swimming itself is force free. In the case of an *E. coli* bacterium, one can envision this as the body of the *E. coli* exerting a drag on the fluid, while the flagellar bundle exerts a driving force on the fluid, see Fig. 11. This is obviously an oversimplified view, since both the head and the bundle experience drag from the fluid and, similarly, they both exert a force onto the fluid, but this model will suffice for now.

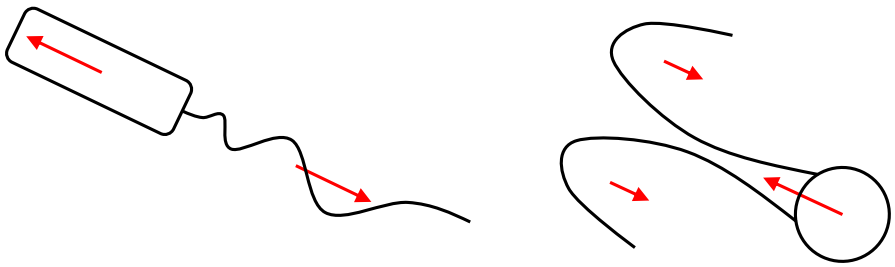

FIG. 11. **Sketches of two microorganisms showing the force free condition for motion.** On the left an *E. coli* is illustrated where the head experiences friction and the tail applies a force onto the fluid. For a *Chlamydomonas* algae on the right, self-propulsion force is applied onto the fluid using two flagella. In both cases the far field flow has a leading-order dipole moment. The sperm generates a far-field extensile flow field (pusher), while the algae has a contractile flow field (puller).

Starting from the Stokeslet $\underline{\boldsymbol{S}}$, we now consider two-point forces $\pm\tilde{\boldsymbol{f}}$ of equal magnitude and opposite directions, separated by a distance l. This construction ensures that the system is force free. Without any loss of generality we place the origin between the two forces, so that they are placed at $\frac{l}{2}\hat{\boldsymbol{p}}$ and $-\frac{l}{2}\hat{\boldsymbol{p}}$, with $\tilde{\boldsymbol{f}} = \pm F\hat{\boldsymbol{p}}$ such that the system is force free. Summing up the two Stokeslets, the velocity field at a point $\boldsymbol{r}$ in the fluid is thus given by

$$\boldsymbol{u}(\boldsymbol{r}) = \frac{F}{8\pi\mu}\left[\underline{\boldsymbol{S}}\left(\boldsymbol{r} - \frac{l}{2}\hat{\boldsymbol{p}}\right) - \underline{\boldsymbol{S}}\left(\boldsymbol{r} + \frac{l}{2}\hat{\boldsymbol{p}}\right)\right]\hat{\boldsymbol{p}}. \tag{118}$$

We now obtain the corresponding expression for the (point) stresslet[49] by taking the limit $l \to 0$. By first multiplying with $1 = l/l$ and defining the (constant) dipole strength $\kappa = Fl$ we now recognize the (negative of) the directional derivative in the limit of $l \to 0$:

$$(\hat{\boldsymbol{p}} \cdot \nabla)\, \underline{\boldsymbol{S}}(\boldsymbol{r}) \equiv \lim_{l \to 0} \frac{1}{l} \left[\underline{\boldsymbol{S}}\left(\boldsymbol{r} + \frac{l}{2}\hat{\boldsymbol{p}}\right) - \underline{\boldsymbol{S}}\left(\boldsymbol{r} - \frac{l}{2}\hat{\boldsymbol{p}}\right) \right]. \tag{119}$$

Using Eq. (119) we can thus write for the stresslet velocity field:

$$\boldsymbol{u}(\boldsymbol{r}) = -\frac{\kappa}{8\pi\mu} \left[(\hat{\boldsymbol{p}} \cdot \nabla)\, \underline{\boldsymbol{S}}(\boldsymbol{r}) \right] \hat{\boldsymbol{p}}. \tag{120}$$

The expression for $\left[(\hat{\boldsymbol{p}} \cdot \nabla)\, \underline{\boldsymbol{S}}\,(\boldsymbol{r}) \right] \hat{\boldsymbol{p}}$ can be derived using the standard tensor index notation. This leads to the well-known expression for the velocity field induced by a point stresslet:

$$\boldsymbol{u}(\boldsymbol{r}) = \frac{\kappa}{8\pi\mu r^2} \left(3(\hat{\boldsymbol{p}} \cdot \hat{\boldsymbol{r}})^2 - 1 \right) \hat{\boldsymbol{r}}, \tag{121}$$

also see the left-hand panel to Fig. 12, which shows a cross-section of the dipolar flow.

Exercise 32: Repeat the above steps to arrive at Eq. (121). Note the obvious analogy to electrostatics. In what way do you expect the analogy to break down, referencing the physical understanding you gained by completing Exercise 29?

In our construction, positive values of κ correspond to pusher (extensile) swimmers and negative values to puller (contractile) swimmers. A well-known pusher is the *E. coli* bacterium, while *Chlamydomonas* algae are archetypical pullers. Note that the flow field around a swimmer decays more quickly r^{-2} than around a point force r^{-1}, as was to be expected. In addition, from this derivation you can start to appreciate that many of the principles you learned in electrostatics carry over to Stokesian hydrodynamics. The Stresslet is simply the second term in a multipole expansion describing the far-away flow field around a general force distribution.

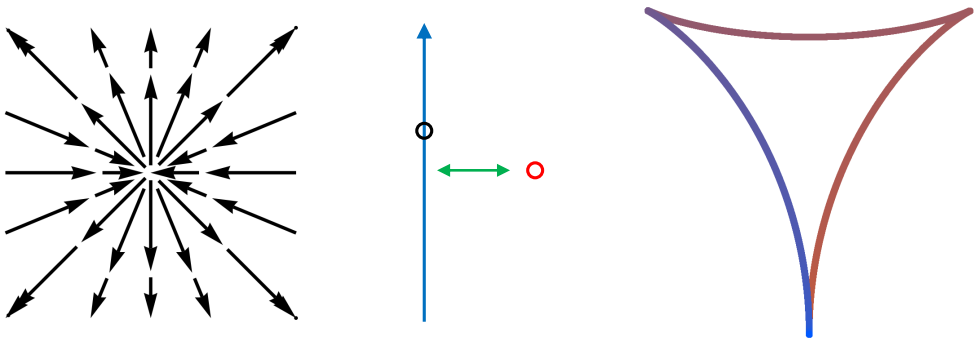

FIG. 12. **The trajectory of a small tracer particle advected in the flow field of a pusher microorganism.** The pusher causes an extensile flow field (left). As it moves past the tracer particle along the blue path, its flow field causes the tracer particle (red) to move (middle). The trajectory of the tracer in this flow is a concave triangle when the swimmer moves from $-\infty$ to ∞; early times are indicated by red and late times in blue (right).

[49] The term "stresslet" is most commonly used to refer to a rank-two tensor object. We abuse the term slightly here by applying it to what is technically the symmetric Stokes doublet, *i.e.*, the tensor sandwiched between radial unit vectors. That is, the stresslet for this situation is given by $\underline{\boldsymbol{\mathcal{S}}} = \kappa \left(\hat{\boldsymbol{p}} \otimes \hat{\boldsymbol{p}} - (1/3)\mathbb{I}_3 \right)$, such that the velocity field can be written as $\boldsymbol{u}(\boldsymbol{r}) = (3/(8\pi\mu r^2))(\hat{\boldsymbol{r}} \cdot \underline{\boldsymbol{\mathcal{S}}}\hat{\boldsymbol{r}})\hat{\boldsymbol{r}}$.

E. Tracer Dynamics near a Swimming Microorganism

Returning to our analogy of a leaf being carried along by the stream, we have one last observation to make regarding the way a microorganism can interact with its surroundings using its flow field. Let us assume that this swimmer is moving along the z-axis and starts off at $z = -L/2$ at time $t = 0$. We track it until it has reached $z = L/2$ at time $t = L/v_s$ with v_s its swim speed, this situation is sketched in Fig. 12. The swim speed can be related to the dipole strength according to $v_s = |\kappa|/(6\pi\mu)$, assuming that the swimmer is a sphere with radius a and experiences an "effective" propulsion force F that is related to a dipole[50], which has a length comparable to a.

A small molecule that is at a radial coordinate r_m with respect to the z-axis and at height $z = 0$ at time $t = 0$ will move along in the flow field produced by the moving swimmer. Let the time-dependent positions of the swimmer and the molecule be given by $\boldsymbol{r}_s$ and $\boldsymbol{r}_m$, respectively. Then the equations of motion describing this problem are given by

$$\frac{\partial \boldsymbol{r}_m}{\partial t}(t) = \boldsymbol{u}(\boldsymbol{r}_m(t) - \boldsymbol{r}_s(t)), \qquad \frac{\partial \boldsymbol{r}_s}{\partial t}(t) = v_s\hat{\boldsymbol{z}}, \tag{122}$$

with $\boldsymbol{u}$ the velocity field generated by the swimmer, as given by Eq. (121).

One can numerically integrate these equations of motion to obtain the trajectory of the small molecule in the flow field of the swimmer. The molecule will follow part of what is a triangle-shaped trajectory, which depends on the ratio $r_m(0)/L$, as well as the sign of κ, see Fig. 12 for an example. What this means is that when a swimmer passes by, it moves around molecules in its surroundings. Typically, these trajectories are not from $-\infty$ to ∞ and therefore not closed[51], also see Exercise 33.

The reason for these finite paths is either rotational Brownian motion, or a process called run-and-tumble, wherein the microorganism periodically and pseudo-stochastically reorients [74]. This is quite different from the situation that is found for driven particles, where the trajectories vanish when a particle is driven along the same path; but not when the path is finite. This implies that bacteria can effectively mix their surroundings through these advection-driven displacements, leading to an enhanced (effective) diffusion of materials in their surroundings. This phenomenon was first reported by Wu *et al.* [75] and later theoretically explained by Underhill *et al.* [76]. Since then, many more have worked on this topic, due to the exciting possibilities for microfluidic mixing.

Exercise 33: Let us numerically solve the equation system (122) and recover the typical trajectories of a small molecule in the flow field of a microorganism, see Fig. 12.

(a) You can use, for example, `Python` or `Mathematica`, whichever you prefer. Start by defining two three vectors for the initial position of the tracer and swimmer, respectively. Next, you can define a function that computes the flow *via* Eq. (121). Assume that the orientation of the swimmer is along the z-axis, $\mu = 1$, and that $\kappa = \pm 1$. What do you obtain for v_s in Eq. (122)? Next use a simple Euler-forward scheme to integrate the trajectory.

(b) Start small (L and $r_m(0)$ both less than 10) and play around a bit with the time step in order to figure out what is an optimal way of obtaining a trajectory. You can improve upon your algorithm and the range you can cover by having a non-uniform time step, which is limited by the size of the speed, but this requires a bit of finesse.

[50] The exact relation is not particularly relevant and will depend on the properties of the swimmer. What is important to acknowledge, is that there should be a linear proportionality between the dipole strength of a swimmer's flow field and the speed of self-propulsion. Note that the sign of the dipole does not impose the direction of swimming.

[51] Technically, the trajectory from $-\infty$ to ∞ is not closed, because of a process referred to as Darwin drift [73]. The trajectory is not invariant under time and parity transformation (a pusher becomes a puller and vice versa), therefore there is no *a priori* reason to expect that the trajectory should be closed. It turns out that it is not, though the degree by which it is not, is rather small compared to the total extent of the trajectory. A driven particle possesses this parity and the net displacement in either direction of traversing the trajectory must be the opposite, hence vanishing in the case of an infinitely long trajectory.

(c) Analyze the separation between the starting point and end point of the molecule's trajectory as a function of the parameters the govern the system: separation, swimmer path length, path asymmetry, and the dipolarity. Can you optimize the tracer displacement? Note that you must be careful with "collisions", wherein the swimmer and tracer separation becomes very small. For such events the numerical solutions become unstable, due to the inherent divergence in the flow field at the swimmer's position.

It should be obvious that the Darwin drift becomes largest in such close-to-touching scenarios. In reality, a large part of tracer displacement is also induced by events where the particles become briefly stuck on the swimmer's surface and detach. This leads them to be carried with the swimmer further than any amount of far-field advection could accomplish.

Where to next? In this chapter, we have seen basic elements to describing the flow around microswimmers. These elements can be built upon to have a simple description of a suspension of self-propelled particles. Such systems are interesting, as they show a form of turbulence that (appears to be) distinct from that found at high Reynolds number, as we will touch upon in Chapter VIII. On a more practical note, the Blake tensor, as shown in Exercise 29 can be a natural starting point for an analysis of the trajectory of a sperm above a wall. It turns out that such trajectories are circular [77], because of hydrodynamic coupling. The point is that you can understand many unexpected behaviors in biology, by simply knowing the behavior of fluids and the limitations that this imposes.

VII. POTENTIAL FLOWS AND INTERACTING SPHERES

A particularly nice feature of *incompressible* Stokes flow in two dimensions (2D), or in three dimensions (3D) with axisymmetry, is that it can be described using a stream function or a velocity potential. Here, we will examine this formalism based on the example of a sedimenting sphere. We will also introduce Faxén's laws, the Lorentz reciprocal relations, and consider the interaction between suspended spheres.

A. Drag Force on a Moving Sphere

In this section, we will consider a spherical particle with radius a moving at a velocity U through an incompressible Newtonian fluid. We will solve the Stokes flow for this problem and arrive at the expression for the Stokes drag. Along the way, make some observations on properties of the hydrodynamic equations in two-dimensional and axisymmetric geometries. In addition, we will learn how to treat flows that result from conservative forces.

We start by noting that for a sphere being dragged through a fluid, the flow in the surrounding (unbounded) medium is prescribed by the boundary conditions only. There is no body force applied to the system[52], which means that we need to solve the coupled differential equations

$$\mu \underline{\boldsymbol{\Delta}}_{\boldsymbol{r}} \boldsymbol{u} = \boldsymbol{\nabla}_{\boldsymbol{r}} p; \tag{123}$$

$$\boldsymbol{\nabla}_{\boldsymbol{r}} \cdot \boldsymbol{u} = 0. \tag{124}$$

We define the vorticity vector $\boldsymbol{\omega}(\boldsymbol{r}, t) = \boldsymbol{\nabla}_{\boldsymbol{r}} \times \boldsymbol{u}$, where '$\times$' denotes the cross product. This allows us to make use of the vector identity $\boldsymbol{\nabla}_{\boldsymbol{r}} \times (\boldsymbol{\nabla}_{\boldsymbol{r}} \times \boldsymbol{A}) = \boldsymbol{\nabla}_{\boldsymbol{r}}(\boldsymbol{\nabla}_{\boldsymbol{r}} \cdot \boldsymbol{A}) - \underline{\boldsymbol{\Delta}}_{\boldsymbol{r}} \boldsymbol{A}$, where $\boldsymbol{A}$ is some vector field depending on $\boldsymbol{r}$. We then obtain the following expression for the momentum transport

$$-\mu \boldsymbol{\nabla}_{\boldsymbol{r}} \times \boldsymbol{\omega} = \boldsymbol{\nabla}_{\boldsymbol{r}} p, \tag{125}$$

which can be further reduced to read

$$\underline{\boldsymbol{\Delta}}_{\boldsymbol{r}} \boldsymbol{\omega} = \boldsymbol{0}; \tag{126}$$

$$\Delta_{\boldsymbol{r}} p = 0, \tag{127}$$

by taking the curl and divergence on both sides of Eq. (125), respectively. Here, we have decoupled flow and pressure, in a manner that is reminiscent of our original Green's function analysis.

If the hydrodynamic problem is 2D or axisymmetric in nature, we can define a stream vector $\boldsymbol{\psi} = (0, 0, \psi)^T$, that evaluates to the fluid velocity field $\boldsymbol{u} = \boldsymbol{\nabla}_{\boldsymbol{r}} \times \boldsymbol{\psi}$. The third component of the stream vector (the scalar function) ψ is referred to as a stream function[53] and its isolines lie along flow lines to the velocity field of the flow. By construction $\boldsymbol{u} \cdot \boldsymbol{\nabla}_{\boldsymbol{r}} \psi = (\boldsymbol{\nabla}_{\boldsymbol{r}} \times \boldsymbol{\psi}) \cdot \boldsymbol{\nabla}_{\boldsymbol{r}} \psi = 0$, thus ψ varies orthogonal to the flow, or in other words, it is constant along streamlines of the flow[54].

Exercise 34: Convince yourself that $\boldsymbol{u} \cdot \boldsymbol{\nabla}_{\boldsymbol{r}} \psi = 0$ by working this out in Cartesian coordinates.

---

[52] Technically, the derivation below will work for any conservative forces applied to the medium.

[53] In the two-dimensional case, the first two components of the $\boldsymbol{\psi}$ vector relate to the x and y coordinates (the flow is planar) and the stream vector points out of the plane. For the axisymmetric case, we can use either cylindrical or spherical-polar coordinates, for which the first components of the stream vector represent the r and z coordinates, or r and θ coordinates, with θ the polar angle, respectively. In both cases, the stream vector lies in the $\hat{\boldsymbol{\phi}}$ direction, where ϕ measures the azimuthal angle. For each representation, the expression for the curl ($\boldsymbol{\nabla}_{\boldsymbol{r}}\times$) should be appropriately adjusted to the coordinate system.

[54] The incompressibility condition $\boldsymbol{\nabla}_{\boldsymbol{r}} \cdot \boldsymbol{u} = 0$ always admits a vector-potential description, making the analogy to classical magnetostatics. However, this description is not unique in general. A necessary condition for uniqueness (a gauge) is $\Delta_{\boldsymbol{r}}(\boldsymbol{\nabla}_{\boldsymbol{r}} \cdot \boldsymbol{\psi}) = 0$, which is met for our axisymmetric system of interest.

We can now return to the sedimenting sphere. This system best lends itself to a description in spherical polar coordinates with distance r and polar angle θ. The radial and polar components of the flow velocity that follow from the stream function $\psi(r,\theta)$ are then given by

$$u_r = \frac{-1}{r^2 \sin\theta}\frac{\partial \psi}{\partial \theta}; \tag{128}$$

$$u_\theta = \frac{1}{r \sin\theta}\frac{\partial \psi}{\partial r}, \tag{129}$$

respectively. A bit of tedious algebraic manipulation reveals that $\underline{\boldsymbol{\Delta}}_{\boldsymbol{r}}\boldsymbol{\omega} = \mathbf{0}$ reduces to $E^4\psi = 0$, where the operator

$$E^2 = \left[\frac{\partial^2}{\partial r^2} + \frac{\sin\theta}{r^2}\frac{\partial}{\partial \theta}\left(\frac{1}{\sin\theta}\frac{\partial}{\partial \theta}\right)\right], \tag{130}$$

is applied twice to the stream function ψ.

We should now solve the differential equation $E^4\psi = 0$ with appropriate boundary conditions to figure out the flow around a sphere. To do so, we transform to a frame where the sphere is stationary in the origin, with velocity boundary condition $\boldsymbol{u} = \mathbf{0}$ at $r = a$, where a is the sphere radius. In the limit of $r \uparrow \infty$, the flow should tend toward $\boldsymbol{u} = U\hat{\boldsymbol{z}}$, where U is the velocity at which the sphere sediments. This means that $u_r = U\cos\theta$ and $u_\theta = U\sin\theta$ very far from the surface of the sphere, a condition which is met by $\psi = (U/2)r^2\sin^2\theta$. This inspires us to examine the trial solution $\psi = g(r)\sin^2\theta$, with $g(r)$ a function only depending on the radial coordinate that is to be determined. Evaluating the expression $E^4\psi = 0$ in terms of this ansatz reveals that

$$\left[\frac{\partial^2}{\partial r^2} - \frac{2}{r^2}\right]^2 g = 0, \tag{131}$$

which is solved by solutions of the form $g \propto r^n$. Specifically, we find $g = A/r + Br + Cr^2 + Dr^4$, where A, B, C, and D are constants to be determined. To satisfy the limiting behavior for $r \uparrow \infty$ we require $D = 0$ and $C = U/2$. The zero-velocity boundary condition on the sphere can be used to derive $A = Ua^3/4$ and $B = -3Ua/4$, which leads to

$$\frac{U}{2}\left[r^2 + \frac{a^3}{2r} - \frac{3ar}{2}\right]\sin^2\theta. \tag{132}$$

From this is straightforward to compute the two velocity components and the pressure (by integrating up the momentum equation). These expressions read

$$u_r = U\cos\theta\left[1 + \frac{a^3}{2r^3} - \frac{3a}{2r}\right]; \tag{133}$$

$$u_\theta = -U\sin\theta\left[1 - \frac{a^3}{4r^3} - \frac{3a}{4r}\right]; \tag{134}$$

$$p = p_\infty - \frac{3}{2}\frac{\mu U a}{r^2}\cos\theta, \tag{135}$$

where p_∞ represents the pressure of say an atmosphere with which the fluid volume is in contact. The surface force on the sphere (traction) due to the flow can be computed from the stress[55] and is found to be parallel to the z-axis (as expected)

$$\boldsymbol{t}\cdot\hat{\boldsymbol{z}} = -p_\infty\cos\theta + \frac{3}{2}\frac{\mu U}{a}. \tag{136}$$

[55] The stress tensor is rank two and is defined by $\sigma_{ij} = -p\delta_{ij} + \mu\dot{\gamma}_{ij}$, with i and j indices, p the pressure, and $\dot{\boldsymbol{\gamma}}$ the strain-rate tensor, which we defined previously. The traction force $\boldsymbol{t}$ is obtained by taking the dot product between the surface normal vector $\hat{\boldsymbol{n}}$ and the stress tensor according to $t_i = \sum_j n_j\sigma_{ji}$, as before.

Integrating this traction over the surface of the sphere leads to the net force $\boldsymbol{F}_{\text{drag}} = 6\pi\mu a\boldsymbol{U}$, which is the sought-after Stokes result.

Exercise 35: Work your way through the above calculations to arrive at $\boldsymbol{F}_{\text{drag}} = 6\pi\mu a\boldsymbol{U}$.

(a) You will need to apply the curl four times to arrive at $E^4\psi = 0$. What is the physical interpretation of doing this?

(b) The most part is the stress calculation using mixed derivatives in spherical-polar coordinates, take your time and use a reference work. Hint: use symmetries to maximum effect.

(c) Suppose that the drag on a disk in a 2D flow is considered instead. What issue do you encounter in your calculation? What does this imply physically?

You should have found that there is something peculiar about 2D, reflecting on Green's functions in 2D this should perhaps not come as a surprise.

Generalizing the outcome of the above calculation, we find that in the rest frame of the sphere, the velocity field of the surrounding fluid is given by

$$\begin{aligned}\boldsymbol{u}(\boldsymbol{r}) &= \left[\frac{3}{4}\frac{a}{r}\left(\mathbb{I}_3 + \hat{\boldsymbol{r}}\otimes\hat{\boldsymbol{r}}\right) + \frac{1}{4}\frac{a^3}{r^3}\left(\mathbb{I}_3 - 3\hat{\boldsymbol{r}}\otimes\hat{\boldsymbol{r}}\right) - \mathbb{I}_3\right]\boldsymbol{U}_\infty \\ &= -\left[\frac{1}{8\pi\mu r}\left(\mathbb{I}_3 + \hat{\boldsymbol{r}}\otimes\hat{\boldsymbol{r}}\right) + \frac{1}{24\pi\mu}\frac{a^2}{r^3}\left(\mathbb{I}_3 - 3\hat{\boldsymbol{r}}\otimes\hat{\boldsymbol{r}}\right) - \frac{1}{6\pi\mu a}\mathbb{I}_3\right]\boldsymbol{F}_{\text{ext}},\end{aligned} \tag{137}$$

with $\boldsymbol{U}_\infty$ the velocity far away from the sphere, and $\boldsymbol{F}_{\text{ext}}$ the force applied to the sphere. Note that the sphere is located at the origin and the flow is undefined for $|\boldsymbol{r}| = r < a$.

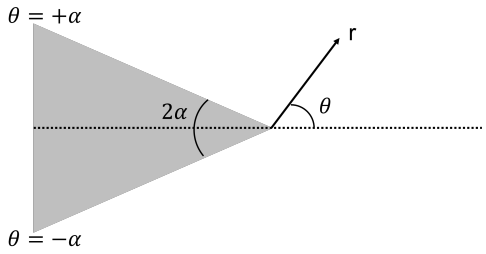

FIG. 13. **Sketch representing the geometry of the wedge.** The opening angle is given by α.

Exercise 36: In this exercise, we will have a closer look at the stream-function formalism for an incompressible, two-dimensional Stokes flow. The goal is to show that low-Re hydrodynamic problems can be treated precisely, using geometry for which the mathematics is slightly less involved than that for the sphere. Let $u_r(r,\theta)$ and $u_\theta(r,\theta)$ express the radial and polar component of the flow that we are considering.

(a) Show that the continuity equation is given by

$$\frac{\partial}{\partial r}(ru_r(r,\theta)) + \frac{\partial u_\theta(r,\theta)}{\partial\theta} = 0, \tag{138}$$

and that this is satisfied by introducing a stream function $\psi(r,\theta)$ such that

$$u_r(r,\theta) = -\frac{1}{r}\frac{\partial\psi(r,\theta)}{\partial\theta} \quad \text{and} \quad u_\theta(r,\theta) = \frac{\partial\psi(r,\theta)}{\partial r}. \tag{139}$$

(b) Show that you obtain the biharmonic equation by eliminating the pressure form the Stokes equation. That is

$$\nabla^4\psi(r,\theta) = \nabla^2(\nabla^2\psi(r,\theta)) = 0, \tag{140}$$

where in polar coordinates

$$\nabla^2\psi(r,\theta) = \frac{\partial^2}{\partial r^2}\psi(r,\theta) + \frac{1}{r}\frac{\partial}{\partial r}\psi(r,\theta) + \frac{1}{r^2}\frac{\partial^2}{\partial\theta^2}\psi(r,\theta). \tag{141}$$

Hint: Recall that you saw the biharmonic equation previously in deriving the Stokeslet.

(c) Use the separated form

$$\psi(r,\theta) = r^{\lambda+1}f_\lambda(\theta), \tag{142}$$

where λ may be complex to write

$$\nabla^2\psi = r^{\lambda-1}\left(f_\lambda^{(2)} + (\lambda+1)^2 f_\lambda\right), \tag{143}$$

where we introduced the notation $f_\lambda^{(j)} = \partial^j f_\lambda/\partial\theta^j$. Obtain the analogous expression for $\nabla^4\psi(r,\theta)$ in terms of r, $f_\lambda(\theta)$ and λ:

$$f_\lambda^{(4)} + \left((\lambda-1)^2 + (\lambda+1)^2\right)f_\lambda^{(2)} + (\lambda-1)^2(\lambda+1)^2 f_\lambda = 0. \tag{144}$$

(d) Substitute $f_\lambda \propto e^{m\theta}$, with a and m constants, in Eq. (144) to obtain an equation in terms of m and λ. Next, use this equation to arrive at the general solution

$$f_\lambda(\theta) = A\cos((\lambda+1)\theta) + B\sin((\lambda+1)\theta) + C\cos((\lambda-1)\theta) + D\sin((\lambda-1)\theta), \tag{145}$$

where A, B, C, and D may be complex. Using this solution, we will now consider the flow around a wedge, which has nice mathematical features. The solutions switch from a flow that smoothly curves around the wedge to an infinite series of counter-rotating vortices depending on the opening angle of the wedge. These counter-rotating vortices can be used, for example, to separate out bacteria that tend to migrate cross-stream (orthogonal to the flow lines). Figure 13 defines the geometry of the wedge, which has an opening angle 2α.

(e) Use the above solution to argue that the boundary conditions on the wedge are given by $\psi(r,\pm\alpha) = 0$ and

$$\left.\frac{\partial\psi(r,\theta)}{\partial\theta}\right|_{\theta=\pm\alpha} = 0, \tag{146}$$

whenever the flow is antisymmetric (*e.g.*, from top to bottom). Use the flow's anti-symmetry to set $B = D = 0$ and argue that $f_\lambda(\pm\alpha) = 0$ and

$$\left.\frac{\partial f_\lambda}{\partial\theta}\right|_{\theta=\pm\alpha} = 0. \tag{147}$$

Using these equations obtain the expressions for A and C. Next, cast these equations into a matrix form M and show that $\det(M) = 0$ gives $\sin(2\lambda\alpha) = -\lambda\sin(2\alpha)$. Why do we demand $\det(M) = 0$? Show that the eigenvalues (other than $\lambda = 0$) are complex when $2\alpha \lesssim 61/75\pi$.

(f) Sketch (or compute) the infinite number of eddies occur for $2\alpha = 0.3\pi$. If $2\alpha \gtrsim 61/75\pi$ the eigenvalues are real. Establish for what value of λ the leading eigenvalue is unity? What kind of flow does this solution represent?

Hint: please do not attempt to complete this exercise by solving for the flow field. The overall structure of the equations should be revealing enough on its own.

Finally, we turn to our curt nod at complex analysis with 2D inviscid flow. It turns out that very elegant connections can be made here to formal mathematics, which if you are interested in viscous, complex 3D flow, are not very useful.

Exercise 37: Consider a two-dimensional (2D) Navier-Stokes equation with incompressibility and without external forcing, *i.e.*, $\boldsymbol{f} = \boldsymbol{0}$.

(a) Write the velocity vector as $\boldsymbol{u}(x,y,t) = (u(x,y,t), v(x,y,t))$ and define the associated vorticity as $\omega = \partial_x v - \partial_y u$. Demonstrate that the momentum transport equation can be rewritten as

$$\rho \frac{D\omega}{Dt} = \mu \nabla^2 \omega, \tag{148}$$

with D/Dt the material derivative, μ the viscosity and ∇^2 the Laplacian. Provide a physical interpretation of Eq. (148), for low Reynolds number, but sufficiently high Strouhal number such that there remains time dependence.

(b) Set $\mu = 0$ and assume that there are no sources of vorticity, *i.e.*, $\omega = 0$ throughout. Introduce the complex notation $z = x + \imath y$ with $\imath^2 = -1$, as well as $w(z) = \phi(x,y) + \imath\psi(x,y)$, where ϕ and ψ are analytic, real-valued functions. Show that $\nabla\phi \cdot \nabla\psi = 0$ and explain what the physical interpretation of ϕ and ψ is in the context of this inviscid flow.

(c) Now consider $w(z) = Az^n$, with A some arbitrary real-valued constant, and n a real-valued power-law coefficient. Explain what the cases $n = 1$, $n = 3/2$, and $n = 2$ correspond to physically. What happens when $n < 0$?

Note that inviscid wedge flow is physically more boring than viscid flow, yet more mathematically pleasing, after a sense.

B. Faxén's Laws and Interacting Spheres

A more general result for the motion of a sphere in an inhomogeneous medium was derived by Hilding Faxén [78, 79]. In fact, he derived several important hydrodynamic results, which bare the name Faxén's laws. His first and second law read

$$\boldsymbol{F} = 6\pi\mu a \left[\left(1 + \frac{a^2}{6} \boldsymbol{\Delta}_{\boldsymbol{r}} \right) \big(\boldsymbol{u}(\boldsymbol{r}) - \boldsymbol{u}_\infty \big) - (\boldsymbol{U} - \boldsymbol{u}_\infty) \right]; \tag{149}$$

$$\boldsymbol{T} = 8\pi\mu a^3 \left[\frac{1}{2} \Big(\nabla_{\boldsymbol{r}} \times \big(\boldsymbol{u}(\boldsymbol{r}) - \boldsymbol{u}_\infty \big) \Big) - (\boldsymbol{\Omega} - \boldsymbol{\Omega}_\infty) \right], \tag{150}$$

respectively. Here, the force acting on the sphere located at $\boldsymbol{r}$ is represented by $\boldsymbol{F}$, the torque by $\boldsymbol{T}$, which come with associated velocity $\boldsymbol{U}$ and angular velocity $\boldsymbol{\Omega}$, respectively. The unperturbed flow far away from the sphere can be decomposed in a linear $\boldsymbol{u}_\infty$ an angular component $\boldsymbol{\Omega}_\infty$. Here,

the choices of the wording 'unperturbed' indicates that the presence of the sphere is not taken into account. Critically, this also holds for $\boldsymbol{u}(\boldsymbol{r})$. That is, this refers to the velocity of the fluid had the sphere not been present. After all, the derivative of the fluid velocity needs to be taken at the sphere's center point, which there would not be any flow, if there was a sphere.

Exercise 38: Write down the velocity $\boldsymbol{U}$ of a sphere in terms of the applied force $\boldsymbol{F}_{\text{app}}$ and perturbation velocity $\boldsymbol{u}(\boldsymbol{r})$, assuming there is no background (angular) velocity to the fluid flow. Do the same for the sphere's angular velocity $\boldsymbol{\Omega}$ given an applied torque $\boldsymbol{T}_{\text{app}}$. You should obtain:

$$\boldsymbol{U} = \frac{\boldsymbol{F}_{\text{app}}}{6\pi\mu a} + \left(1 + \frac{a^2}{6}\underline{\boldsymbol{\Delta}}_{\boldsymbol{r}}\right)\boldsymbol{u}(\boldsymbol{r})\Big|_{\boldsymbol{r}=\boldsymbol{r}_c}; \tag{151}$$

$$\boldsymbol{\Omega} = \frac{\boldsymbol{T}_{\text{app}}}{8\pi\mu a^3} + \frac{1}{2}\nabla_{\boldsymbol{r}} \times \boldsymbol{u}(\boldsymbol{r})\Big|_{\boldsymbol{r}=\boldsymbol{r}_c}, \tag{152}$$

where $\boldsymbol{r}_c$ is the center-point of the sphere.

Faxén's laws do not fall out of thin air. In order to obtain these, we will make use of the Lorentz reciprocity, as you may recall from your studies of electromagnetism. Let us derive this relation below. Suppose we are interested in incompressible zero-Re flow, prescribed by $\nabla_{\boldsymbol{r}} \cdot \boldsymbol{u} = 0$ and $\nabla_{\boldsymbol{r}} \cdot \underline{\boldsymbol{\sigma}} = \boldsymbol{f}$, with $\boldsymbol{f}$ the external force (per volume) and $\underline{\boldsymbol{\sigma}}$ the (full) stress tensor. The fluid velocity is specified by boundary conditions, which for this specific flow problem are complicated. We also have a complementary solution to the incompressible Stokes equations $\nabla_{\boldsymbol{r}} \cdot \boldsymbol{u}' = 0$ and $\nabla_{\boldsymbol{r}} \cdot \underline{\boldsymbol{\sigma}}' = \boldsymbol{f}'$. For this known flow, the boundary conditions are generally more simple. This is a bit nebulous at present, so to make this more explicit, we can think, *e.g.*, of the 'simple' problem as a sphere translating through a fluid at constant velocity and the problem of interest the motion of a sphere with a complicated surface velocity distribution[56], like the one on the cover. Taking the dot product with the unknown and known velocity, respectively, we arrive at

$$\boldsymbol{u}' \cdot \nabla_{\boldsymbol{r}} \cdot \underline{\boldsymbol{\sigma}} - \boldsymbol{u} \cdot \nabla_{\boldsymbol{r}} \cdot \underline{\boldsymbol{\sigma}}' = \boldsymbol{u}' \cdot \boldsymbol{f} - \boldsymbol{u} \cdot \boldsymbol{f}', \tag{153}$$

where we are free to rearrange $\boldsymbol{u}' \cdot \nabla_{\boldsymbol{r}} \cdot \underline{\boldsymbol{\sigma}}$ to $(\nabla_{\boldsymbol{r}} \cdot \underline{\boldsymbol{\sigma}}) \cdot \boldsymbol{u}'$. Using the product rule, we can then rewrite this as $\nabla_{\boldsymbol{r}} \cdot \left(\underline{\boldsymbol{\sigma}}\boldsymbol{u}'\right) = (\nabla_{\boldsymbol{r}} \cdot \underline{\boldsymbol{\sigma}}) \cdot \boldsymbol{u}' + \underline{\boldsymbol{\sigma}} : \left(\nabla_{\boldsymbol{r}}\boldsymbol{u}'\right)$. Using this relation, we find

$$\nabla_{\boldsymbol{r}} \cdot \left(\underline{\boldsymbol{\sigma}}\boldsymbol{u}'\right) - \nabla_{\boldsymbol{r}} \cdot \left(\underline{\boldsymbol{\sigma}}'\boldsymbol{u}\right) = \boldsymbol{u} \cdot \boldsymbol{f}' - \boldsymbol{u}' \cdot \boldsymbol{f}, \tag{154}$$

where the double-dot product term can be cancelled using the relation $\underline{\boldsymbol{\sigma}} = -p\mathbb{I}_3 + \mu\underline{\dot{\boldsymbol{\gamma}}}$, incompressibility of the fluid, and symmetry. Integrating up this equation over the volume gives rise to the familiar form provided in Eq. (157).

Exercise 39: Let us now derive Faxén's first law by making use of Lorentz reciprocity. Start by considering the Stokes equations

$$\mu\underline{\boldsymbol{\Delta}}_{\boldsymbol{r}}\boldsymbol{u} = \nabla_{\boldsymbol{r}}p - \boldsymbol{f}; \tag{155}$$

$$\nabla_{\boldsymbol{r}} \cdot \boldsymbol{u} = 0. \tag{156}$$

Rewrite this in the form of the stress tensor $\underline{\boldsymbol{\sigma}}$ and derive the following form for the reciprocity relation

$$\int_{\partial V} \mathrm{d}S\, \hat{\boldsymbol{n}} \cdot \underline{\boldsymbol{\sigma}} \cdot \boldsymbol{u}' - \int_{\partial V} \mathrm{d}S\, \hat{\boldsymbol{n}} \cdot \underline{\boldsymbol{\sigma}}' \cdot \boldsymbol{u} = \int_V \mathrm{d}V\, \boldsymbol{u} \cdot \boldsymbol{f}' - \int_V \mathrm{d}V\, \boldsymbol{u}' \cdot \boldsymbol{f}, \tag{157}$$

[56] In electrostatics, the simple problem is often a situation with uniform surface charge and the (more complicated) problem of interest a heterogeneous charge distribution.

where the unprimed quantities belong to the solved problem, while primed quantities belong the unknown problem. Use Eq. (157) and the expression for the traction force on a moving sphere — do not compute this, just copy it from the notes — to prove Faxén's first law. You will have to make use of a Taylor expansion about the center point and realize that all odd terms cancel by integration. Above a certain exponent all even terms cancel as well. Is Faxén's first law exact? Explain using a few words.

We can now compute the interaction between two moving (no-slip) spheres. We will restrict ourselves to two idealized situations, identical spheres (radius a) moving in the direction of the line connecting their centers and spheres moving perpendicular to it in an otherwise stationary fluid. Let the spheres be separated by a length $L \gg 2a$ — they are positioned at $\boldsymbol{r}_1 = (-L/2, 0, 0)$ and $\boldsymbol{r}_2 = (L/2, 0, 0)$, respectively — and both subjected to an external force $\boldsymbol{F}_{\text{ext}}$. In our calculation, we approximate the velocity fields $\boldsymbol{u}_1$ and $\boldsymbol{u}_2$ induced by the moving spheres by the Stokeslet solution, *i.e.*, by the ones generated by two point forces centered on $\boldsymbol{r}_1$ and $\boldsymbol{r}_2$, respectively. This is appropriate when the spheres are well separated.

The Stokes equations are linear, hence the sum of solutions $\boldsymbol{u}_1 + \boldsymbol{u}_2$ is again a solution to the Stokes equations. Note, however, that $\boldsymbol{u}_2(\boldsymbol{r}_1 + \boldsymbol{d}) \neq$ constant for $|\boldsymbol{d}| = a$. The same holds for the effect of sphere 1 on sphere 2. This means that simply adding two solutions for isolated spheres in bulk induces a(n admittedly small) violation of the required boundary condition on the spheres. It is possible to resolve this issue *via* higher-order multipole corrections, as we did for the Blake tensor. However, we will not consider this here.

Now turning to Faxén's laws, we can determine the velocity perturbation of one sphere on the other. Truncating Eq. (151) to zeroth order in a, we obtain for the velocity induced by sphere 1 on sphere 2, $\boldsymbol{U}_{1\to2} = \boldsymbol{u}_1(\boldsymbol{r}_2)$ and *vice versa* $\boldsymbol{U}_{2\to1} = \boldsymbol{u}_2(\boldsymbol{r}_1)$. Note the symmetry in these expressions, when both spheres experience a force of equal magnitude and direction. The drag force on sphere 1 and 2 now reduces to the Stokes drag

$$\boldsymbol{F}_{\text{drag},1} = 6\pi\mu a(\boldsymbol{U}_{2\to1} - \boldsymbol{V}_1); \tag{158}$$

$$\boldsymbol{F}_{\text{drag},2} = 6\pi\mu a(\boldsymbol{U}_{1\to2} - \boldsymbol{V}_2), \tag{159}$$

The force balance reads $\boldsymbol{F}_{\text{ext}} + \boldsymbol{F}_{\text{drag},n} = \boldsymbol{0}$ for either sphere, with n the index. We conclude that both spheres must have the same terminal velocity $\boldsymbol{V} = \boldsymbol{V}_1 = \boldsymbol{V}_2$ based on symmetry and isolating this velocity we obtain

$$\boldsymbol{V} = \frac{1}{6\pi\mu a}\left[\mathbb{I}_3 + \frac{3a}{4L}\left(\mathbb{I}_3 + \frac{(\boldsymbol{r}_2 - \boldsymbol{r}_1)\otimes(\boldsymbol{r}_2 - \boldsymbol{r}_1)}{L^2}\right)\right]\boldsymbol{F}_{\text{ext}}. \tag{160}$$

For a force parallel to the alignment of spheres, the terminal velocity is

$$V_{\parallel} = \frac{F_{\text{ext}}}{6\pi\mu a}\left(2 + \frac{3a}{2L}\right), \tag{161}$$

while in the perpendicular direction the same force magnitude results in

$$V_{\perp} = \frac{F_{\text{ext}}}{6\pi\mu a}\left(2 + \frac{3a}{4L}\right). \tag{162}$$

In both cases, the particle velocities of the two particles are greater than that of a single suspended sphere. However, there is a directional preference for two particles to follow each other. This is a first step in understanding how clustered objects can move faster in certain directions, which

allows hydrodynamic interactions to favor local heterogeneities [80, 81].

Exercise 40: We can take the above result for two spheres and extend it to model the behavior of a rod. Consider the so-called 'shish-kebab' model of a cylinder of length L and radius a. This consists of a line of spheres of radius a for which the position of the m-th sphere — provided the cylinder is aligned with the x-axis — is given by $r(m) = (2am, 0, 0)$, where $m \in [-N, N]$. The total length of the cylinder is, therefore, $L = 2a(2N + 1)$.

(a) Argue that the drag force on the shish-kebab rod is given by

$$\boldsymbol{F}_{\text{drag}} = -6\pi\mu a \sum_{m=-N}^{N} (\boldsymbol{U} - \boldsymbol{W}_m)\,, \tag{163}$$

where $\boldsymbol{U}$ is the velocity of the rod and $\boldsymbol{W}_m$ is the effect of all the other spheres on the sphere located at position $r(m)$.

(b) What is the force that the n-th sphere ($n \neq m$) applies to the fluid? Use this to provide an expression for $\boldsymbol{W}_m$, approximating the flow caused by each sphere using the Oseen tensor (stokeslet). You should arrive at the self-consistent equation

$$\boldsymbol{W}_m = \sum_{\substack{n=-N \\ n\neq m}}^{N} \frac{3}{4|n-m|}\left[\mathbb{I}_3 + \begin{pmatrix}1\\0\\0\end{pmatrix}\otimes\begin{pmatrix}1\\0\\0\end{pmatrix}\right](\boldsymbol{U} - \boldsymbol{W}_n)\,. \tag{164}$$

Clearly, $\boldsymbol{W}_m$ depends on the position along the rod, but for a sufficiently long rod, it will only weakly depend on the position. The physical intuition is that the ends will contribute little to the behavior of the rod and we may therefore approximate all $\boldsymbol{W}_m$ by the center value $\boldsymbol{W}_0$, which turns out to work surprisingly well.

(c) Rewrite Eq. (164) using this approximation and realize that

$$\boldsymbol{W} \equiv \boldsymbol{W}_0 = \frac{3}{4}\left[\mathbb{I}_3 + \begin{pmatrix}1\\0\\0\end{pmatrix}\otimes\begin{pmatrix}1\\0\\0\end{pmatrix}\right](\boldsymbol{U} - \boldsymbol{W}) \sum_{\substack{n=-N \\ n\neq 0}}^{N} \frac{1}{|n|}. \tag{165}$$

(d) Approximate the sum by an integral (that evaluates to $2\log N$) and use this to solve for $\boldsymbol{W}$ as a function of $\boldsymbol{U}$. Putting this back into the expression for $\boldsymbol{F}_{\text{drag}}$ you should arrive at

$$F_\parallel = -6\pi\mu a \frac{2N+1}{1 + (3/2)\log N} U_\parallel \approx -\frac{2\pi\mu L}{\log(L/a) - 2\log 2 + 2/3} U_\parallel; \tag{166}$$

$$F_\perp \approx -\frac{4\pi\mu L}{\log(L/a) - 2\log 2 + 4/3} U_\perp, \tag{167}$$

for motion along and perpendicular to the rod, respectively.

(e) show that the ratio in friction coefficient for the two motions reduces to $1/2$ in the case of an infinitely long rod. Use this result to compute the sedimentation angle α of a rod with uniform mass density in a very viscous fluid, as a function of its initial angle θ with respect to the direction of gravity ($\theta = 0$ for the rod aligned parallel to gravity with its long axis). Argue why the rod does not reorient on the basis of symmetry and compute the maximum sedimentation angle $\alpha^* = (1/2)\arccos(1/3)$.

This is the first step toward understanding the sedimentation of more involved shapes in a viscous fluid [82, 83], which is governed by the center of mass and the hydrodynamic center.

Exercise 41: In this exercise, we build upon Exercise 29 to consider the behavior of a small sphere or microorganism near a wall. We will make use of Eqs. (102) and (103) and Faxén's laws.

(a) Argue *in words* why a small sphere dragged parallel to a wall does not experience a lateral velocity toward or away from the wall. Hint: This requires a symmetry argument only, no actual calculation.

(b) Approximate the flow field generated by a moving sphere by that of a Stokeslet and use the above image convention and Faxén's laws to determine the effect of the wall on the sphere's velocity and angular velocity, when it is dragged parallel to the wall. You should recover

$$U_x = \frac{(a^2 - 9h^2)F}{96h^3\pi\mu}, \tag{168}$$

whenever the force is the applied force in the x-direction (denoted here by the scalar F).

The above shows the obvious limitations of the approximation. Full analysis of the hydrodynamic equations for a very small fluid layer in between the wall and sphere, show that sphere slips and its effective velocity V and angular velocity Ω (accounting for fluid friction induced by the wall) are related via $a\Omega/V = 1/4$ [84]. This is a fascinating result, as it implies that fluid friction and mechanical friction are distinguishable. This led to debate within the field on the validity of the zero-velocity boundary condition and how reasonable the smooth-surface approximation is.

(c) Discuss *in words* how you can improve the far-field estimate of a point force acting on the fluid. Hint: Think in terms of the boundary condition on the traveling sphere.

In the case of a self-propelled particle, there is no force acting on the swimmer. The expression for the velocity and angular velocity of the swimmer in the presence of a wall are

$$\boldsymbol{U} = \boldsymbol{u}_{\text{swim}} + \left(1 + \frac{a^2}{6}\underline{\boldsymbol{\Delta}}_{\boldsymbol{r}}\right)\boldsymbol{u}(\boldsymbol{r})\Big|_{\boldsymbol{r}=\boldsymbol{r}_s}; \tag{169}$$

$$\boldsymbol{\Omega} = \frac{1}{2}\nabla_{\boldsymbol{r}} \times \boldsymbol{u}(\boldsymbol{r})\Big|_{\boldsymbol{r}=\boldsymbol{r}_s}, \tag{170}$$

respectively, with $\boldsymbol{u}(\boldsymbol{r})$ the velocity field caused by the image and $\boldsymbol{u}_{\text{swim}}$ the swimmer's intrinsic self-propulsion velocity. Recall that for a simple dipole swimmer $\boldsymbol{u}_{\text{swim}} = |\kappa|\hat{\boldsymbol{p}}/(8\pi\mu)$, with κ the dipole strength and $\hat{\boldsymbol{p}}$ the swimmers orientation. Further recall that the bulk velocity field of such a dipole swimmer is given by $\boldsymbol{u}_{\text{dip}}(\boldsymbol{r}-\boldsymbol{r}_{\text{s}}) = -\kappa\left[(\hat{\boldsymbol{p}}\cdot\nabla_{\boldsymbol{r}_{\text{s}}})\,\underline{\boldsymbol{S}}_{\text{O}}(\boldsymbol{r}-\boldsymbol{r}_{\text{s}})\right]\hat{\boldsymbol{p}}$ with the Stokeslet as defined in Eq. (104).

(d) Argue in words why it is possible to replace $\underline{\boldsymbol{S}}_{\text{O}}(\boldsymbol{r}-\boldsymbol{r}_{\text{s}})$ by $\underline{\boldsymbol{S}}_{\text{I}}(\boldsymbol{R})$ in the above equation for the dipole flow to obtain the flow field caused by the dipole's image.

(e) Is a puller swimming parallel to the wall repelled from or attracted toward the wall? Is the swimmer slowed down by the presence of the wall? Is swimming parallel to the wall stable for a pusher or for a puller? Assume there is an interaction potential that keeps it from crashing into or moving away from the wall.

C. Intro to Rotne-Prager-Yamakawa: Looking toward Stokesian Dynamics

We now have most of the elements at our disposal to start to understand the way in which one can simulate many hydrodynamically interacting spheres at low Reynolds number. Suppose we have an unbounded fluid volume filled with N identical spheres of radius a that are spaced far apart. The positions of the i-th sphere's center is given by $\boldsymbol{r}_i$, and the force acting on it is denoted $\boldsymbol{F}_i$. Then, using Faxén's first law (151), we know that the velocity of this sphere is given by

$$\boldsymbol{U}_i = \frac{\boldsymbol{F}_k}{6\pi\mu a} + \left(1 + \frac{a^2}{6}\nabla^2_{\boldsymbol{r}_i}\right)\boldsymbol{u}(\boldsymbol{r}_i), \tag{171}$$

where the velocity of the fluid unperturbed by the presence of the i-th sphere, can be approximated

$$\boldsymbol{u}(\boldsymbol{r}_i) = \sum_{\substack{k=1\\k\neq i}}^{N} \frac{1}{8\pi\mu}\underline{\boldsymbol{S}}(\boldsymbol{r})\boldsymbol{F}_k, \tag{172}$$

using the Oseen tensor. This then gives rise to a matrix equation

$$\boldsymbol{\mathcal{U}} = \underline{\boldsymbol{\mathcal{M}}}\boldsymbol{\mathcal{F}}, \tag{173}$$

where $\boldsymbol{\mathcal{U}}$ is the $3N$ vector comprising all particle velocities, $\boldsymbol{\mathcal{F}}$ similarly holds all particle forces, and $\underline{\boldsymbol{\mathcal{M}}}$ connects the two *via* Eqs. (171) and (172).

Note that the matrix depends on the instantaneous particle positions and will need to be updated as the particles displace. This requires integrating the differential equation system in Eq. (173), though in practice a simple time-stepping method may be used to do this numerically. We know that $\underline{\boldsymbol{\mathcal{M}}}$ must be symmetric to satisfy Newton's second law. It is real-valued and it must be positive definite, because each mode of particle motion is dissipative. That is, $\underline{\boldsymbol{\mathcal{M}}}$ has only strictly positive eigenvalues and is therefore invertible. These properties must hold in general, even when we make more sophisticated approximations for $\underline{\boldsymbol{\mathcal{M}}}$.

In the above, we have used the Oseen tensor to arrive at a form for $\underline{\boldsymbol{\mathcal{M}}}$. This is only suited for point-like particles. A better approximation would follow by taking into account the finite size of the spheres, using a suitably modified form of the expression in Eq. (137). This approximation is referred to as the Rotne-Prager-Yamakawa formalism [85]: the translation of spheres is accounted by building up $\underline{\boldsymbol{\mathcal{M}}}$ from pairwise terms. This way of approaching the problem can be useful in the dilute regime. However, there are several weaknesses:

- Higher-order terms would have to be accounted for to accurately capture the dynamics of spheres that come in close contact.
- While $\underline{\boldsymbol{\mathcal{M}}}$ couples each particle to each other particle, the dynamics derived above is not truly many body.

Both points come with subtleties that need a bit more clarification. In the interest of expediency, we will only highlight these issues here and not go into the development of the machinery behind a more sophisticated method like Stokesian dynamics [86].

When two perfectly smooth spheres are brought into near contact — surface-to-surface separation $s \equiv |\boldsymbol{r}| - 2a \ll a$ — in a Newtonian fluid medium, the friction they experience diverges as s^{-1} [22]. Their effective sliding friction, orthogonal to the vector connecting the two spheres, is proportional to $\log s$. These divergences originate from the fact that the small gap between the particles gives rise to strong momentum dissipation. The behavior is often referred to as 'lubrication,' since it is relevant to the behavior of oil-lubricated ball bearings. However, it also plays a critical

role in colloidal suspensions at sufficiently high density [87]. It should be strongly emphasized that lubricated hydrodynamics are not a separate form of hydrodynamic interactions; as some, even very senior researchers, sometimes claim. They follow from solving the Stokes equations, where an expansion is made in the small parameter s/a. We will not pursue this here and instead refer the interested reader to the book by Kim and Karilla [22]. One might naively expect that adding an increasing number of terms to the expansion that starts from the Oseen tensor, would help in resolving these lubrication effects, *i.e.*, terms that go beyond Eq. (137). However, this proves impractical for most intents and purposes and instead explicit corrections using the small expansion parameter are taken [88, 89].

The second point of interest is more subtle. Technically, the dynamics prescribed by $\underline{\boldsymbol{\mathcal{M}}}$ couples all particles to each other. However, there is an issue. Consider the situation where a particle, say 1, moves due to an applied force and as a consequence another particle, say 2, moves due to hydrodynamic interactions. Then the motion of particle 2 causes a flow, that acts on particle 1, via Faxén's laws, which causes a subtle change in the movement of particle 1, which in turn modifies the way particle 2 moves. This means that an infinite series of recursive corrections has to be applied. It turns out that the mobility formulation of the problem, as in Eq. (173), is generally inappropriate to deal with the issue [86]. A pairwise construction of the coupling tensor in the resistive framework, *i.e.*, where the velocity prescribes a force can be used to circumvent the issue. The analogy that can be made is that to electric resistors being in parallel, where working with the resistance or the conductance changes the problem of finding the net value from an involved one requiring inversion to a simple sum, respectively.

Lastly, we have casually omitted that spheres can rotate, either when they are subjected to a torque or a shear flow. A more complete description of hydrodynamic interactions needs to account for these aspects. Presently, Stokesian dynamics [86] is one of the most powerful [90] and actuate means by which all these effects can be taken into account. However, even it is approximative in nature and has well-known limitations.

Exercise 42: Read through the paper "Hydrodynamic Interactions in Particle Suspensions: A Perspective on Stokesian Dynamics" to learn more about the Stokesian Dynamics algorithm" [91] to gain a flavor of the approach. You should be able to understand large parts of the text with the knowledge that you have gained thus far, though please do not bother with specific details. Next, have a look at the paper "Python-JAX-based Fast Stokesian Dynamics" [92].

(a) Install the `JAX`-based solver on your machine.

(b) Reproduce the three-dancing sphere trajectory from Fig. 1b of Ref. [92].

In principle the `JSFD` solver is capable of much more, but the three-body problem should be feasible to solve on most modern laptops.

Where to next? In this chapter, we have seen how spheres interact with each other in a basic formalism. Dealing with long-range hydrodynamic interactions in a sufficiently exact and efficient manner, when multiple spheres are involved, is still a challenge to this day. In particular, scientists interested in the dynamics of colloidal suspensions will need to take these into account, when their system is brought sufficiently out of equilibrium [81]. Another, intriguing direction to take this topic is to build rigid bodies up from assemblies of spheres [93] and consider their dynamics when sedimenting or in shear flow. Such systems also lend themselves to analysis by (analytic) theory, using either resistive force theory — for which we made the first steps above in deriving the mobility tensor for a rod — or the slender-body approximation [94].

VIII. COMPLEX AND ACTIVE FLUIDS

This chapter closes our discussion of low-Reynolds-number hydrodynamics. We will build upon the definition of an upper-convected derivative, see Section III B, to overcome the issues in generalizing the Maxwell model that we identified in Section II C. This allows us to obtain the Oldroyd-B constitutive relation for the flow of a dilute polymer suspension. We also consider briefly a simple description for an active-matter system with many particles, the Vicsek model, and examine further the consequences of having many active particles suspended in a fluid medium, briefly touching upon the concept of active turbulence and its relation to elastic turbulence.

A. Flows in Polymer Suspensions

Recall from our discussion of rheology in Chapter II that a Maxwell fluid satisfies the differential equation

$$\tau + \frac{\mu}{G_0}\dot{\tau} = \mu\dot{\gamma}, \tag{174}$$

where $\lambda = \mu/G_0$ represents the time scale of relaxation. Transitioning to a tensorial form for the shear rate, we must change the time derivative to an upper-convected derivative. This leads to the constitutive relation for the *upper-convected Maxwell fluid*

$$\underline{\boldsymbol{\tau}} + \lambda\, \overset{\triangledown}{\underline{\boldsymbol{\tau}}} = \mu\underline{\dot{\boldsymbol{\gamma}}}; \tag{175}$$

$$\overset{\triangledown}{\underline{\boldsymbol{\tau}}} = \left(\frac{\partial}{\partial t} + \boldsymbol{u}\cdot\nabla_{\boldsymbol{r}}\right)\underline{\boldsymbol{\tau}} - \left(\nabla_{\boldsymbol{r}}\boldsymbol{u}\right)^{T}\underline{\boldsymbol{\tau}} - \underline{\boldsymbol{\tau}}\left(\nabla_{\boldsymbol{r}}\boldsymbol{u}\right). \tag{176}$$

The physical interpretation of this equation is that when shear is ceased ($\underline{\dot{\boldsymbol{\gamma}}} = \underline{\mathbf{0}}$), the deviatoric stress relaxes exponentially to zero with rate λ^{-1}.

In a dilute polymer suspension, it is reasonable to assume that the polymeric contribution to the stress satisfies the upper-convected Maxwell relation. That is, the first departure away from pure viscous dissipation is given by a Hookean elastic contribution. This leaves the presence of the Newtonian suspending medium, *e.g.*, water, unaccounted for in Eq. (176). We solve this by adding the viscous and elastic stresses $\underline{\boldsymbol{\tau}} = \mu_s\underline{\dot{\boldsymbol{\gamma}}} + \underline{\boldsymbol{\tau}}_p$, where the term $\underline{\boldsymbol{\tau}}_p$ satisfies Eq. (175) with $\underline{\boldsymbol{\tau}} \to \underline{\boldsymbol{\tau}}_p$ and $\mu \to \mu_p$. This leads to the following relation

$$\underline{\boldsymbol{\tau}} + \lambda\, \overset{\triangledown}{\underline{\boldsymbol{\tau}}} = \mu\left(\underline{\dot{\boldsymbol{\gamma}}} + \lambda_r\, \overset{\triangledown}{\underline{\dot{\boldsymbol{\gamma}}}}\right). \tag{177}$$

Here, $\mu = \mu_s + \mu_p$ represents the total viscosity of the fluid, accounting for both the fluid μ_s and polymeric component μ_p. The relaxation rate $\lambda_r = \lambda\mu_s/\mu$ is the polymer rate weighted by the polymer-to-solvent viscosity ratio. The parameter λ represents the elastic relaxation of the polymer component, as was the case in the upper-convected Maxwell fluid.

For an incompressible, Oldroyd-B fluid we can recast the above and obtain the following equations describing the flow

$$\nabla_{\boldsymbol{r}}\cdot\boldsymbol{u} = 0; \tag{178}$$

$$\rho\left(\frac{\partial}{\partial t} + \boldsymbol{u}\cdot\nabla_{\boldsymbol{r}}\right)\boldsymbol{u} = \nabla_{\boldsymbol{r}}\cdot\underline{\boldsymbol{\sigma}} + \boldsymbol{f}_{\text{ext}}; \tag{179}$$

$$\underline{\boldsymbol{\sigma}} = -p\mathbb{I}_3 + \mu_s\underline{\dot{\boldsymbol{\gamma}}} + \underline{\boldsymbol{\tau}}_p; \tag{180}$$

$$\lambda\, \overset{\triangledown}{\underline{\boldsymbol{\tau}}}_p + \underline{\boldsymbol{\tau}}_p = \mu_p\underline{\dot{\boldsymbol{\gamma}}}. \tag{181}$$

Exercise 43: Derive Eq. (177) yourself from the definitions provided. Next, show that the flow can be rewritten to the following form

$$\nabla_{\boldsymbol{r}} \cdot \boldsymbol{u} = 0; \tag{182}$$

$$\rho\left(\frac{\partial}{\partial t} + \boldsymbol{u}\cdot\nabla_{\boldsymbol{r}}\right)\boldsymbol{u} = -\nabla_{\boldsymbol{r}} p + \mu_s \underline{\boldsymbol{\Delta}}_{\boldsymbol{r}}\boldsymbol{u} + \frac{\mu_p}{\lambda}\nabla_{\boldsymbol{r}}\cdot\underline{\boldsymbol{\sigma}}_p + \boldsymbol{f}_{\text{ext}}; \tag{183}$$

$$\overset{\triangledown}{\underline{\boldsymbol{\sigma}}}_p = -\frac{1}{\lambda}\left(\underline{\boldsymbol{\sigma}}_p - \mathbb{I}_3\right). \tag{184}$$

and provide the form of $\underline{\boldsymbol{\sigma}}_p$. You will need to make use of the upper-convected derivative of the identity tensor to arrive at Eq. (184). What is the physical interpretation of $\underline{\boldsymbol{\sigma}}_p$?

Exercise 44: The Oldroyd-B model can be derived from a model of Hookean dumbbells with zero rest length, suspended in a Newtonian fluid [20, 29]. The Hookean character of the springs leads to issues in this model, which can be understood by examining the continuum constitutive relations. Consider a simple, 2D, and time-independent extensional flow $\boldsymbol{u} = (\dot{\epsilon}x, -\dot{\epsilon}y)$, with $\dot{\epsilon}$ a constant that is similar in nature to $\dot{\gamma}$ but instead measures the rate of uniaxial stretching rather than shear. Note that we have the signs chosen such that the flow is incompressible. Define the extensional viscosity[57] as

$$\mu_{\text{ext}} = \frac{\sigma_{xx} - \sigma_{yy}}{\dot{\epsilon}}. \tag{185}$$

What is the value of μ_{ext} for a Newtonian fluid? And how does that compare to the expression for an Oldroyd-B fluid? The fluid strain hardens, *i.e.*, with increasing $\dot{\epsilon}$ the effective viscosity increases. However, there is a divergence at $2\lambda\dot{\epsilon} = 1$. Explain what happens physically at this point and why this is not a problem for shear flow. How would you amend the model to solve the issue?

Having arrived at a set of equations for Oldroyd-B flow[58], the natural step is to perform a dimensional analysis, as we already performed for the Newtonian Navier-Stokes equations in Section V A. We begin by noting that Eqs. (182) - (184) contain four dimensionful quantities ρ, μ_s, μ_p, and λ. Unlike the situation with the Newtonian flow, there is now a natural time scale, λ, so we should see this reflected in our reduction. Introducing a time scale T, length scale L, and velocity U, and introducing tildes for reduced parameters as before, we arrive at

$$\mathsf{Re}\left(\mathsf{St}\frac{\partial}{\partial\tilde{t}} + \tilde{\boldsymbol{u}}\cdot\nabla_{\tilde{\boldsymbol{r}}}\right)\tilde{\boldsymbol{u}} = -\nabla_{\tilde{\boldsymbol{r}}}\tilde{p} + \underline{\boldsymbol{\Delta}}_{\tilde{\boldsymbol{r}}}\tilde{\boldsymbol{u}} + \frac{\mu_p}{\mu_s}\frac{\mathsf{L}}{\lambda\mathsf{U}}\nabla_{\tilde{\boldsymbol{r}}}\cdot\underline{\boldsymbol{\sigma}}_p + \tilde{\boldsymbol{f}}_{\text{ext}}; \tag{186}$$

$$\left(\mathsf{St}\frac{\partial}{\partial\tilde{t}} + \tilde{\boldsymbol{u}}\cdot\nabla_{\tilde{\boldsymbol{r}}}\right)\underline{\boldsymbol{\sigma}}_p - \left(\nabla_{\tilde{\boldsymbol{r}}}\tilde{\boldsymbol{u}}\right)^T\underline{\boldsymbol{\sigma}}_p - \underline{\boldsymbol{\sigma}}_p\left(\nabla_{\tilde{\boldsymbol{r}}}\tilde{\boldsymbol{u}}\right) = -\frac{\mathsf{L}}{\lambda\mathsf{U}}\left(\underline{\boldsymbol{\sigma}}_p - \mathbb{I}_3\right), \tag{187}$$

with Re the usual Reynolds number and St the Strouhal number, and $\tilde{\boldsymbol{u}}$, $\tilde{p}$, and $\tilde{\boldsymbol{f}}_{\text{ext}}$ reduced as in Section V A. Note that $\underline{\boldsymbol{\sigma}}_p$ is already reduced and that we encounter a new dimensionless group that is paired with this quantity

$$\frac{\mathsf{L}}{\lambda\mathsf{U}}, \tag{188}$$

which is related to the Weissenberg number Wi. The Weissenberg number is defined as the ratio between elastic and viscous forces. In a simple, 2D, and time-independent shear flow $\boldsymbol{u} = (\dot{\gamma}y, 0)$,

[57] Do not mix up μ_{ext} with the dilatational viscosity μ' we defined in Section IV A 3!
[58] There is such a thing as Oldroyd-A flow as well, see Ref. [95].

this can be represented by the difference between the normal stress over the shear stress

$$\mathsf{Wi} = \frac{\sigma_{xx} - \sigma_{yy}}{\sigma_{xy}} = \frac{2\lambda\mu_p\dot{\gamma}^2}{(\mu_s - \mu_p)\dot{\gamma}} = \frac{2\mu_p}{\mu_s - \mu_p}\lambda\dot{\gamma}, \tag{189}$$

where we can recognize $\dot{\gamma} = \mathsf{U}/\mathsf{L}$ and hence the proportionality in Eq. (188).

Exercise 45: Derive Eq. (189) from Eq (184) and the definition of the stress on the fluid. Note that the excess stress in the xx-direction is acting along the flow lines but is oppositely directed to the pressure. Thus, it can be interpreted as a form of tension. This tension is what drives effects like viscoelastic rod climbing [96], as we will see shortly in Exercise 47.

We will henceforth choose to ignore the viscosity prefactors and define the Weissenberg number

$$\mathsf{Wi} \equiv \lambda\dot{\gamma}, \tag{190}$$

where $\dot{\gamma}$ is a representative shear for the fluid of interest. This reveals an issue in Eqs. (186) and (187), when setting the time scale to the elastic relaxation value $T = \lambda$. Namely that $\mathsf{St} = \mathsf{Wi}^{-1}$ and the limit $\mathsf{Wi} \downarrow 0$ is poorly behaved, even though it is a natural one to take. We can eliminate one such issue by formally taking $\mathsf{Re} \downarrow 0$, though it feels somewhat unsatisfying. Alternatively, we can reduce the constitutive equation as

$$\frac{\lambda}{\mathsf{T}}\frac{\partial}{\partial\tilde{t}}\underline{\tilde{\boldsymbol{\tau}}}_p = \frac{\lambda\mathsf{U}}{\mathsf{L}}\left[(\nabla_{\tilde{\boldsymbol{r}}}\tilde{\boldsymbol{u}})^{\mathrm{T}}\,\underline{\tilde{\boldsymbol{\tau}}}_p + \underline{\tilde{\boldsymbol{\tau}}}_p\,(\nabla_{\tilde{\boldsymbol{r}}}\tilde{\boldsymbol{u}}) - (\tilde{\boldsymbol{u}}\cdot\nabla_{\tilde{\boldsymbol{r}}})\,\underline{\tilde{\boldsymbol{\tau}}}\right] + \frac{\mu_p}{\mu_s}\underline{\tilde{\dot{\boldsymbol{\gamma}}}} - \underline{\tilde{\boldsymbol{\tau}}}_p. \tag{191}$$

which, upon writing $\underline{\tilde{\boldsymbol{\tau}}} \equiv \Gamma\underline{\tilde{\boldsymbol{s}}}$ and setting $\mathsf{T} = \lambda$ can be further manipulated. Explicitly requiring that $\mathsf{Re} = 0$, the reduced momentum transport and constitutive equation read

$$\underline{\boldsymbol{\Delta}}_{\tilde{\boldsymbol{r}}}\tilde{\boldsymbol{u}} = \nabla_{\tilde{\boldsymbol{r}}}\tilde{p} - \Gamma\nabla_{\tilde{\boldsymbol{r}}}\cdot\underline{\tilde{\boldsymbol{s}}} - \tilde{\boldsymbol{f}}_{\mathrm{ext}}; \tag{192}$$

$$\frac{\partial}{\partial\tilde{t}}\underline{\tilde{\boldsymbol{s}}} = \underline{\tilde{\dot{\boldsymbol{\gamma}}}} - \underline{\tilde{\boldsymbol{s}}} + \mathsf{Wi}\left[(\nabla_{\tilde{\boldsymbol{r}}}\tilde{\boldsymbol{u}})^{\mathrm{T}}\,\underline{\tilde{\boldsymbol{s}}} + \underline{\tilde{\boldsymbol{s}}}\,(\nabla_{\tilde{\boldsymbol{r}}}\tilde{\boldsymbol{u}}) - (\tilde{\boldsymbol{u}}\cdot\nabla_{\tilde{\boldsymbol{r}}})\,\underline{\tilde{\boldsymbol{s}}}\right]. \tag{193}$$

Here, we can appreciate the way in which Wi charts the departure from $\underline{\boldsymbol{s}} = \underline{\dot{\boldsymbol{\gamma}}}$. At low Wi, this provides an excellent initial guess for any iterative solving scheme. However, Eq. (193) is also unsatisfying in the sense that the key components of the definition of the upper-convected derivative can now be scaled out. This, however, should not be problematic in the limit $\mathsf{Wi} \downarrow 0$, since then there will be no elastic stress component.

A final thing to note for Eq. (193) is that for $\mathsf{Wi} \gtrsim 1$, we can have situations where $\underline{\boldsymbol{s}} \propto (\boldsymbol{u})^2$. This is because the elastic stress itself scales with velocity and the convected-derivative terms contain products of gradients of $\boldsymbol{u}$ and $\underline{\boldsymbol{s}}$. Thus, even at zero Reynolds number, we reintroduce time-dependence and more importantly nonlinearities in the dependence of the momentum transport equation on the velocity *via* the $\Gamma\nabla_{\tilde{\boldsymbol{r}}}\cdot\underline{\tilde{\boldsymbol{s}}}$ term. This can lead to the emergence of zero-Re turbubulence, often referred to as elastic turbulence, at often surprisingly low values of Wi [3, 97, 98].

Exercise 46: In this exercise, we revisit the scenario sketched in Exercise 31, albeit for an Oldroyd-B fluid rather than a Newtonian one. Examine the script "oldroyd_b_force_roller_exercise.py". This gives a `Python` implementation the discrete-projection solver, which has been modified to deal with the reduced form of the Oldroyd-B equation provided in Eq. (193).

(a) Read through the provided scripts and try to understand how the projection formalism has been implemented.

(b) Look up the paper "Emergence of singular structures in Oldroyd-B fluids" by Becca Thomases and Michael Shelly [99] and quickly read through the text.

(c) Complete the script and reproduce their $\mathsf{Wi} = 0.3$ and 0.6 results for the stress field in their Fig. 2. N.B. you do not need to go to their level of grid refinement.

(d) What is the physical interpretation of the stress patterns that you observe?

If you are feeling ambitious, you can circumvent the time-dependent solving by using iterative minimization. Alternatively, you can try your hand at the $\mathsf{Wi} = 5$ solution.

B. Going beyond Oldroyd-B

As we have seen in Exercise 44, there can be issues in working with this model for extensional flows. Referencing Chapter III, we realize that we can modify the Oldroyd-B constitutive equation with terms that are objective to compensate for unphysical behavior. A standard addition would be $\underline{\dot{\gamma}}\underline{\dot{\gamma}}$, *i.e.*, the rate-of-strain tensor acting on itself, which makes the medium a *second-order fluid*. Taking this to its limiting form, we can, for example, include all possible (independent) tensorial invariants up to second order [20], resulting in the Oldroyd 8-constant model

$$\underline{\boldsymbol{\tau}} + \lambda_1 \overset{\triangledown}{\underline{\boldsymbol{\tau}}} + \lambda_2 \left(\underline{\dot{\gamma}}\underline{\boldsymbol{\tau}} + \underline{\boldsymbol{\tau}}\underline{\dot{\gamma}} \right) + \lambda_3 \mathrm{Tr}\left(\underline{\boldsymbol{\tau}}\right) \underline{\dot{\gamma}} + \lambda_4 \left(\underline{\boldsymbol{\tau}} : \underline{\dot{\gamma}} \right) \mathbb{I}_3 = \mu \left[\underline{\dot{\gamma}} + \lambda_5 \overset{\triangledown}{\underline{\dot{\gamma}}} + \lambda_6 \underline{\dot{\gamma}}\underline{\dot{\gamma}} + \lambda_7 \left(\underline{\dot{\gamma}} : \underline{\dot{\gamma}} \right) \mathbb{I}_3 \right]. \tag{194}$$

In practice, this form has limited use, as there are too many fit parameters to be determined in most reasonable experiments and too large a parameter space to scan in order to do theory.

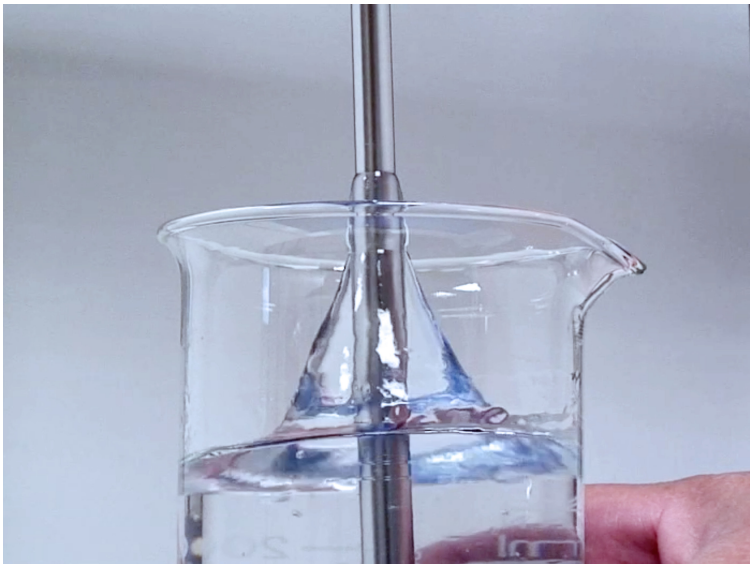

FIG. 14. **Visualization of the rod-climbing effect.** A 2% solution of high molecular weight polyacrylamide is stirred in a beaker using a smooth metal rod. Source: Wikimedia Commons.

Exercise 47: Consider the geometry of the rod climbing problem, see Fig. 14. A cylinder of radius a is rotating concentrically within a cylinder of larger radius R with angular frequency Ω. The bottom half of the cylinder is filled with a second-order fluid satisfying the stress $\underline{\boldsymbol{\sigma}}$ to shear-rate $\underline{\dot{\gamma}}$ relation

$$\underline{\boldsymbol{\sigma}} = -p\mathbb{I} + \mu_s \underline{\dot{\gamma}} - \mu_p \overset{\triangledown}{\underline{\dot{\gamma}}} + \beta \underline{\dot{\gamma}}\underline{\dot{\gamma}}, \tag{195}$$

where p is the pressure, μ_s the dynamic viscosity of the fluid and μ_p that of the second (let us say the polymer) fraction, β is a higher-order viscosity. We can assume that the last two terms are small compared to the first two on the right-hand side of Eq. (195), *i.e.*, the effect of the polymers is small. The top half is filled with say air and there is an interface that separates the viscoelastic fluid from the air. Let $z = h(r)$ measure the height profile of this interface, where r measures the radial distance and z the height along the cylinder. For convenience, you may assume that $h(r) = 0$ when the rod does not rotate.

(a) Consider the expression for $\underline{\boldsymbol{\sigma}}$ in cylindrical coordinates and derive expressions for σ_{rr}, $\sigma_{\theta r}$, σ_{zz}, and $\sigma_{\theta\theta}$, where θ is the azimuthal component. Show that in steady state the expression

$$0 = \frac{\partial \sigma_{rr}}{\partial r} + \frac{\sigma_{rr} - \sigma_{\theta\theta}}{r}, \tag{196}$$

holds and use it to establish the pressure profile

$$p(r) = \frac{1}{2}\left(\mu_p + \beta\right)\dot{\gamma}^2 - f(z), \tag{197}$$

where $f(z)$ is a function that will need to be specified.

(b) Show that the axial hydrostatic balance reads

$$\frac{\partial \sigma_{zz}}{\partial z} + g\rho = 0, \tag{198}$$

with g the gravitational acceleration and ρ the net fluid mass, and integrate this to obtain $p(r) = g\rho\left(h(r) - z\right)$, where we assume that $p = 0$ at the interface. Choose $f(z)$ appropriately to obtain the final expression

$$h(r) = \frac{1}{g\rho}\left(\mu_p + \beta\right)\frac{\Omega^2 a^4}{r^4}. \tag{199}$$

We can conclude that as long as $\mu_p + \beta > 0$, there will be some rod climbing in the fluid. Note, however, that we have not accounted for the fact that rotation will also cause part of the fluid to spin outward, provided we are rotating sufficiently fast.

Another way to improve the Oldroyd-B model is to introduce a maximum extension length to the springs that make up the polymer fluid. This is known as the *finitely extensible nonlinear elastic Peterlin* model, or *FENE-P* model, after Anton Peterlin. The equations for FENE-P read

$$\nabla_{\boldsymbol{r}} \cdot \boldsymbol{u} = 0; \tag{200}$$

$$\rho\left(\frac{\partial}{\partial t} + \boldsymbol{u}\cdot\nabla_{\boldsymbol{r}}\right)\boldsymbol{u} = -\nabla_{\boldsymbol{r}} p + \mu_s \underline{\boldsymbol{\Delta}}_{\boldsymbol{r}}\boldsymbol{u} + \nabla_{\boldsymbol{r}}\cdot\underline{\boldsymbol{\tau}}_p + \boldsymbol{f}_{\text{ext}}; \tag{201}$$

$$\overset{\triangledown}{\underline{\boldsymbol{\sigma}}}_p = -\frac{1}{\lambda}\left(f(\sigma_p^t)\underline{\boldsymbol{\sigma}}_p - \mathbb{I}_3\right); \tag{202}$$

$$\underline{\boldsymbol{\tau}}_p = -\mu_p \overset{\triangledown}{\underline{\boldsymbol{\sigma}}}_p, \tag{203}$$

where $\sigma_p^t = \text{Tr}\left(\underline{\boldsymbol{\sigma}}_p\right)$ and

$$f(x) = \frac{l^2 - 3}{l^2 - x^2}, \tag{204}$$

which diverges as $x \to l$ with l the maximal extension [100].

Exercise 48: Consider the FENE-P model. Here, we will show that this improves upon the issues that were identified in Exercise 44 for the Oldroyd-B model.

(a) Perform dimensional reduction on this set of equations and identify the Weissenberg number.

Consider a simple, 2D, zero-Reynolds-number, and time-independent extensional flow $\boldsymbol{u} = (\dot{\epsilon}x, -\dot{\epsilon}y)$, with $\dot{\epsilon}$ a constant that is similar in nature to $\dot{\gamma}$, but instead measures the rate of uniaxial stretching rather than shear. Note that we have the signs chosen such that the flow is incompressible. Define the extensional viscosity as

$$\mu_{\text{ext}} = \frac{\sigma_{xx} - \sigma_{yy}}{\dot{\epsilon}}. \tag{205}$$

(b) What is the value of μ_{ext} for a Newtonian fluid? And how does that compare to the expression for the FENE-P fluid? Hint: assume that $\underline{\boldsymbol{\sigma}}_p$ is independent of time and position, and use `Mathematica` to express μ_{ext} in terms of σ_p^t (reduced polymer stress). You will find that when $l \neq \sqrt{3}$

$$2\lambda\dot{\epsilon}\sigma_p^t = f(\sigma_p^t)\left(\sigma_{p,xx} - \sigma_{p,yy}\right). \tag{206}$$

(c) Referencing the relation between l and σ_p^t explain using this expression how FENE-P resolves the issue that is present in the Oldroyd-B mode, for which we have instead $f(x) = 1$.

C. Active Particles

Let us now turn our attention to systems that are intrinsically far away from equilibrium. Active matter is a term that describes a class of systems, in which energy is constantly consumed to perform work, and broadly can be found in all the known phases: gas, liquid, fluid, solid, and several (presumably all) liquid-crystalline mesophases. These systems defy description using the standard framework of statistical mechanics, due to their strong departure from equilibrium, despite having apparent similarities to their passive counterparts. We have seen an example of active particles already in Chapter VI, where we discussed the motion of a microorganism in water and how this impacts particles in the swimmer's surrounding.

Activity is the norm in biology. On our length scale, we encounter flocks of birds [101], schools of fish [102], and, of course, human crowds [103–105]; on the mesoscopic level examples are found in dividing and moving bacteria [106–108], sperm [109–111], and algae [112, 113]; and on the nanoscopic level, transport along the cytoskeleton is achieved by myosin motors [114].

Recent years have seen a huge increase in studies into systems consisting of self-propelled particles, in particular artificial ones in the colloidal regime [115–128]. These self-propelled colloids show promise as physical model systems for complex biological behavior (bacteria moving collectively) and could be used to answer fundamental questions concerning out-of-equilibrium statistical physics [129, 130]. From the perspective of physical chemistry, much remains poorly understood about the way many of these artificial swimmers move [126, 131–137] and form collective states. This makes the field of active matter fruitful for experimental study and provides ample opportunity for interaction with theory.

The above exemplifies the range of length and time scales, which the field of active matter encompasses, as well as its diversity. Physical features of interest in these systems are the apparent

ability to 'phase separate' at much lower density than in equilibrium. One form of such a *non-equilibrium* phase transition is found in the *Vicsek model*, which was derived by Tamás Vicsek and collaborators in 1995 [138]. We will see how this model works, comment on why it is an example of 'dry' active matter [139], and discuss the effective hydrodynamic theory that is associate it with it. Then we turn to wet active matter, which we discussed before in Chapter VI, and see a surprising connection to Oldroyd-B fluids, as we introduced in this chapter.

D. The Vicsek Model

The *Vicsek model* was developed by Vicsek *et al.* [138], who hybridized elements of classical equilibrium models with non-equilibrium features that made the system active. In many regards, the Vicsek model has more the flavor of an algorithm, as we will see shortly, and it has been studied computationally by the original authors and many others. The work by Refs. [140, 141] greatly helped clarify features of the model, but many (often subtle) variants have been proposed and considered. It can be argued that the Vicsek model serves as fundamental a role to the (motile) active-matter community, as the Ising model does for the classical statistical-physics community.

The Vicsek model is defined by the *overdamped* dynamics of a collection of self-propelled particles (originally) in 2D at density ρ_0. For the purpose of an algorithm, this will typically be a square simulation volume with periodic boundary conditions and edge length L. The particles are at positions $\boldsymbol{r}_i(t)$ moving along the direction specified by the unit vector $\hat{\boldsymbol{n}}_i(t)$. Here, i is the index and t denotes the time. All particles move with the same constant speed v_0, according to the time-discrete (step size Δt) dynamics

$$\boldsymbol{r}_i(t+\Delta t) = \boldsymbol{r}_i(t) + v_0 \Delta t \hat{\boldsymbol{n}}_i(t), \tag{207}$$

so that orientation and particle velocity have the same direction. There is no momentum conservation in the Vicsek model, which makes it an example of 'dry' active matter, *i.e.*, which captures motion of particles not suspended in a fluid medium.

Recall that the ferromagnetic variant of the Ising model has the property that alignment lowers the local energy. Borrowing from the Ising model, Vicsek made the analogy that the direction of motion of a particle is modified by the direction of its neighbors. Because the model is off lattice, this interaction has a range R_0, see Fig. 15 for an illustration. In 2D, we can capture the i-th particle's orientation using an angle $\theta_i(t)$ (recall the ABP argument), leading to the following angular dynamics

$$\theta_i(t+\Delta t) = \langle \theta_j(t) \rangle_{|\boldsymbol{r}_j(t)-\boldsymbol{r}_i(t)|<R_0} + \Delta\theta, \tag{208}$$

where $\Delta\theta$ is chosen with uniform probability from the interval $[-\eta/2, \eta/2]$. The alignment of a given particle becomes the average — indicated here using the angular brackets and subscript — of all particles in the interaction range. One could think of birds in a flock coordinating with their neighbors but making small mistakes in doing so.

The parameters defining the Vicsek model are ρ_0, v_0, R_0, and η. However, v_0 can be used to set a time scale in combination with R_0, leaving only ρ_0 and η to control the phase behavior, for a given v_0-R_0 combination. The phase behavior is illustrated in Fig. 15. Note specifically that the microphase separated system exhibits a dynamical behavior that is reminiscent of flocking in biological systems. The simple nature of the Vicsek model and its ability to have qualitative similarities to intricate dynamics in biology prompted considerable attention. This has led to an overall shift of the activities of the physics community toward the open problems that are present in biological and even social systems. Considerable time and effort have been spent figuring out the

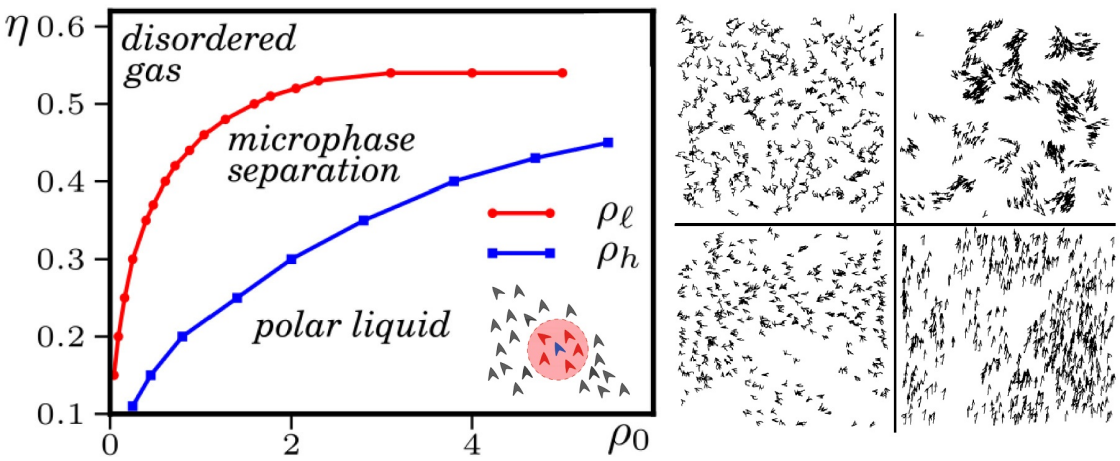

FIG. 15. **The Vicsek Model:** (left panel) The phase diagram for the Vicsek model — density ρ_0 and the strength of the noise interfering with alignment η are on the respective axes — identifying the three major phases and the parameters for which the transitions occur, taken from Ref. [142]. The colored curves indicate the binodals to the phase separating region. The bottom-right inset visualizes the alignment rule, which was taken from Ref. [143]. (right panel) Snapshots of various phases from the original paper by Vicsek *et al.* [138], showing $N = 300$ self-propelled particles using small wedges. (top-left) Initial condition given by the isotropic phase. (top-right) Low-density and low-noise lead to flocking or equivalently a microphase-separated system. (bottom-left) High-density and high-noise lead to a disordered phase. (bottom-right) High-density and low-noise lead to a polar liquid.

order of the phase transition in the Vicsek model, which turns out to be quite sensitive to finite-size effects in numerical calculations. Guillaume Grégoire and Hugues Chaté eventually determined that the transition is *first* order [140].

Exercise 49: Implement the Vicsek model and study its phase behavior numerically. Reproduce the isotropic, flocking, and polar liquid states.

In relation to the theme of the course, it should be noted that the Vicsek model is particle conserving and that the speed of the particles is not lost. That is, there is conservation of the activity. It turns out that on sufficiently long length and time scales, the behavior is amenable to an effective hydrodynamic description, in terms of the mass density ρ and particle velocity $\boldsymbol{v}$. The equations that follow from either a lengthy derivation [144] or understanding of the underlying symmetries of the problem [31]. John Toner and Yuhai Tu took the latter route [145] and postulated equations that read

$$\frac{\partial}{\partial t}\rho + \nabla_{\boldsymbol{r}} \cdot (\rho \boldsymbol{v}) = 0, \tag{209}$$

which is simply a statement of mass conservation or equivalently particle conservation, as we have seen before for hydrodynamic models. The velocity changes according to

$$\begin{aligned}\frac{\partial}{\partial t}\boldsymbol{v} + \lambda_1(\boldsymbol{v}\cdot\nabla_{\boldsymbol{r}})\boldsymbol{v} + \lambda_2(\nabla_{\boldsymbol{r}}\cdot\boldsymbol{v})\boldsymbol{v} + \lambda_3\nabla_{\boldsymbol{r}}(v^2) = \\ (\alpha - \beta v^2)\boldsymbol{v} - \nabla_{\boldsymbol{r}}P + D_{\mathrm{B}}\nabla_{\boldsymbol{r}}\left(\nabla_{\boldsymbol{r}}\cdot\boldsymbol{v}\right) + D_{\mathrm{T}}\underline{\boldsymbol{\Delta}}_{\boldsymbol{r}}\boldsymbol{v} + D_2\left(\boldsymbol{v}\cdot\nabla_{\boldsymbol{r}}\right)^2\nabla_{\boldsymbol{r}} + \boldsymbol{f},\end{aligned} \tag{210}$$

which should look reminiscent of momentum transport equations, with a bunch of extra terms. Let us go through the equations one step at a time.

Here, we have that the parameters β, D_B, D_2, and D_T are all positive, and $\alpha < 0$ in the disordered phase and $a > 0$ in the ordered state. You will recognize a second-order Landau-theory like argument for the speed $v = |\boldsymbol{v}|$ in the factor $\alpha - \beta v^2$. This ensures that $\boldsymbol{v}$ has a nonzero local magnitude given by $\sqrt{\alpha/\beta}$ in the ordered phase when $\alpha > 0$. The various diffusion coefficients D_i reflect that a localized fluctuation in the velocity spreads out, because of coupling between neighboring particles. The term $\boldsymbol{f}$ introduces a noise, which may be assumed Gaussian, or tuned to the specifics of the problem.

Exercise 50: What is the physical interpretation of the D_B, D_2, and D_T terms in Eq. (210)? That is, what kind of diffusion are they capturing, explain your answer in a *few* words. Hint: your answer should reflect how diffusion is commonly associated with a spreading out of a quantity, but here the terms are meant to do something different for the flocks that form.

Turning to the left-hand side of Eq. (210), we see that there are terms and weights other than the usual $\partial/(\partial t) - \boldsymbol{v} \cdot \nabla_{\boldsymbol{r}}$ that we have derived for momentum transport. All λ terms are analogs of the usual convective derivative of the coarse-grained velocity field $\boldsymbol{u}$ in the Navier-Stokes equations (2). However, for an active system, Galilean invariance is not assumed to hold, which allows all three combinations of one spatial gradient and two velocities that transform like vectors to be present. If Galilean invariance did apply here, as it would for flow problems, it would force $\lambda_2 = \lambda_3 = 0$ and $\lambda_1 = 1$. The former is appropriate for creatures moving in the presence of friction over (or through) a static medium, *e.g.*, wildebeest moving over the surface of the Serengeti plane, bacteria crawling over the surface of a Petri dish, *etc.* The latter, is appropriate for creatures moving through a medium which is itself fluid (*e.g.*, the air birds fly through, the water fish swim through). In these cases, there should be conservation laws for the total momentum of flock plus background fluid. At the level of the theory by Toner and Tu [31, 145], all three coefficients are nonzero phenomenological parameters whose nonuniversal values are determined by the microscopic rules.

Finally, because the Vicsek flocks have spatially varying density, we require an expression for the pressure as a function of density. This would need to be determined for a specific model, but can be formally written as

$$P = \sum_{n=1}^{\infty} b_n \left(\rho - \rho_0\right)^n , \tag{211}$$

in an almost virial-expansion type manner, with the b_n expansion weights. Here, instead, an expansion about the mean density ρ_0 was chosen. Toner and Tu remark that here too, strictly speaking, the most general form of the expression should allow for gradients along and transverse to $\boldsymbol{v}$. In equilibrium isotropy of the pressure is guaranteed by Pascal's law, but this cannot be invoked for a non-equilibrium system.

We refer the interested reader to Refs. [31, 146] for additional details. Therein a theoretical analysis of Eq. (210) is performed that shows the way the system phase transitions and to which universality class its critical behavior belongs. Numerically solving the Toner-Tu model is also possible [147], but goes beyond the scope of these notes.

E. Wet Active Matter and Active Turbulence

Finally, let us turn to the topic of wet active matter and its relation to active turbulence[59]. This is another form of turbulence that is observed at low values of the Reynolds number. Spontaneous chaotic flows were found in a bacterial suspension [148]. Hence, they were initially called

[59] This section of the notes largely follows the discussion in Ref. [33] initially. The second part takes more inspiration from the discussion in Ref. [32].

bacterial turbulence. In the following decade, turbulent-like flows were discovered and characterized in several other active fluids, often of biological origin. Examples include different bacterial suspensions [106, 148, 149], swarming sperm [150], suspensions of microtubules and molecular motors [151–154], tissue cell monolayers [155, 156], and suspensions of artificial self-propelled particles [157]. A key difference between active, and inertial and elastic turbulence is that for the latter, the scale at which energy is injected is imposed by external driving. In contrast, active flows are autonomous, and the pattern of energy injection is self-organized. In other words, the spectrum of energy injection is not an input of the problem but part of its solution. Consequently, both energy injection and dissipation are peaked at similar scales, and hence one may not expect energy cascades spanning an arbitrarily large range of scales as in traditional turbulence. Nevertheless, the spectra of energy injection and dissipation need not be exactly equal, thus allowing for energy transfer across scales, like the ones observed in the well-known initial Kolmogorov cascade [158]; for inertial turbulence we expect to see $E(k) \propto k^{-5/3}$ in Fourier space. Regardless of the nature of the energy cascade, active turbulence can exhibit scale-free correlations.

Active turbulence has been studied extensively theoretically and computationally. Recent studies have focused on the spectral properties of continuum models [159–163], where the active fluid is described as an effective medium, whose equations are inspired by nematodynamics [164–166] and pattern formation [167]. In many approaches, the concentration of active particles is highly, such that excluded volume and alignment (collisional dynamics) dominate. In the dilute suspensions, it has been shown that hydrodynamic interactions can cause active turbulence [32, 168, 169].

Now let us briefly make the connection to the elastic Oldroyd-B model that we have seen previously for the topic of active turbulence. Hydrodynamic theories describe wet active suspensions in terms of the concentration field ρ for the microorganisms or swimmers. This is complemented by a description of the incompressible fluid velocity field $\boldsymbol{u}$ and an order parameter quantifying the degree of local orientation $\boldsymbol{p}$, which represents the average, within a fluid element, of the swimmers' direction, *i.e.*, $\boldsymbol{p} \propto \langle \hat{\boldsymbol{n}}_i \rangle$ and is thus not a unit vector. In semi-dilute suspensions, hydrodynamic interactions can induce local (even global) alignment, which makes $\boldsymbol{p}$ a meaningful measure.

Exercise 51: Convince yourself that two swimmers moving along non-quite parallel trajectories, will align themselves, by making use of the expressions for their flow field and Faxés laws.

Assuming for simplicity that microswimmer density remains roughly constant, which is very much unlike the situation that we encountered in the Vicsek model, and that $\boldsymbol{p}$ is divergence free, then the equations of motion for the system read

$$\nabla_{\boldsymbol{r}} \cdot \boldsymbol{u} = 0; \tag{212}$$

$$\rho \left(\frac{\partial}{\partial t} + \boldsymbol{u} \cdot \nabla_{\boldsymbol{r}} \right) \boldsymbol{u} = -\nabla_{\boldsymbol{r}} p + \mu \underline{\boldsymbol{\Delta}}_{\boldsymbol{r}} \boldsymbol{u} + \zeta \nabla_{\boldsymbol{r}} \cdot (\boldsymbol{p} \otimes \boldsymbol{p}) ; \tag{213}$$

$$\left(\frac{\partial}{\partial t} + (\boldsymbol{u} + \xi \boldsymbol{p}) \cdot \nabla_{\boldsymbol{r}} \right) \boldsymbol{p} = \frac{1}{2} \underline{\boldsymbol{\omega}} \boldsymbol{p} - \Gamma \boldsymbol{p} + D \underline{\boldsymbol{\Delta}}_{\boldsymbol{r}} \boldsymbol{p}. \tag{214}$$

Here, we have the usual incompressibility condition in Eq. (212). Because the whole system is Galilei invariant, the left-hand side of Eq. (213) has the usual form. On the right-hand side, we see pressure and viscosity (μ) terms, as well as one $\zeta \boldsymbol{p} \otimes \boldsymbol{p}$ that represents the active stress, with ζ a proportionality constant. Note that the local orientation $\boldsymbol{p}$ has a corrected material derivative, see Exercise 52. The tensor $\underline{\boldsymbol{\omega}}$ represents the anti-symmetric part of the velocity gradient, as defined in Eq. (60). The prefactor Γ acts like a friction to local reorientation, which suppresses the natural tendency of the orientation to diffuse (coefficient D) through, *e.g.*, collisions and thermal noise.

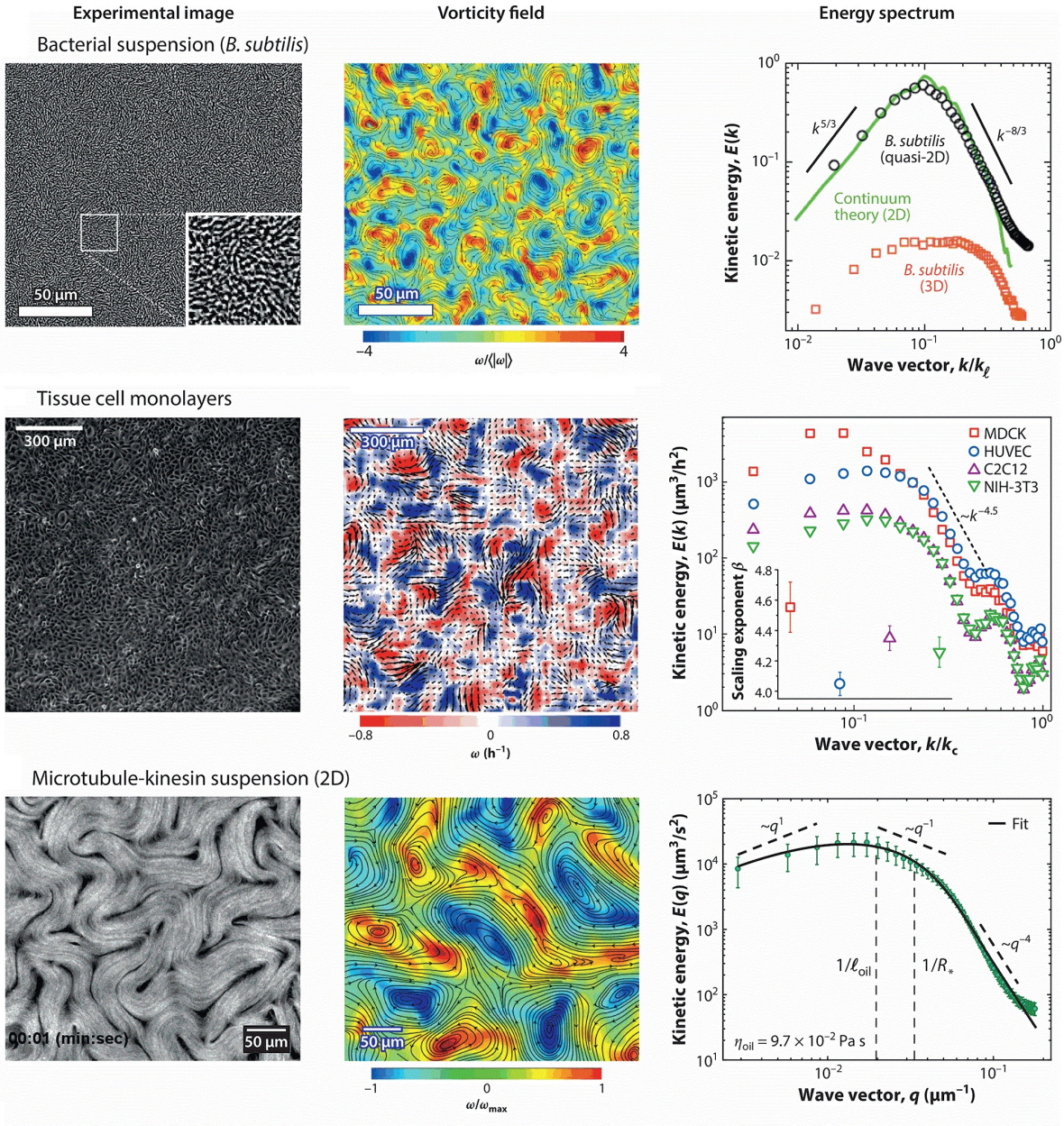

FIG. 16. **Signatures of active turbulence in experimental systems:** The columns show from left to right: an image of the system, a snapshot of the vorticity field (with either streamlines or the flow field), and the measured energy spectrum. For the MDCK cells, the different spectra correspond to different cell types. The experiments on bacteria are from Ref. [149], the epithelial monolayer results come from Ref. [156], and the microtubule panels are from Refs. [152, 154]. Image layout was adopted from Ref. [33].

Exercise 52: In this exercise, we are going to gain further understanding of how to arrive at Eqs. (213) and (214). Assume that we consider an upper-convected-Maxwell-like fluid, where the stress tensor can be written as $\underline{\boldsymbol{\tau}} = \boldsymbol{p} \otimes \boldsymbol{p}$, *i.e.*, as a dyadic product of a vectorial quantity.

(a) What does $\boldsymbol{p} \otimes \boldsymbol{p}$ represent physically in terms of the swimmer's orientation and why is it appropriate for this to induce a stress on the fluid? Explain your answer in a *few* words.

(b) Write down the appropriately transforming time derivative for the vector $\boldsymbol{p}$, referencing the expressions in Section III B.

(c) Assume there is a single relaxation time λ to this problem and write down the appropriate differential equation for the relaxation of $\boldsymbol{p}$. How do Γ (in Eq. (214)) and λ relate? Show that you can also get the regular material derivative and $\underline{\boldsymbol{\omega}}\boldsymbol{p}/2$ term from this. Why does that make sense, if you think in terms of Faxén's laws? Explain using a *few* words only.

(d) Why should we *not* have a term that accounts for contributions of $\underline{\dot{\boldsymbol{\gamma}}}$ on $\boldsymbol{p} \otimes \boldsymbol{p}$, as we are used to from the upper-convected Maxwell model, if we think of small spherical swimmers? Explain this in a *few* words, referencing what this term's effect is on a fluid of dumbbels connected by springs. Argue why a term like $\underline{\boldsymbol{\omega}}\boldsymbol{p}$ should, however, appear in Eq. (214) for a suspension of swimmers in a *few* words.

(e) We had already explained the term D in the main text, so that the only term remaining that needs clarification is $\xi\,(\boldsymbol{p}\cdot\nabla_{\boldsymbol{r}})\,\boldsymbol{p}$. Examine Ref. [30], which we had already encountered in Section III B, and establish its origin. What does ξ represent and when can this be set to zero? Explain your answer using a *few* words.

(f) Argue from the shape of the equations or from the analogy to the *vectorial* form of the Oldroyd-B model, how the active suspension can exhibit turbulence.

The equation system can be examined further using a method called the *shell model*, which has seen use in the study of elastic turbulence, we refer the interested reader to Ref. [32] for more information.

Where to next? In this chapter, we have seen how to formulate general constitutive equations and how simple non-Newtonian fluids behave. Recently, there is renewed attention in the community for the discrete nature of the medium, rather than describing this as a continuum. Often, local microstructure is relevant to understanding the dynamics of such systems, rather than its continuum properties, *e.g.*, see Refs. [170, 171] when this involves microswimmers. There are also many questions that need resolution, when it comes to the behavior of active particles in complex fluids, which can be both fundamental in nature and simultaneously have medical relevance. Lastly, we should note that in general the field of soft (active) matter is moving more toward the study of systems with intelligence [172] or which can proliferate [173].

[1] J. Blake, *A spherical envelope approach to ciliary propulsion*, J. Fluid Mech. **46**, 199 (1971).
[2] A. Mathijssen, M. Lisicki, V. Prakash, and E. Mossige, *Culinary fluid mechanics and other currents in food science*, Rev. Mod. Phys. **95**, 025004 (2023).
[3] A. Groisman and V. Steinberg, *Elastic turbulence in a polymer solution flow*, Nature **405**, 53 (2000).
[4] S. Frontinus and C. Herschel, *The Two Books on the Water Supply of the City of Rome of Sextus Julius Frontinus, Water Commissioner of the City of Rome AD 97: A Photographic Reproduction of the Sole Original Latin Manuscript, and Its Reprint in Latin* (D. Estes & Company, Boston (USA), 1899).
[5] L. Euler, *Principes Généraux du Mouvement des Fluides*, Acad. Roy. Sci. Belles-Lett. Berlin **11**, 1 (1755).
[6] J. L. R. d'Alembert, *Essai d'une Nouvelle Théorie de la Résistance des Fluides* (David l'aîné, Paris (FR), 1752).
[7] R. Bird, E. Lightfoot, and W. Stewart, *Transport Phenomena* (John Wiley & Sons, Hoboken (USA), 1960).
[8] P. Kapitza, *Viscosity of liquid helium below the λ-point*, Nature **141**, 74 (1938).
[9] C. Navier, *Sur les Lois des Mouvement des Fluides, en Ayant Egard a L'adhesion des Molecules*, Ann. Chim. Paris **19**, 244 (1821).
[10] S. Marbach and L. Bocquet, *Active osmotic exchanger for efficient nanofiltration inspired by the kidney*, Phys. Rev. X **6**, 031008 (2016).
[11] M. Lighthill, *On the squirming motion of nearly spherical deformable bodies through liquids at very small Reynolds numbers*, Commun. Pure Appl. Math. **5**, 109 (1952).
[12] E. Purcell, *Life at low Reynolds number*, Am. J. Phys. **45**, 3 (1977).
[13] P. Lynch, *The emergence of numerical weather prediction: Richardson's dream* (Cambridge University Press, Cambridge (UK), 2006).
[14] G. Vallis, *Geophysical fluid dynamics: whence, whither and why?*, Proc. Roy. Soc. A **472**, 20160140 (2016).
[15] C. Hill and J. Marshall, *Parallel Computational Fluid Dynamics 1995* (Elsevier, Amsterdam (NL), 1996), p. 545.
[16] W. Freeden, C. Gerhards, and H. Nutz, *Modeling Oceanic Flow: From Global Navier–Stokes to Local Geostrophic Wavelet Modeling*, Encyclopedia of Geodesy **2015**, 1 (2015).
[17] P. Melchior, *The physics of the earth's core: an introduction* (Elsevier, Amsterdam (NL), 2013).
[18] S. Shore, *Astrophysical hydrodynamics: an introduction* (John Wiley & Sons, Hoboken (USA), 2008).
[19] H. Alfvén, *Existence of electromagnetic-hydrodynamic waves*, Nature **150**, 405 (1942).
[20] A. Morozov and S. Spagnolie, *Complex Fluids in Biological Systems* (Springer, New York (USA), 2015), pp. 3–52.
[21] A. Brunk, J. Chaudhuri, M. Lukacova-Medvidova, and B. Duenweg, *Fundamentals of the Oldroyd-B model revisited: Tensorial vs. vectorial theory*, arXiv **2308.01326**, 1 (2023).
[22] S. Kim and S. Karrila, *Microhydrodynamics: Principles and Selected Applications* (Courier Corporation, Mineola (USA), 2013).
[23] L. Landau and E. Lífshítz, *Fluid Mechanics* (Pergamom Press, Oxford (UK), 1959), Vol. 6.
[24] G. Łukaszewicz and P. Kalita, *Navier–Stokes Equations: An Introduction with Applications* (Springer, New York (USA), 2016).
[25] D. Olbers, J. Willebrand, and C. Eden, *Ocean dynamics* (Springer Science & Business Media, Berlin (Germany), 2012).
[26] J. Serrin, *Fluid Dynamics I/Strömungsmechanik I* (Springer, New York (USA), 1959), p. 125.
[27] F. Bampi and A. Morro, *Objectivity and objective time derivatives in continuum physics*, Found. Phys. **10**, 905 (1980).
[28] M. Frewer, *Covariance and objectivity in mechanics and turbulence*, arXiv **1611.07002**, 1 (2016).
[29] H. Wilson, *Polymeric Fluids*, 2006.
[30] H. Stone, M. Shelley, and E. Boyko, *A note about convected time derivatives for flows of complex fluids*, Soft Matter **19**, 5353 (2023).
[31] J. Toner, Y. Tu, and S. Ramaswamy, *Hydrodynamics and phases of flocks*, Ann. Phys. **318**, 170 (2005).
[32] A. Gascó, I. Pagonabarraga, and A. Scagliarini, *Three-dimensional active turbulence in microswimmer*

suspensions: simulations and modelling, arXiv **2304.03662**, 1 (2023).
[33] R. Alert, J. Casademunt, and J.-F. Joanny, *Active turbulence*, Ann. Rev. Cond. Mat. Phys. **13**, 143 (2022).
[34] D. Bonn, M. Denn, L. Berthier, T. Divoux, and S. Manneville, *Yield stress materials in soft condensed matter*, Rev. Mod. Phys. **89**, 035005 (2017).
[35] R. Bird, R. Armstrong, and O. Hassager, *Dynamics of polymeric liquids. Vol. 1: Fluid mechanics* (John Wiley and Sons Inc., New York (USA), 1987).
[36] J. Choi, F. Nettesheim, and S. Rogers, *The unification of disparate rheological measures in oscillatory shearing*, Phys. Fluids **31**, 073107 (2019).
[37] C. Dreiss, *Wormlike micelles: where do we stand? Recent developments, linear rheology and scattering techniques*, Soft Matter. **3**, 956 (2007).
[38] K. Glaser, A. Manduca, and R. Ehman, *Review of MR elastography applications and recent developments*, J. Magn. Reson. Imaging **36**, 757 (2012).
[39] A. Amon, P. Born, K. Daniels, J. Dijksman, K. Huang, D. Parker, M. Schröter, R. Stannarius, and A. Wierschem, *Preface: Focus on imaging methods in granular physics*, Rev. Sci. Instrum. **88**, 051701 (2017).
[40] J. Oldroyd, *On the formulation of rheological equations of state*, Proc. Roy. Soc. Lond. Series A **200**, 523 (1950).
[41] R. Bird, C. Curtiss, R. Armstrong, and O. Hassager, *Dynamics of polymeric liquids. Vol. 2: Kinetic theory* (John Wiley and Sons Inc., New York (USA), 1987).
[42] M. Šilhavŷ, *On Cauchy's stress theorem*, Atti Accad. Naz. dei Lincei Cl. Sci. Fis. Mat. Nat. Rend. Lincei Mat. Appl. **1**, 259 (1990).
[43] F. Koenemann, *Cauchy's stress theory in a modern light*, Euro. J. Phys. **35**, 015010 (2013).
[44] I. Torres-Diaz, A. Cortes, Y. Cedeno-Mattei, O. Perales-Perez, and C. Rinaldi, *Flows and torques in Brownian ferrofluids subjected to rotating uniform magnetic fields in a cylindrical and annular geometry*, Phys. Fluids **26**, 012004 (2014).
[45] J. Maxwell, *V. Illustrations of the dynamical theory of gases.—Part I. On the motions and collisions of perfectly elastic spheres*, Philos. Mag. **19**, 19 (1860).
[46] J. Maxwell, *Xiii. the bakerian lecture.—on the viscosity or internal friction of air and other gases*, Philos. Trans. Royal Soc. London **156**, 249 (1866).
[47] R. Flood, M. McCartney, and A. Whitaker, *James Clerk Maxwell: perspectives on his life and work* (Oxford University Press, Oxford (UK), 2014).
[48] J. Perrin, *Mouvement Brownien et Réalité Moléculaire*, Ann. Chim. Phys. **18**, 5 (1909).
[49] E. Rutherford, *LXXIX. The scattering of α and β particles by matter and the structure of the atom*, Philos. Mag. **21**, 669 (1911).
[50] C. Brennen, *Fundamentals of multiphase flow*, (2005).
[51] O. Reynolds, *XXIX. An experimental investigation of the circumstances which determine whether the motion of water shall he direct or sinuous, and of the law of resistance in parallel channels*, Philos. Trans. Royal Soc. London **174**, 935 (1884).
[52] FlowKit, *FlowKit CFD Solutions*, `http://wiki.palabos.org/_media/numerics:lbmflowaroundcylinder.py.zip`, 2013, accessed: 2018-03-11.
[53] C. Williamson, *Vortex dynamics in the cylinder wake*, Ann. Rev. Fluid Mech. **28**, 477 (1996).
[54] T. von Kármán, *Über den Mechanismus des Widerstandes, den ein bewegter Körper in einer Flüssigkeit erfährt*, Nachr. Ges. Wissenschaft. Göttingen **1911**, 509 (1911).
[55] A. Mallock, *On the resistance of air*, Proc. Royal Soc. **A79**, 262 (1907).
[56] Bénard, *Formation périodique de centres de giration à l'arrière d'un obstacle en mouvement*, Comptes Rendus Acad. Sci **147**, 839 (1908).
[57] H. Schlichting, K. Gersten, E. Krause, H. Oertel, and K. Mayes, *Boundary-layer theory* (Springer, New York (USA), 1955), Vol. 7.
[58] B. Eckhardt, T. Schneider, B. Hof, and J. Westerweel, *Turbulence transition in pipe flow*, Annu. Rev. Fluid Mech. **39**, 447 (2007).
[59] T. Bergman, F. Incropera, D. DeWitt, and A. Lavine, *Fundamentals of heat and mass transfer* (John Wiley & Sons, Hoboken (USA), 2011).
[60] K. Burns, G. Vasil, J. Oishi, D. Lecoanet, and B. Brown, *Dedalus: A flexible framework for numerical simulations with spectral methods*, Phys. Rev. Research **2**, 023068 (2020).

[61] V. Girault and P.-A. Raviart, *Finite element methods for Navier-Stokes equations: theory and algorithms* (Springer Science & Business Media, Berlin (Germany), 2012).

[62] T. Krüger, H. Kusumaatmaja, A. Kuzmin, O. Shardt, G. Silva, and E. Viggen, *The Lattice Boltzmann Method* (Springer, New York (USA), 2017).

[63] G. Gompper, T. Ihle, D. Kroll, and R. Winkler, *Advanced computer simulation approaches for soft matter sciences III* (Springer-Verlag, Berlin (Germany), 2009).

[64] A. Najafi and R. Golestanian, *Propulsion at low Reynolds number*, J. Phys.: Cond. Mat. **17**, S1203 (2005).

[65] H. Berg, *The rotary motor of bacterial flagella*, Ann. Rev. Biochem. **72**, 19 (2003).

[66] C. Brokaw, D. Luck, and B. Huang, *Analysis of the movement of Chlamydomonas flagella: the function of the radial-spoke system is revealed by comparison of wild-type and mutant flagella*, J. Cell Biol. **92**, 722 (1982).

[67] L. af Klinteberg, D. Shamshirgar, and A.-K. Tornberg, *Fast Ewald summation for free-space Stokes potentials*, Res. Math. Sci. **4**, 1 (2017).

[68] J. de Graaf and J. Stenhammar, *Stirring by periodic arrays of microswimmers*, J. Fluid Mech. **811**, 487 (2017).

[69] C. Beenakker, *Ewald sum of the Rotne–Prager tensor*, J. Chem. Phys. **85**, 1581 (1986).

[70] J. Blake, *A note on the image system for a Stokeslet in a no-slip boundary*, Mat. Proc. Cambridge Phil. Soc. **70**, 303 (1971).

[71] H. Lorentz, *Abhandlungen über theoretische Physik* (B.G. Teubner, Leipzig & Berlin (Germany), 1907).

[72] Y. von Hansen, M. Hinczewski, and R. Netz, *Hydrodynamic screening near planar boundaries: Effects on semiflexible polymer dynamics*, J. Chem. Phys. **134**, 06B609 (2011).

[73] D. Pushkin, H. Shum, and J. Yeomans, *Fluid transport by individual microswimmers*, J. Fluid Mech. **726**, 5 (2013).

[74] H. Berg and D. Brown, *Chemotaxis in Escherichia coli analysed by three-dimensional tracking*, Nature **239**, 500 (1972).

[75] X.-L. Wu and A. Libchaber, *Particle diffusion in a quasi-two-dimensional bacterial bath*, Phys. Rev. Lett. **84**, 3017 (2000).

[76] P. Underhill, J. Hernandez-Ortiz, and M. Graham, *Diffusion and spatial correlations in suspensions of swimming particles*, Phys. Rev. Lett. **100**, 248101 (2008).

[77] J. Elgeti, U. Kaupp, and G. Gompper, *Hydrodynamics of sperm cells near surfaces*, Biophys. J. **99**, 1018 (2010).

[78] H. Faxén, Ph.D. thesis, Uppsala, 1921.

[79] H. Faxén, *Simplified representation of the generalized Green's equations for the constant motion of translation of a rigid body in a viscous fluid*, Ark. Mat. Astr. Fys. **20**, 1 (1927).

[80] J. de Graaf, K. Torre, W. Poon, and M. Hermes, *Hydrodynamic stability criterion for colloidal gelation under gravity*, Phys. Rev. E **107**, 034608 (2023).

[81] K. Torre and J. de Graaf, *Hydrodynamic lubrication in colloidal gels*, Soft Matter **19**, 7388 (2023).

[82] L. Koens and E. Lauga, *Slender-ribbon theory*, Phys. Fluids **28**, 013101 (2016).

[83] M. Palusa, J. de Graaf, A. Brown, and A. Morozov, *Sedimentation of a rigid helix in viscous media*, Phys. Rev. Fluids **3**, 124301 (2018).

[84] A. Goldman, R. Cox, and H. Brenner, *Slow viscous motion of a sphere parallel to a plane wall—I Motion through a quiescent fluid*, Chem. Eng. Sci. **22**, 637 (1967).

[85] J. Rotne and S. Prager, *Variational treatment of hydrodynamic interaction in polymers*, J. Chem. Phys. **50**, 4831 (1969).

[86] J. Brady and G. Bossis, *Stokesian dynamics*, Ann. Rev. Fluid Mech. **20**, 111 (1988).

[87] J. Morris, *Lubricated-to-frictional shear thickening scenario in dense suspensions*, Phys. Rev. Fluids **3**, 110508 (2018).

[88] D. Jeffrey and Y. Onishi, *Calculation of the resistance and mobility functions for two unequal rigid spheres in low-Reynolds-number flow*, J. Fluid Mech. **139**, 261 (1984).

[89] D. Jeffrey, *The calculation of the low Reynolds number resistance functions for two unequal spheres*, Phys. Fluids A **4**, 16 (1992).

[90] A. Fiore and J. Swan, *Fast stokesian dynamics*, J. Fluid Mech. **878**, 544 (2019).

[91] K. Torre and J. de Graaf, *Hydrodynamic Interactions in Particle Suspensions: A Perspective on Stokesian Dynamics*, arXiv **2503.16083**, 1 (2025).

[92] K. Torre, R. Schram, and J. de Graaf, *Python-JAX-based Fast Stokesian Dynamics*, arXiv **2503.07847**, 1 (2025).

[93] D. Palanisamy and W. den Otter, *Efficient Brownian Dynamics of rigid colloids in linear flow fields based on the grand mobility matrix*, J. Chem. Phys. **148**, 194112 (2018).

[94] R. Johnson and C. Brokaw, *Flagellar hydrodynamics. A comparison between resistive-force theory and slender-body theory*, Biophys. J. **25**, 113 (1979).

[95] J. Hinch and O. Harlen, *Oldroyd B, and not A?*, J. Nonnewton. Fluid Mech. **298**, 104668 (2021).

[96] G. Schramm, *A practical approach to rheology and rheometry* (Haake, Karlsruhe (Germany), 1994).

[97] V. Steinberg, *Elastic turbulence: an experimental view on inertialess random flow*, Ann. Rev. Fluid Mech. **53**, 27 (2021).

[98] S. Datta *et al.*, *Perspectives on viscoelastic flow instabilities and elastic turbulence*, Phys. Rev. Fluids **7**, 080701 (2022).

[99] B. Thomases and M. Shelley, *Emergence of singular structures in Oldroyd-B fluids*, Phys. Fluids **19**, 103103 (2007).

[100] K. Khambhampati and K. Rajagopal, *The derivation of the FENE-P model within the context of a thermodynamic perspective for bodies with evolving natural configurations*, Int. J. Non.Linear Mech. **134**, 103729 (2021).

[101] M. Ballerini *et al.*, *Interaction ruling animal collective behavior depends on topological rather than metric distance: Evidence from a field study*, Proc. Natl. Acad. Sci. **105**, 1232 (2008).

[102] Y. Katz, K. Tunstrøm, C. Ioannou, C. Huepe, and I. Couzin, *Inferring the structure and dynamics of interactions in schooling fish*, Proc. Nat. Acad. Sci. **108**, 18720 (2011).

[103] D. Helbing, I. Farkas, and T. Vicsek, *Simulating dynamical features of escape panic*, Nature **407**, 487 (2000).

[104] J. Zhang, W. Klingsch, A. Schadschneider, and A. Seyfried, in *Traffic and Granular Flow '11*, edited by V. V. Kozlov, A. P. Buslaev, A. S. Bugaev, M. V. Yashina, A. Schadschneider, and M. Schreckenberg (Springer, Berlin (Germany), 2013), p. 241.

[105] J. Silverberg, M. Bierbaum, J. Sethna, and I. Cohen, *Collective motion of humans in mosh and circle pits at heavy metal concerts*, Phys. Rev. Lett. **110**, 228701 (2013).

[106] A. Sokolov, I. Aranson, J. Kessler, and R. Goldstein, *Concentration dependence of the collective dynamics of swimming bacteria*, Phys. Rev. Lett. **98**, 158102 (2007).

[107] J. Schwarz-Linek, C. Valeriani, A. Cacciuto, M. E. Cates, D. Marenduzzo, A. N. Morozov, and W. C. K. Poon, *Phase separation and rotor self-assembly in active particle suspensions*, Proc. Nat. Acad. Sci. **109**, 4052 (2012).

[108] M. Reufer, R. Besseling, J. Schwarz-Linek, V. Martinez, A. Morozov, J. Arlt, D. Trubitsyn, F. Ward, and W. Poon, *Switching of swimming modes in magnetospirillium gryphiswaldense*, Biophys. J. **106**, 37 (2014).

[109] D. Woolley, *Motility of spermatozoa at surfaces*, Reproduction **126**, 259 (2003).

[110] I. Riedel, K. Kruse, and J. Howard, *A self-organized vortex array of hydrodynamically entrained sperm cells*, Science **309**, 300 (2005).

[111] R. Ma, G. Klindt, I. Riedel-Kruse, F. Jülicher, and B. Friedrich, *Active phase and amplitude fluctuations of flagellar beating*, Phys. Rev. Lett. **113**, 048101 (2014).

[112] M. Polin, I. Tuval, K. Drescher, J. Gollub, and R. Goldstein, *Chlamydomonas swims with two "gears" in a eukaryotic version of run-and-tumble locomotion*, Science **325**, 487 (2009).

[113] V. Geyer, F. Jülicher, J. Howard, and B. Friedrich, *Cell-body rocking is a dominant mechanism for flagellar synchronization in a swimming alga*, Proc. Nat. Acad. Sci. **110**, 18058 (2013).

[114] D. Mizuno, C. Tardin, C. Schmidt, and F. MacKintosh, *Nonequilibrium mechanics of active cytoskeletal networks*, Science **315**, 370 (2007).

[115] R. Ismagilov, A. Schwartz, N. Bowden, and G. Whitesides, *Autonomous movement and self-assembly*, Angew. Chem. Int. Ed. **41**, 652 (2002).

[116] W. F. Paxton, K. C. Kistler, C. C. Olmeda, A. Sen, S. K. St. Angelo, Y. Cao, T. E. Mallouk, P. E. Lammert, and V. H. Crespi, *Catalytic nanomotors: Autonomous movement of striped nanorods*, J. Am. Chem. Soc. **126**, 13424 (2004).

[117] Y. Wang, R. M. Hernandez, D. J. Bartlett, J. M. Bingham, T. R. Kline, A. Sen, and T. E. Mallouk, *Bipolar electrochemical mechanism for the propulsion of catalytic nanomotors in hydrogen peroxide solutions*, Langmuir **22**, 10451 (2006).

[118] J. R. Howse, R. A. L. Jones, A. J. Ryan, T. Gough, R. Vafabakhsh, and R. Golestanian, *Self-motile colloidal particles: From directed propulsion to random walk*, Phys. Rev. Lett. **99**, 048102 (2007).
[119] A. A. Solovev, Y. Mei, E. Bermúdez Ureña, G. Huang, and O. G. Schmidt, *Catalytic microtubular jet engines self-propelled by accumulated gas bubbles*, Small **5**, 1688 (2009).
[120] L. F. Valadares, Y.-G. Tao, N. S. Zacharia, V. Kitaev, F. Galembeck, R. Kapral, and G. A. Ozin, *Catalytic nanomotors: Self-propelled sphere dimers*, Small **6**, 565 (2010).
[121] H.-R. Jiang, N. Yoshinaga, and M. Sano, *Active motion of a janus particle by self-thermophoresis in a defocused laser beam*, Phys. Rev. Lett. **105**, 268302 (2010).
[122] Y. Mei, A. A. Solovev, S. Sanchez, and O. G. Schmidt, *Rolled-up nanotech on polymers: from basic perception to self-propelled catalytic microengines*, Chem. Soc. Rev. **40**, 2109 (2011).
[123] S. Ebbens, M.-H. Tu, J. R. Howse, and R. Golestanian, *Size dependence of the propulsion velocity for catalytic janus-sphere swimmers*, Phys. Rev. E **85**, 020401 (2012).
[124] I. Buttinoni, G. Volpe, F. Kümmel, G. Volpe, and C. Bechinger, *Active brownian motion tunable by light*, J. Phys.: Condens. Matter **24**, 284129 (2012).
[125] L. Baraban, R. Streubel, D. Makarov, L. Han, D. Karnaushenko, O. G. Schmidt, and G. Cuniberti, *Fuel-free locomotion of janus motors: Magnetically induced thermophoresis*, ACS Nano **7**, 1360 (2013).
[126] A. Brown and W. Poon, *Ionic effects in self-propelled pt-coated janus swimmers*, Soft Matter **10**, 4016 (2014).
[127] S. Ebbens, D. Gregory, G. Dunderdale, J. Howse, Y. Ibrahim, T. Liverpool, and R. Golestanian, *Electrokinetic effects in catalytic platinum-insulator janus swimmers*, Euro. Phys. Lett. **106**, 58003 (2014).
[128] J. Simmchen, V. Magdanz, S. Sanchez, S. Chokmaviroj, D. Ruiz-Molina, A. Baeza, and O. Schmidt, *Effect of surfactants on the performance of tubular and spherical micromotors – a comparative study*, RSC Adv. **4**, 20334 (2014).
[129] M. Cates, *Diffusive transport without detailed balance in motile bacteria: does microbiology need statistical physics?*, Rep. Prog. Phys. **75**, 042601 (2012).
[130] M. Cates and J. Tailleur, *Motility-induced phase separation*, Annu. Rev. Condens. Matter Phys. **6**, 219 (2015).
[131] T. E. Mallouk and A. Sen, *Powering nanorobots*, Sci. Am. **300**, 72 (2009).
[132] M. Popescu, S. Dietrich, M. Tasinkevych, and J. Ralston, *Phoretic motion of spheroidal particles due to self-generated solute gradients*, Eur. Phys. J. E **31**, 351 (2010).
[133] S. Das, A. Garg, A. Campbell, J. Howse, A. Sen, D. Velegol, R. Golestanian, and S. Ebbens, *Boundaries can steer active janus spheres*, Nat. Commun. **6**, 8999 (2015).
[134] J. de Graaf, G. Rempfer, and C. Holm, *Diffusiophoretic self-propulsion for partially catalytic spherical colloids*, IEEE Trans. Nanobiosci. **14**, 272 (2015).
[135] A. Brown, W. Poon, C. Holm, and J. De Graaf, *Ionic screening and dissociation are crucial for understanding chemical self-propulsion in polar solvents*, Soft Matter **13**, 1200 (2017).
[136] S. Ketzetzi, J. De Graaf, R. Doherty, and D. Kraft, *Slip length dependent propulsion speed of catalytic colloidal swimmers near walls*, Phys. Rev. Lett. **124**, 048002 (2020).
[137] S. Ketzetzi, J. De Graaf, and D. Kraft, *Diffusion-based height analysis reveals robust microswimmer-wall separation*, Phys. Rev. Lett. **125**, 238001 (2020).
[138] T. Vicsek, A. Czirók, E. Ben-Jacob, I. Cohen, and O. Shochet, *Novel type of phase transition in a system of self-driven particles*, Phys. Rev. Lett. **75**, 1226 (1995).
[139] M. Marchetti, J.-F. Joanny, S. Ramaswamy, T. Liverpool, J. Prost, M. Rao, and R. Simha, *Hydrodynamics of soft active matter*, Rev. Mod. Phys. **85**, 1143 (2013).
[140] G. Grégoire and H. Chaté, *Onset of collective and cohesive motion*, Phys. Rev. Lett. **92**, 025702 (2004).
[141] H. Chaté, F. Ginelli, G. Grégoire, and F. Raynaud, *Collective motion of self-propelled particles interacting without cohesion*, Phys. Rev. E **77**, 046113 (2008).
[142] A. Solon, H. Chaté, and J. Tailleur, *From phase to microphase separation in flocking models: The essential role of nonequilibrium fluctuations*, Phys. Rev. Lett. **114**, 068101 (2015).
[143] M. Zumaya, H. Larralde, and M. Aldana, *Delay in the dispersal of flocks moving in unbounded space using long-range interactions*, Sci. Reports **8**, 1 (2018).
[144] K. Grosvenor, N. Obers, and S. Patil, *Hydrodynamics without Boost-Invariance from Kinetic Theory: From Perfect Fluids to Active Flocks*, arXiv **2501.00025**, 1 (2024).
[145] J. Toner and Y. Tu, *Flocks, herds, and schools: A quantitative theory of flocking*, Phys. Rev. E **58**,

4828 (1998).
[146] F. Ginelli, *The physics of the vicsek model*, Euro. Phys. J. S.T. **225**, 2099 (2016).
[147] X. Yang and M. Marchetti, *Hydrodynamics of turning flocks*, Phys. Rev. Lett. **115**, 258101 (2015).
[148] C. Dombrowski, L. Cisneros, S. Chatkaew, R. Goldstein, and J. Kessler, *Self-concentration and large-scale coherence in bacterial dynamics*, Phys. Rev. Lett. **93**, 098103 (2004).
[149] H. Wensink, J. Dunkel, S. Heidenreich, K. Drescher, R. Goldstein, H. Löwen, and J. Yeomans, *Meso-scale turbulence in living fluids*, Proc. Nat. Acad. Sci. **109**, 14308 (2012).
[150] A. Creppy, O. Praud, X. Druart, P. Kohnke, and F. Plouraboué, *Turbulence of swarming sperm*, Phys. Rev. E **92**, 032722 (2015).
[151] T. Sanchez, D. Chen, S. DeCamp, M. Heymann, and Z. Dogic, *Spontaneous motion in hierarchically assembled active matter*, Nature **491**, 431 (2012).
[152] P. Guillamat, J. Ignés-Mullol, and F. Sagués, *Taming active turbulence with patterned soft interfaces*, Nat. Commun. **8**, 564 (2017).
[153] A. Tan, E. Roberts, S. Smith, U. Olvera, J. Arteaga, S. Fortini, K. Mitchell, and L. Hirst, *Topological chaos in active nematics*, Nat. Phys. **15**, 1033 (2019).
[154] B. Martínez-Prat, R. Alert, F. Meng, J. Ignés-Mullol, J.-F. Joanny, J. Casademunt, R. Golestanian, and F. Sagués, *Scaling regimes of active turbulence with external dissipation*, Phys. Rev. X **11**, 031065 (2021).
[155] C. Blanch-Mercader, V. Yashunsky, S. Garcia, G. Duclos, L. Giomi, and P. Silberzan, *Turbulent dynamics of epithelial cell cultures*, Phys. Rev. Lett. **120**, 208101 (2018).
[156] S.-Z. Lin, W.-Y. Zhang, D. Bi, B. Li, and X.-Q. Feng, *Energetics of mesoscale cell turbulence in two-dimensional monolayers*, Commun. Phys. **4**, 21 (2021).
[157] H. Karani, G. Pradillo, and P. Vlahovska, *Tuning the random walk of active colloids: From individual run-and-tumble to dynamic clustering*, Phys. Rev. Lett. **123**, 208002 (2019).
[158] A. Kolmogorov, *On degeneration (decay) of isotropic turbulence in an incompressible viscous liquid*, Dokl. Akad. Nauk SSSR **31**, 538 (1941).
[159] J. Słomka and J. Dunkel, *Spontaneous mirror-symmetry breaking induces inverse energy cascade in 3D active fluids*, Proc. Nat. Acad. Sci. **114**, 2119 (2017).
[160] M. Linkmann, G. Boffetta, M. Marchetti, and B. Eckhardt, *Phase transition to large scale coherent structures in two-dimensional active matter turbulence*, Phys. Rev. Lett. **122**, 214503 (2019).
[161] L. Carenza, L. Biferale, and G. Gonnella, *Cascade or not cascade? Energy transfer and elastic effects in active nematics*, Europhys. Lett. **132**, 44003 (2020).
[162] R. Alert, J.-F. Joanny, and J. Casademunt, *Universal scaling of active nematic turbulence*, Nat. Phys. **16**, 682 (2020).
[163] C. Rorai, F. Toschi, and I. Pagonabarraga, *Coexistence of active and hydrodynamic turbulence in two-dimensional active nematics*, Phys. Rev. Let. **129**, 218001 (2022).
[164] K. Kruse, J.-F. Joanny, F. Jülicher, J. Prost, and K. Sekimoto, *Asters, vortices, and rotating spirals in active gels of polar filaments*, Phys. Rev. Lett. **92**, 078101 (2004).
[165] L. Giomi, M. Marchetti, and T. Liverpool, *Complex spontaneous flows and concentration banding in active polar films*, Phys. Rev. Lett. **101**, 198101 (2008).
[166] E. Tjhung, M. Cates, and D. Marenduzzo, *Nonequilibrium steady states in polar active fluids*, Soft Matter **7**, 7453 (2011).
[167] J. Słomka and J. Dunkel, *Generalized Navier-Stokes equations for active suspensions*, Euro. Phys. J. S.T. **224**, 1349 (2015).
[168] D. Bárdfalvy, H. Nordanger, C. Nardini, A. Morozov, and J. Stenhammar, *Particle-resolved lattice Boltzmann simulations of 3-dimensional active turbulence*, Soft Matter **15**, 7747 (2019).
[169] V. Škultéty, C. Nardini, J. Stenhammar, D. Marenduzzo, and A. Morozov, *Swimming suppresses correlations in dilute suspensions of pusher microorganisms*, Phys. Rev. X **10**, 031059 (2020).
[170] C. Abaurrea-Velasco, C. Lozano, C. Bechinger, and J. de Graaf, *Autonomously probing viscoelasticity in disordered suspensions*, Phys. Rev. Lett. **125**, 258002 (2020).
[171] N. Narinder, M. Bos, C. Abaurrea-Velasco, J. de Graaf, and C. Bechinger, *Understanding enhanced rotational dynamics of active probes in rod suspensions*, Soft Matter **18**, 6246 (2022).
[172] V. Baulin *et al.*, *Intelligent soft matter: Towards embodied intelligence*, arXiv **2502.13224**, 1 (2025).
[173] O. Hallatschek, S. Datta, K. Drescher, J. Dunkel, J. Elgeti, B. Waclaw, and N. Wingreen, *Proliferating active matter*, Nat. Rev. Phys. **5**, 407 (2023).